ELASTIC AND INELASTIC RESPONSES OF COLUMNS AFTER SUDDEN LOSS OF BRACING

by

Rae Hak Yoo

Dissertation submitted to the Faculty of the

Virginia Polytechnic Institute and State University

on partial fulfillment of the requirements for the degree of

Doctor of Philosophy

in

Civil Engineering

APPROVED:

Raymond H. Plaut, Chairman

Richard M. Barker

William S. Easterling

Robert A. Heller

Siegfried M. Holzer

December, 1995

Blacksburg, Virginia

c.2

ELASTIC AND INELASTIC RESPONSES OF COLUMNS AFTER SUDDEN LOSS OF BRACING

by

Rae Hak Yoo

Raymond H Plaut, Chairman

(ABSTRACT)

A pinned column with initial deflection and an internal brace is investigated. The brace is modeled as a translational spring. Axial compressive loads are applied at the brace and the top of the column, and the equilibrium shape of the column is determined. The critical loads for the perfect column are computed analytically for several load combinations.

The dynamic response of the column after sudden loss of bracing is analyzed using Galerkin's method. With the consideration of the effects of the bracing location and the bracing stiffness, the maximum deflection of the column during motion is determined. The contribution of damping effects to the maximum deflection of the column is examined. Damping effects in the Galerkin method are compared to results from the finite element method (based on ABAQUS).

The plastic dynamic analysis is carried out using ABAQUS. Both residual stresses and damping effects are considered, and the spread of plasticity during the motion is investigated. The cases studied include equal and unequal spans, and axial loads below and above the load which causes the column to collapse.

ACKNOWLEDGMENTS

I wish to acknowledge all who have provided the support, assistance and guidance necessary to complete my education.

First, I express my sincere appreciation to my chairman, Dr. Raymond H. Plaut for his guidance and assistance. I have learned a lot from him, academically and otherwise. His love and devotion to students will be firmly retained in my memory throughout my life.

I also acknowledge the members of my committee, Dr. Barker, Easterling, Heller and Dr. Holzer, for their academic criticism while reviewing this work.

I am deeply indebted to my father and my mother who gave me support, encouragement and sacrifice. I would never return countless love they gave me.

Special thanks must be given to my wife, Jung Hee Lee, and my son, Dongseop for their love, constant support, and willingness to share difficulties and happiness throughout many years of study.

Finally, I would like to thank my friends and colleagues, Jae-geun Yang, Seungbum Ahn, Chulho Bang, Hojong Baik, Sang-Gyun Kim, Wonkyu Kim, Suwan Park, Dongwoo Son, Do H. Nam and Sang-Keon Lee for thier support.

TABLE OF CONTENTS

LIST OF TABLES

LIST OF FIGURES

1. INTRODUCTION

It is clear that the capacity of a column carrying a compressive load can be increased remarkably by adding rotational or translational spring supports between its ends.

The design guide for column bracing, developed by Winter [1], suggests an ideal spring stiffness for columns with two or more internal braces, equal span lengths, and only end loading [2]. However, this ideal stiffness may not be adequate for actual column design, since span lengths are not always equal and at each bracing point a compressive load may be applied. For the unequal-span column, a modified ideal spring stiffness is suggested [2], but this is an approximation.

Plaut and J. Yang [3] and Plaut and Y. Yang [4] investigated some examples and proved that no ideal spring stiffness exists for unequal-span columns except under special conditions. Modification of the design guidelines for lateral bracing requirements of two-span columns was recommended by Plaut [5]. These recommendations were discussed by Yura [6].

Even though some investigations studied the optimal location of bracing and the required bracing force to ensure that structures are stable [7,8], the effect of a sudden loss of bracing on columns has not been examined. The loss of column bracing results in a decrease of the critical load and may cause the whole structure to fail catastrophically.

When an imperfect column loses its bracing, it is no longer in an equilibrium state, which makes the column change its shape. This change of shape is caused by the elastic stresses which are released when the applied loads are removed [9]. The abrupt change of the elastic stresses due to the sudden loss of bracing makes the column vibrate. This vibration may fade away or may grow, depending on the magnitude of the applied axial force and the material behavior in the column.

Only a few papers can be found on this effect on structures. The plastic bending and "springback" of a cantilever beam subjected to a concentrated force and an axial load at its tip was examined by Yu and Johnson [10] when the concentrated force was removed. In that study, the behavior of the beam was regarded as static rather than dynamic, and the moment due to the axial load was neglected in the analysis. Since one of the main concerns in column design is the moment caused by the axial forces, this assumption seems to be inappropriate for column design.

Amman [11] studied the effect of sudden loss of support for reinforced and prestressed concrete beams with experiments. However, the behavior of massive, heavy, horizontal, concrete beams is much different from that of an axial, compressed, vertical, steel column.

A large number of papers on the response of elastic-plastic structures under dynamic loading have been published [12-17]. The effect of an impact load on column behavior would not be the same as that of a sudden loss of bracing. Unlike the dynamic

loading, the loss of bracing does not provide an initial velocity to a column. Studies on the dynamic response following a sudden loss of support were not found.

If the loading on the structure is very high, the behavior does not remain elastic; hence, structural behavior should be analyzed based on inelastic theory. In general, there are two basic types of plastic analysis. The first one is the plastic hinge or rigid plastic analysis. The second is called the plastic zone method or the distributed plasticity method.

For a rigid, perfectly plastic, simply supported beam subjected to compressive loads, a plastic hinge is located at the point where the maximum moment occurs if that moment reaches the value of the plastic moment. Based on the assumption of the plastic hinge existing, the derived dynamic mode of deflection is a function of the distance from the supporting points and the plastic moment only, excluding the compressive load. However, the stability of columns is mainly determined by the axial forces. According to papers by Cowper and Symonds [18] and Hall et al. [19], the rigid-plastic theory was found to give a discrepancy between the measured deflection and the analytical prediction for dynamic loading problems. The rigid-plastic theory for dynamic problems involves the following assumptions: (1) it rules out the elastic effects for ductile materials, and (2) it neglects the geometric shape changes during motion, so this method requires some corrections in analyzing a rate-sensitive material such as a mild steel. These shortcomings of the rigid-plastic theory were discussed by Martin and Symonds [20]. Here, the plastic zone method will be applied to the study of a braced column.

The main purpose of this study is to analyze the behavior of a column after a sudden loss of bracing, which has not been considered previously, and to provide a basis for future design guidelines. Collapse of the column will be examined. For loads smaller than the collapse load, maximum dynamic responses will be computed.

An unequal-span column with one internal brace having various spring stiffnesses will be analyzed by elastic, viscoelastic, and plastic theories. The critical loads are determined by the exact solution of the governing equations for several load combinations, and an approximate method is used to find the dynamic mode shape after sudden loss of bracing for elastic and viscoelastic behavior. The plastic zone analysis will be done using ABAQUS, which permits one to determine the region of plasticity at any time during the motion. Initial crookedness of the column is assumed, using the summation of a sine series so that various initial shapes could be considered.

2. MODEL FOR COLUMN ANALYSIS

For unequal-span columns, the current design guidelines recommend the following formula as an ideal brace stiffness [2]:

$$\bar{k}_{ideal} = \frac{\pi^2 EI}{\bar{a}^3} + \frac{\pi^2 EI}{\bar{b}^3} \tag{2.1}$$

where $\bar{a}$ and $\bar{b}$ are shown in Fig. 2.1 and EI is the constant bending stiffness of the beam.

Plaut [5] and Plaut and Yang [4] investigated some columns with two or three spans and showed that, for certain conditions, the spring stiffness required for the critical load to be at least the Euler load P_e of the longest span is sometimes higher than the ideal spring stiffness in equation (2.1). In order to ensure the safety of the structure, it is apparent that design guidelines must be modified for adequate design of column bracing. In this study, a two-span column will be analyzed and some aspects not involved in the current design guides, such as a load at the bracing point, will be studied.

The static analysis is carried out to investigate the responses of a column with two unequal spans as shown in Fig. 2.1. Based on the elastic theory, the behavior of the column is analyzed exactly. For the perfect column, the critical loads are sought theoretically. A typical column size $(W8 \times 40)$, in the finite element method, is modeled with different bracing locations, spring stiffnesses, and load combinations. To investigate

an imperfect column, the column is assumed to be initially deflected. Only the deflection in the direction of the weak axis of the column is assumed in the analysis.

In the Load and Resistance Factor Design (LRFD) specifications, the design strength is based on a maximum out-of-straightness of about 1/1500 of the column length [21]. But, in the American Society of Testing and Materials specification A6, the maximum permitted camber of a rolled structural shape is specified less than L/1000 for all sections less than 30 feet long (the permissible variation in straightness for W shape column less than 45 feet long is limited to 1/8 in × number of feet of column length but not over 3/8 in.) [22,23]. To provide conservative results from the analysis, the maximum initial deflection of the column is limited to 1/1000 of the column length. The bracing between the ends of the column is modeled as a translational spring. The spring is allowed to displace in the weak axis direction only. The effect of an axial force at the bracing point will be considered.

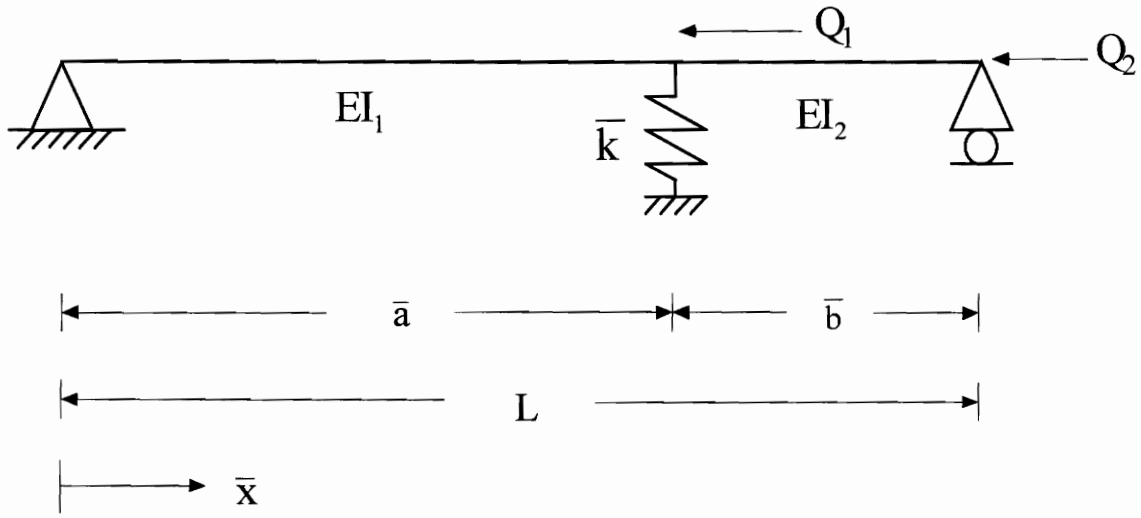

Fig. 2.1 Loading System and Column Configuration

After the sudden loss of the column bracing, the behavior of the column is analyzed elastically by an approximate dynamic analysis, first using Galerkin's method and then the finite element method. In the dynamic analysis, the load acting at the bracing point is no longer present, since the load disappears with the bracing. The effect of the residual stresses is also studied in the plastic analysis. The distribution of residual stresses is specified in section 4.2.2. Due to the complexity, plastic dynamic analysis is carried out using the finite element method. The decaying motions of the column are investigated by including damping coefficients with both Galerkin's method and the finite element method.

3. STATIC ANALYSIS

3.1 Elastic analysis

Elastic analysis is carried out on a two-span column with length L as depicted in Fig. 2.1. The bending stiffness is EI_1 in the first span and EI_2 in the second span. The compressive loads Q_1 and Q_2 are assumed to act at $\bar{x} = \bar{a}$ and $\bar{x} = L$, respectively. Both ends of the column ($\bar{x} = 0$ and $\bar{x} = L$) are simply supported, and a translational spring with stiffness $\bar{k}$ is located at $\bar{x} = \bar{a}$, where $\bar{a}$ is the distance from the left end of the column. The initial deflection, $\bar{w}_0$, is defined as the column shape when no axial forces are applied and the spring is unstretched. Under the axial loads, the column deflection $\bar{w}$ is also measured from the $\bar{x}$ axis. Deflections are positive if upward in Fig. 2.1.

If the deflection is small, the equilibrium equations of the system in Fig. 2.1 are:

$$EI_1\left(\bar{w}_1''''(\bar{x}) - \bar{w}_0''''(\bar{x})\right) + (Q_1 + Q_2)\bar{w}_1''(\bar{x}) = 0, \quad \text{for } 0 \le \bar{x} \le \bar{a}$$

$$EI_2\left(\bar{w}_2''''(\bar{x}) - \bar{w}_0''''(\bar{x})\right) + Q_2\bar{w}_2''(\bar{x}) = 0, \qquad \text{for } \bar{a} \le \bar{x} \le L, \tag{3.1}$$

where primes denote differentiation with respect to $\bar{x}$.

To simplify the calculations, the following nondimensional quantities are introduced:

$$x = \frac{\bar{x}}{L}, \quad w_0 = \frac{\bar{w}_0}{L}, \quad w = \frac{\bar{w}}{L},$$

$$a = \frac{\bar{a}}{L}, \quad b = \frac{\bar{b}}{L}$$

$$k = \frac{\bar{k}L^3}{EI_1},\ \gamma_1^{\,2} = \frac{(Q_1 + Q_2)L^2}{EI_1},\ \gamma_2^{\,2} = \frac{Q_2 L^2}{EI_2} \tag{3.2}$$

$$P_1 = \frac{Q_1 L^2}{EI_1},\ P_2 = \frac{Q_2 L^2}{EI_2} = \gamma_2^{\,2}$$

By applying these relations, the equilibrium equations are non-dimensionalized as follows:

$$w_1''''(x) - w_0''''(x) + \gamma_1^2 w_1''(x) = 0, \quad \text{for } 0 \le x \le a$$

$$w_2''''(x) - w_0''''(x) + \gamma_2^2 w_2''(x) = 0, \quad \text{for } a \le x \le 1 \tag{3.3}$$

Equation (3.3) has the following general solution:

$$w_1(x) = A_1 \sin\gamma_1 x + A_2 \cos\gamma_1 x + A_3 x + A_4 + W_{P1}(x),\ (0 \le x \le a)$$

$$w_2(x) = B_1 \sin\gamma_2 x + B_2 \cos\gamma_2 x + B_3 x + B_4 + W_{P2}(x),\ (a \le x \le 1) \tag{3.4}$$

where $W_{P1}(x)$ and $W_{P2}(x)$ are particular solutions.

The boundary and transition conditions are:

at x=0: $w_1 = 0$

$$w_1'' - w_0'' = 0$$

at x=a: $w_1 = w_2$

$$w_1' = w_2'$$

$$w_1'' - w_0'' = \varepsilon(w_2'' - w_0'')$$

$$w_1''' - w_0''' + q w_1' = \varepsilon(w_2''' - w_0''') + k(w_1 - w_0)$$

at x=1: $w_2 = 0$

$$w_2'' - w_0'' = 0 \tag{3.5}$$

where $\varepsilon = \frac{EI_2}{EI_1}$ and $q = \gamma_1^2 - \varepsilon\gamma_2^2$.

Boundary conditions at the ends and transition conditions at the spring location give eight equations for the eight unknowns (A_i, B_i), so solutions for the deflection can be obtained. Detailed solutions are shown in the Appendix.

3.2 Critical loads of perfect column

When a column possesses no initial deflection, it is called perfect . If the column is perfect and the loads act along the centerline, the set of algebraic equations obtained from equation (3.5) is homogeneous. A nontrivial solution of the homogeneous equation exists only if the determinant of the 8×8 coefficient matrix is zero. The nondimensional critical load is defined from the lowest root of the determinantal equation. To verify the formulation, the critical load is calculated when P_1 and k approach zero. In that case, the critical load must approach the Euler load for a simply supported column. In the calculation, as k decreases to a small value, the critical value of P_2 approaches the nondimensional Euler load, π^2, for the unbraced column.

In order to calculate the critical load for the combination of loads, the ratio of $\frac{P_1}{P_2}$ is fixed. Here, the relative critical load P_{rc} is introduced to define the critical ratio load

based on P_2. For example, if the spans have the same bending stiffness EI, and if $P_1:P_2$=2:1, k=100 and a=0.6, the relative critical load P_{rc}=10.25 means that the column buckles when $\frac{Q_1L^2}{EI}$=20.50 and $\frac{Q_2L^2}{EI}$=10.25, i.e., P_{rc} in Figs 3.1 to 3.7 is the critical value of P_2.

Figure 3.1 indicates that an ideal spring stiffness exists if $Q_1 = 0$ and $a = 0.5$. If k is larger than $16\pi^2$=157.91 and $a = 0.5$, no increment of the critical load occurs for this case. Figures 3.1 to 3.4 show the critical load as a function of the left span length for several spring stiffnesses and for $Q_1:Q_2$=0:1, $Q_1:Q_2$=0.5:1, $Q_1:Q_2$=1:1, and $Q_1:Q_2$=2:1, respectively. For these three cases, as k is increased, the critical load always becomes larger. Unlike the case of end loading only, the symmetric bracing, however, does not provide the maximum critical load for each case. The maximum critical load usually occurs when the brace is located between $a = 0.3$ and 0.5.

Figures 3.5 to 3.7 show the relative critical load variation versus spring location for different load ratios and fixed spring stiffnesses. As seen in these figures, if a load is applied at the bracing (i.e., the load ratio is other than zero), the optimal spring location to produce the maximum strength of the column is not at the center of the column. It depends on the spring stiffness and load combination. As the spring stiffness becomes large, the optimal location is moved to the left.

3.3 Imperfect column

A perfect column is an idealized one for a theoretical analysis. When the axial load is applied to a perfect column, theoretically no moment is induced. Therefore column bending cannot be expected unless the applied load is higher than the critical load. To get a relationship between applied loads and bracing requirement, an analysis is performed for the imperfect column with initial deflection. Actual columns are not perfectly straight, and even if the initial deflection is small, it affects the column behavior and reduces the load carrying capacity of the column.

In Plaut and Yang [4], the initial deflection was assumed to be a symmetric quadratic function or an anti-symmetric cubic function. These functions do not represent all the shapes of columns. This study assumes the initial crookedness as the summation of a sine series, so that many types can be considered.

The expression assumed for the nondimensional initial deflection is as follows:

$$w_0(x) = \sum_{m=1}^{M} R_m \sin(m\pi x) \tag{3.6}$$

The maximum amplitude of the dimensional initial deflection is assumed to be L/1000. The deflection under given loads can be obtained by substituting $w_0(x)$ into equations (3.2) and (3.3) and solving the boundary value problem.

Figure 3.8 depicts the static deflection under $\frac{Q_1 L^2}{EI}=8$ and $\frac{Q_2 L^2}{EI}=8$ and the initial deflection $w_0(x)=0.001\sin(\pi x)$ for a=0.4 and k=100. The net deflection, u(x), is

measured from the initial deflection. The spring location is not at the center in this example, so the column is displaced unsymmetrically.

a	k=50	k=100	k=150	k=200	k=300	k=400	k=500
0.1	10.79	11.63	12.40	13.09	14.30	15.29	16.12
0.2	13.04	15.58	17.56	19.08	21.17	22.46	23.32
0.3	15.88	20.45	23.58	25.61	27.82	28.91	29.54
0.4	18.57	25.78	30.52	32.95	34.81	35.48	35.82
0.5	19.81	29.29	38.14	39.48	39.48	39.48	39.48
0.6	18.57	25.78	30.52	32.95	34.81	35.48	35.82
0.7	15.88	20.45	23.58	25.61	27.82	28.91	29.54
0.8	13.04	15.58	17.56	19.08	21.17	22.46	23.32
0.9	10.79	11.63	12.40	13.09	14.30	15.29	16.12

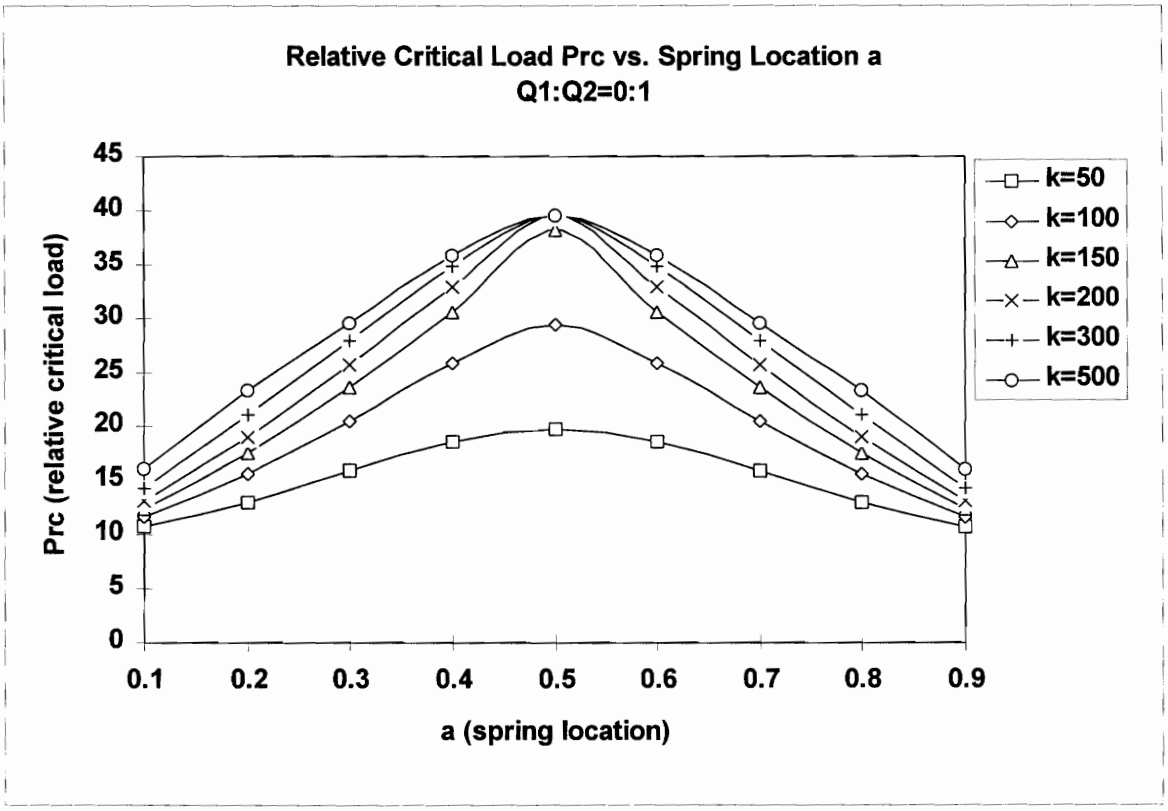

Fig. 3.1 Relative critical load P_{rc} vs. spring location a, $Q_1:Q_2 = 0:1$ and different k's

a	k=50	k=100	k=150	k=200	k=300	k=400	k=500
0.1	9.88	10.72	11.51	12.23	13.51	14.58	15.49
0.2	11.32	13.88	16.02	17.75	20.23	21.80	22.82
0.3	13.33	17.90	21.47	24.01	26.81	28.11	28.81
0.4	15.16	21.92	27.55	30.76	32.36	32.72	32.86
0.5	15.71	22.80	27.72	29.44	30.18	30.38	30.47
0.6	14.30	18.91	21.52	22.88	24.09	24.62	24.90
0.7	11.92	14.78	16.57	17.70	18.95	19.60	19.99
0.8	9.55	11.16	12.37	13.27	14.48	15.24	15.74
0.9	7.62	8.17	8.67	9.11	9.87	10.50	11.01

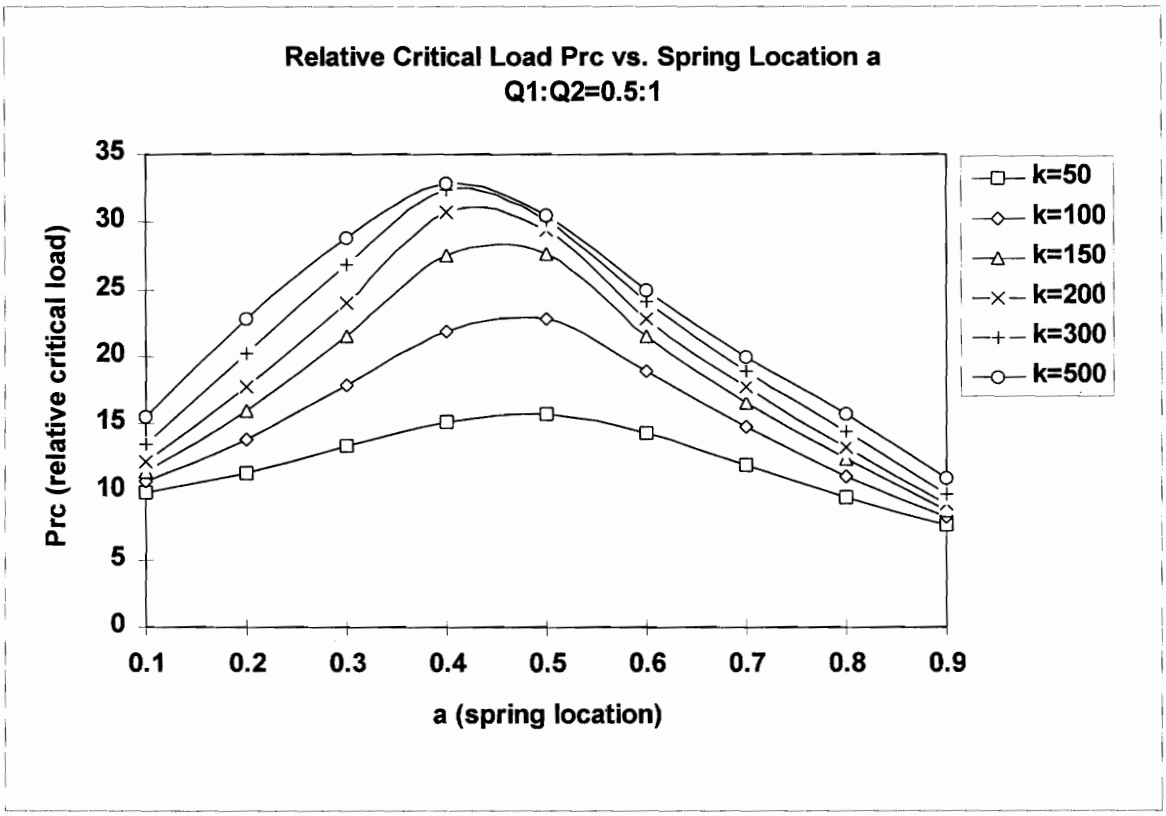

Fig. 3.2 Relative critical load P_{rc} vs. spring location a, Q_1:Q_2 = 0.5:1 and different k's

a	k=50	k=100	k=150	k=200	k=300	k=400	k=500
0.1	9.05	9.89	10.67	11.40	12.72	13.86	14.83
0.2	9.89	12.35	14.51	16.36	19.17	21.03	22.26
0.3	11.35	15.61	19.30	22.21	25.69	27.23	27.99
0.4	12.68	18.59	24.17	28.52	29.21	29.25	29.26
0.5	12.90	18.25	21.50	22.84	23.70	23.98	24.12
0.6	11.52	14.80	16.55	17.48	18.37	18.77	19.00
0.7	9.47	11.49	12.72	13.49	14.36	14.82	15.10
0.8	7.50	8.66	9.51	10.14	10.99	11.52	11.88
0.9	5.88	6.29	6.65	6.98	7.53	7.98	8.35

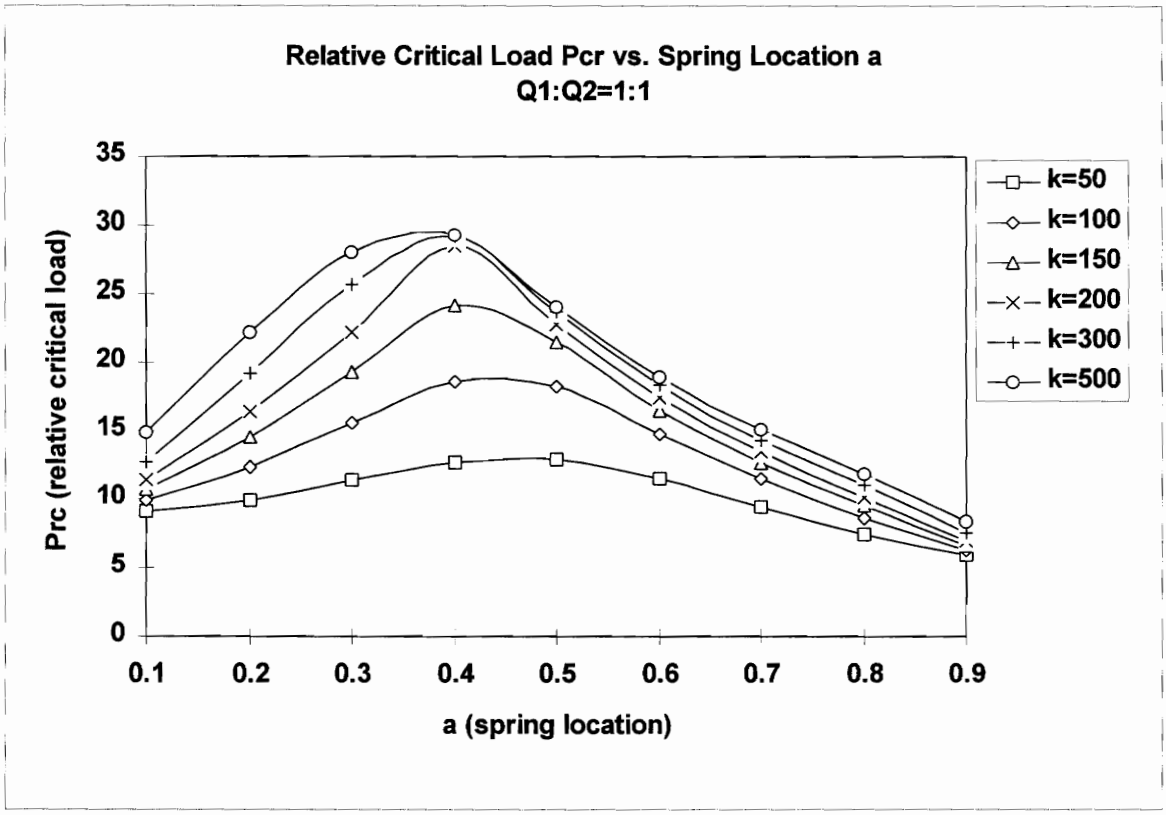

Fig. 3.3 Relative critical load P_{rc} vs. spring location a, $Q_1:Q_2 = 1:1$ and different k's

a	k=50	k=100	k=150	k=200	k=300	k=400	k=500
0.1	7.66	8.44	9.19	9.90	11.23	12.42	13.48
0.2	7.78	9.90	11.89	13.73	16.87	19.24	20.90
0.3	8.63	12.12	15.44	18.49	23.13	25.27	26.08
0.4	9.45	13.88	18.00	21.07	22.26	22.40	22.45
0.5	9.42	12.88	14.79	15.67	16.36	16.63	16.77
0.6	8.23	10.25	11.29	11.86	12.43	12.70	12.86
0.7	6.67	7.92	8.66	9.13	9.66	9.95	10.13
0.8	5.22	5.96	6.49	6.88	7.41	7.74	7.96
0.9	4.03	4.30	4.53	4.74	5.10	5.39	5.63

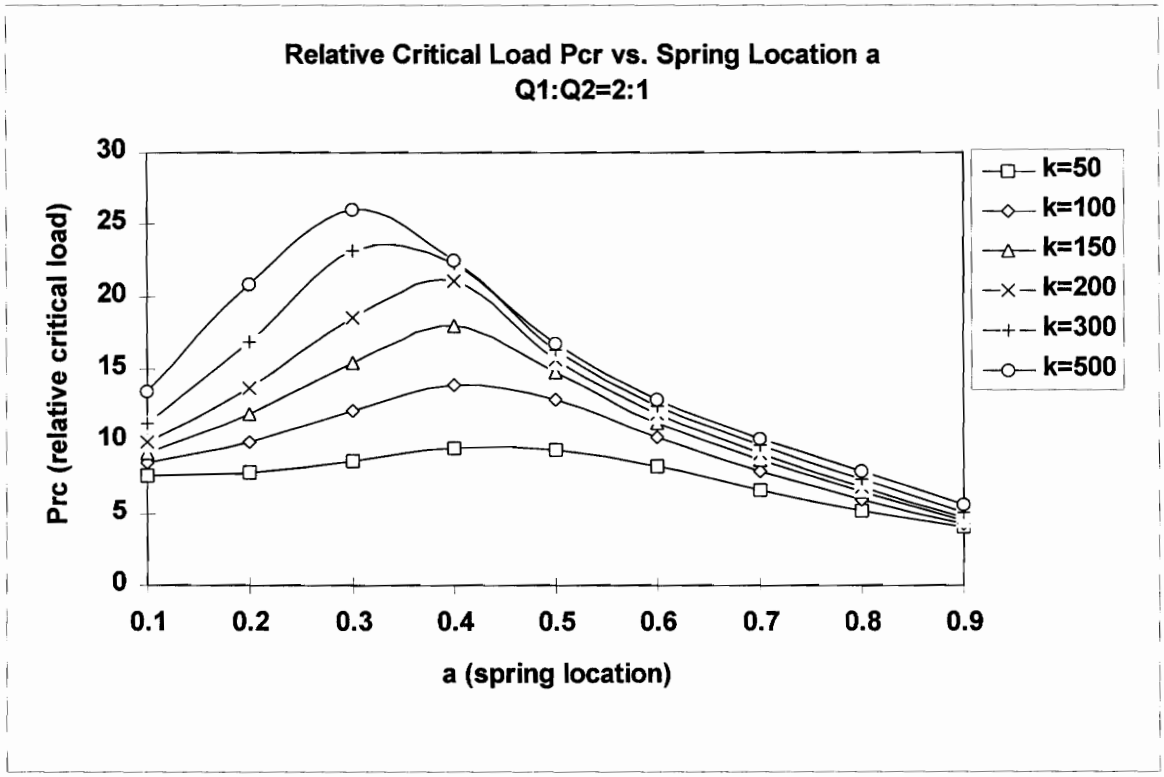

Fig. 3.4 Relative critical load P_{rc} vs. spring location a, $Q_1:Q_2 = 2:1$ and different k's

a	RATIO=0	RATIO=0.5	RATIO=1	RATIO=2
0.1	11.63	10.72	9.89	5.36
0.2	15.58	13.88	12.35	6.94
0.3	20.45	17.90	15.61	8.95
0.4	25.78	21.92	18.59	10.96
0.5	29.29	22.80	18.25	11.40
0.6	25.78	18.91	14.80	9.45
0.7	20.45	14.78	11.49	7.39
0.8	15.58	11.16	8.66	5.58
0.9	11.63	8.17	6.29	4.08

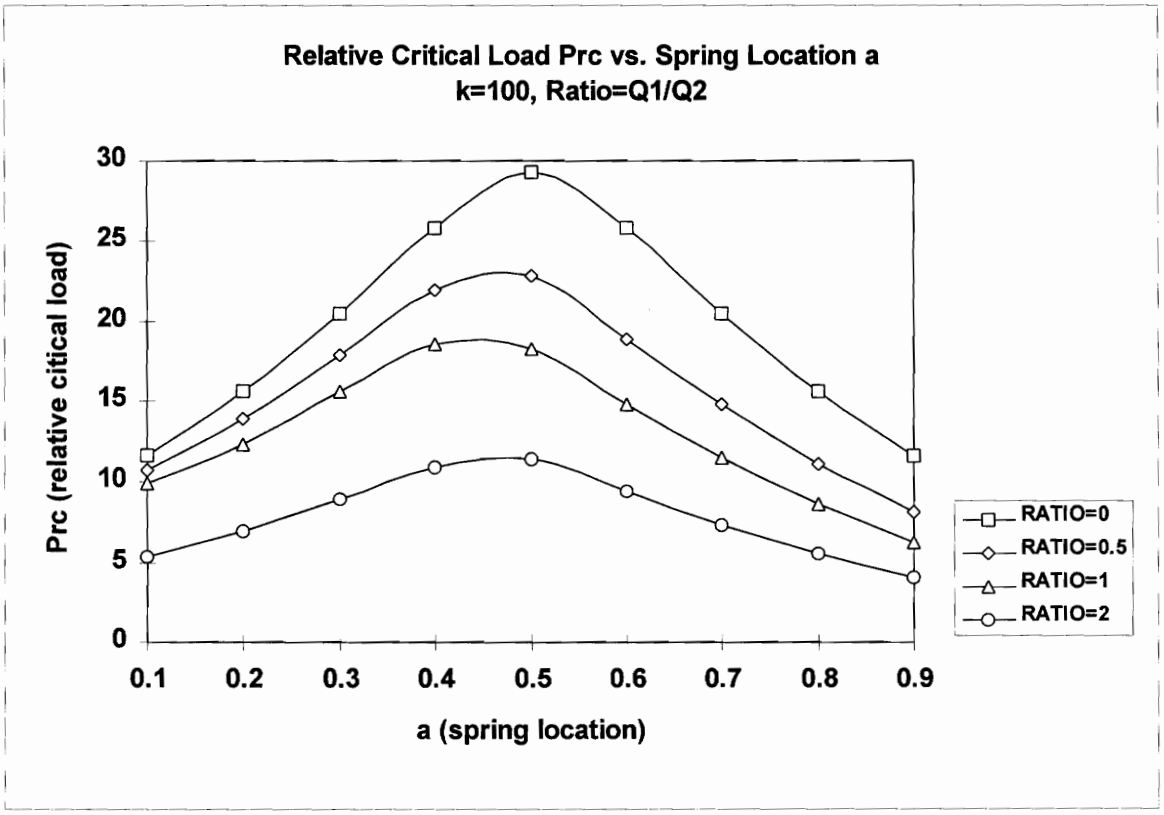

Fig. 3.5 Relative critical load vs. a, k=100

a	RATIO=0	RATIO=0.5	RATIO=1	RATIO=2
0.1	13.09	12.23	11.40	6.11
0.2	19.08	17.75	16.36	8.87
0.3	25.61	24.01	22.21	12.00
0.4	32.95	30.76	28.52	15.38
0.5	39.48	29.44	22.84	14.72
0.6	32.95	22.88	17.48	11.44
0.7	25.61	17.70	13.49	8.85
0.8	19.08	13.27	10.14	6.63
0.9	13.09	9.11	6.98	4.55

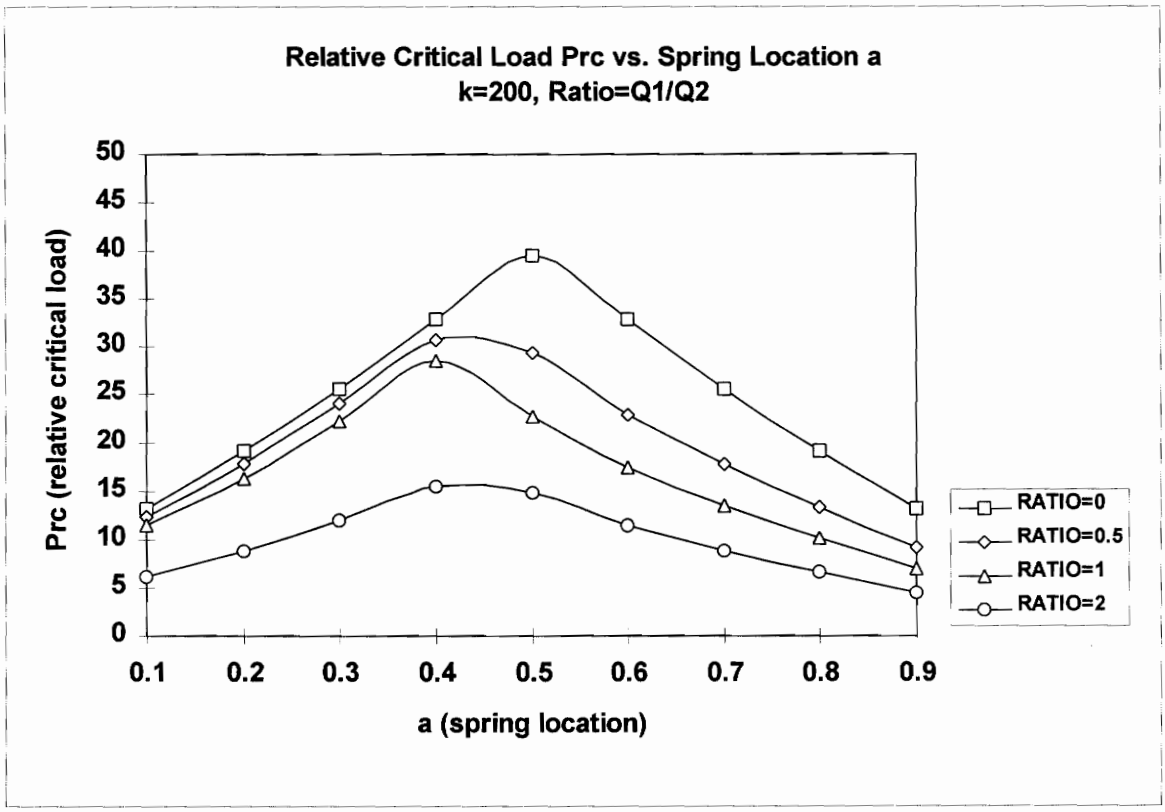

Fig. 3.6 Relative critical load vs. a, k=200

a	RATIO=0	RATIO=0.5	RATIO=1	RATIO=2
0.1	16.12	15.49	14.83	7.74
0.2	23.32	22.82	22.26	11.41
0.3	29.54	28.81	27.99	14.40
0.4	35.82	32.86	29.26	16.43
0.5	39.48	30.47	24.12	15.23
0.6	35.82	24.90	19.00	12.45
0.7	29.54	19.99	15.10	9.99
0.8	23.32	15.74	11.88	7.87
0.9	16.12	11.01	8.35	5.50

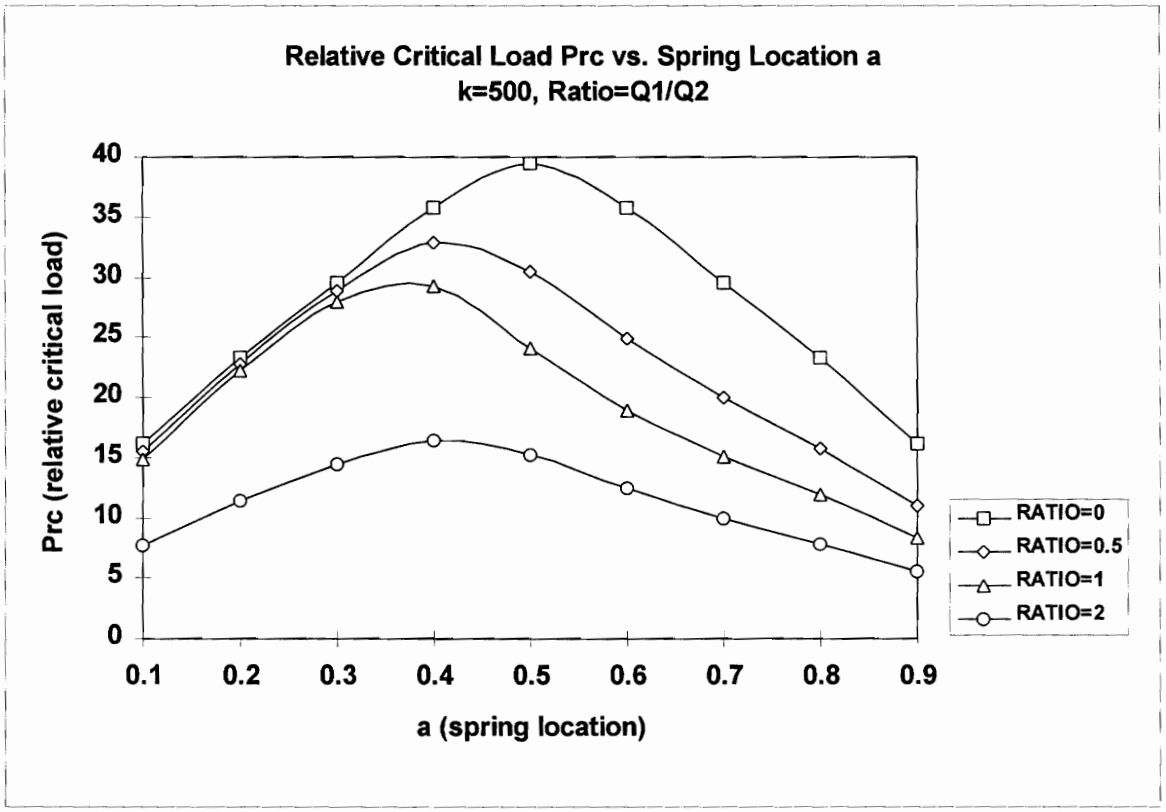

Fig. 3.7 Relative critical load vs. a, k=500

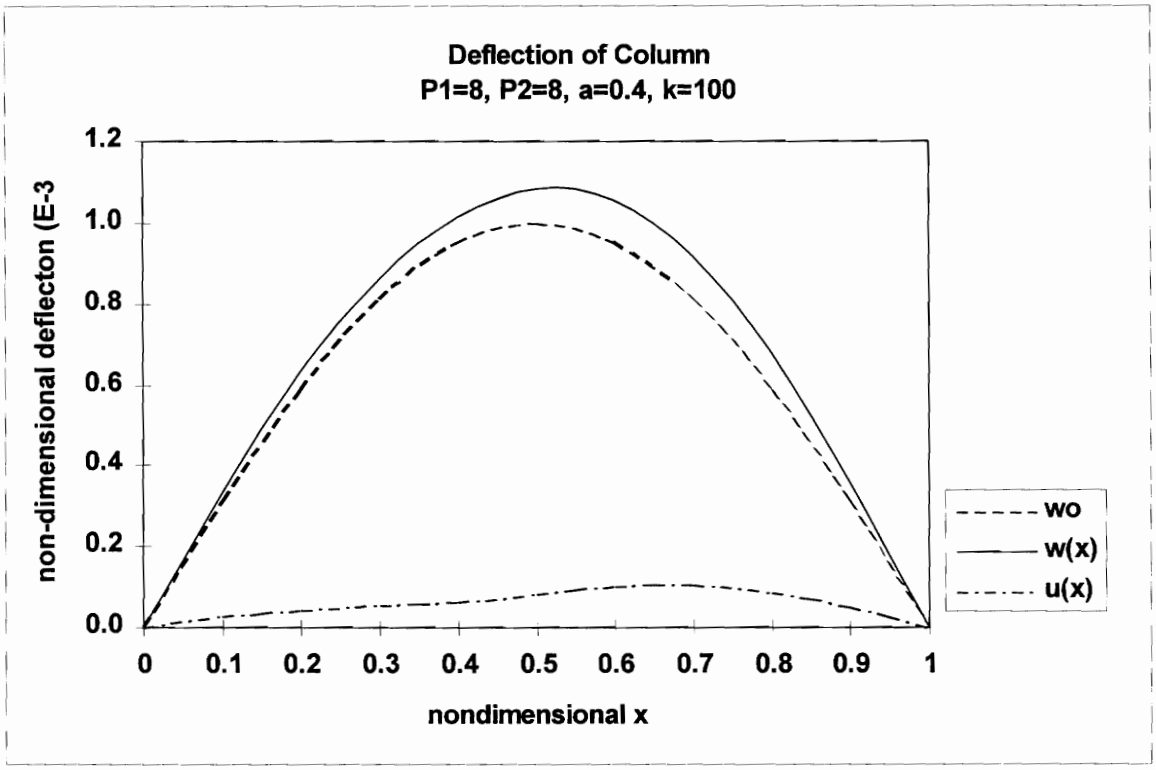

Fig. 3.8 Deflection of column, P_1=8, P_2=8, k=100, a=0.4

3.4 ABAQUS

The response of a column can be approximated using the finite element method. For a column which has more than 3 spans, or different boundary conditions or transition conditions, the finite element method can eliminate the rigorous and cumbersome procedures required in the analytical solution of the equilibrium equation. This section shows a comparison between the finite element method and the analytical solution. The finite element analysis is carried out using the well-known commercial program ABAQUS [24].

A typical wide flange I section column $(W8 \times 40, A36)$ is selected in the analysis, and the deflections associated with the applied loads are found and compared to the results from the exact analysis. A 240 inch-long column is examined. The geometry, loading, and section properties of the column are shown in Figs. 3.9 and 3.10. The modulus of elasticity is quantified for steel as 29000 $kips / in^2$. The shape of the initial deflection is assumed to be a half-sine function and only the initial deflection in the weak axis direction is considered. The maximum initial deflection at the midpoint of the column is chosen as L/1000.

3.4.1 Type of element

The analysis, so far, follows Euler-Bernoulli beam theory, which does not include the transverse shear deformation. To satisfy this assumption, cubic beam elements, in which the response of the column is estimated using cubic interpolation, are used in the

analysis. ABAQUS also provides various cross-section beam elements for the beam type element. A B33 (2-node cubic beam element in space) with I-beam section is selected, and the geometric properties are defined in the input data in Fig. 3.9. The cubic beam element in ABAQUS is provided for small strain and large rotation analysis based on Euler-Bernoulli beam theory. To consider the geometric nonlinearity, the large displacement effects are included by taking the NLGEOM parameter on the *STEP option.

3.4.2 Bracing and boundary conditions

The internal support can be interpreted as a spring which has rotational or translational resisting stiffness. ABAQUS provides three types of spring element. In this analysis, the SPRING1 element is used, which is provided for connection between a node and ground. When the axial load is applied, the column tends to bend about the weak axis due to the moment and the initial deflection of the column, so the deformation about the strong axis is ruled out in the analysis. As shown in Fig. 3.10, a translational spring is placed at the internal support, and it is assumed that the spring is stretched perpendicular to the $\bar{x} \cdot \bar{y}$ plane. Like the theoretical analysis, the effect of rotational stiffness of the brace is not considered. A B33 element has 6 degrees of freedom at each node $(u_x, u_y, u_z, \phi_x, \phi_y, \phi_z)$ [24]. At the left support, all the degrees of freedom but ϕ_y are constrained. At the right support, only u_x and ϕ_y are released.

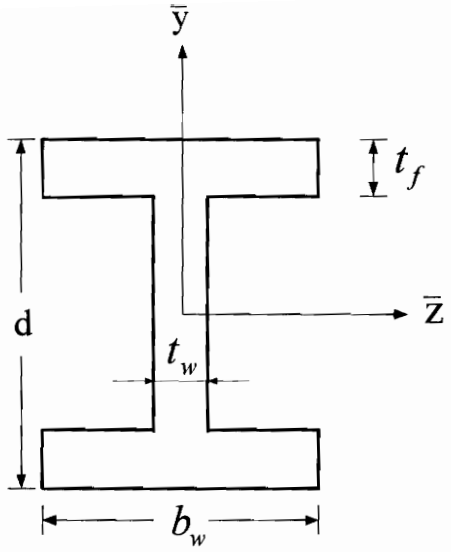

d	t_w	b_w	t_f	A	$I_{\bar{y}}$	$I_{\bar{z}}$
8.25	0.36	8.07	0.56	11.7	49.1	146.1

Fig. 3.9. The section data for the I-beam column (base unit=inch)

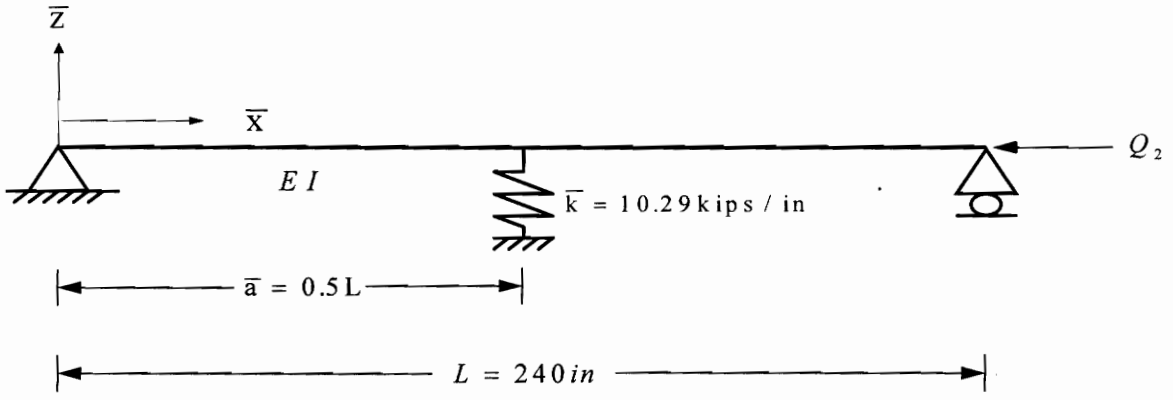

Fig. 3.10 Simply supported column with spring support and an end loading

3.4.3 Element discretization and convergence

The accuracy of the ABAQUS results is checked for some element discretizations. For the system in Fig. 3.10, the deflections at some points (x) are calculated and compared to those from the exact solution in Table 3.1. Four cases of the element discretization are tested and the average errors are estimated for each case. The last row of Table 3.1 represents the corresponding averaged errors relative to the exact solution.

The exact deflections can be calculated by solving the equation of motion of the system with the boundary conditions. Solutions were described in the elastic analysis in section 3.1 and the Appendix.

It is obviously true that a finer column discretization provides more accurate results. However, the computational expense should be considered when deciding on the discretization to apply. Even though a 40-element model provides closer results (0.01 % error) to the exact solution, a 20-element model which allows 0.05% error is chosen in

Table 3.1. Deflection at point x, unit=in.$\times 10^{-1}$

x	Exact	8 elements	10 elements	20 elements	40 elements
0.1	0.981	-	0.979	0.981	0.981
0.125	1.214	1.210	-	-	-
0.2	1.858	-	1.854	1.857	1.858
0.25	2.229	2.222	-	-	-
0.3	2.541	-	2.536	2.540	2.541
0.375	2.886	2.877	-	-	-
0.4	2.967	-	2.961	2.965	2.966
0.5	3.108	3.098	3.101	3.106	3.107
Ave. Err.(%)	-	**0.3**	**0.2**	**0.05**	**0.01**

the analysis. This amount of error causes less than 1/1000 inch of deviation in this system, and can be considered negligible.

3.4.4 The critical load for the perfect column in ABAQUS

The critical load for the perfect column can be found theoretically. The basic concept of the finite element method is that buckling is expected when the tangent stiffness matrix has a small determinant, which approaches zero (i.e., the tangent stiffness matrix is singular) [2,24]. Following is the procedure used to find the buckling load. At the base load P_N (below the buckling load), the elastic tangent stiffness matrix, $[K_P]$, is computed. By adding a perturbation load Q_N, the differential stiffness matrix $[K_Q]$, which is the sum of the load stiffness and the stress stiffness associated with Q_N, is computed. The tangent stiffness matrix for the load $P_N + \lambda Q_N$ is written as $[K_P + \lambda K_Q]$. The load-displacement rate relationship becomes

$$[K_P + \lambda K_Q]du = dF. \tag{3.7}$$

A nontrivial solution for this equation, when dF=0, is possible only if the determinant of the stiffness matrix is zero. This is an eigenvalue problem and the buckling load is calculated in terms of the lowest eigenvalue λ_i. The estimated buckling load is provided as $P_N + \lambda Q_N$. In ABAQUS, *BUCKLE step is provided to predict the buckling load.

A 240 inch-long $W8 \times 40$ column in Fig. 3.10 is selected for the finite element analysis. The column is assumed to be straight. Table 3.2 shows the critical loads for different spring stiffnesses. The buckling analysis in the finite element method shows good accuracy. The critical loads from the perfect column for different spring locations are compared to the ABAQUS results in Table 3.3.

Table 3.2 The nondimensional relative critical load P_{rc} for varying spring stiffness, where Q_1:Q_2=0:1 and a=0.5

k	50	100	150	200	300	400	500
Perfect	19.81	29.29	38.14	39.48	39.48	39.48	39.48
ABAQUS	19.81	29.30	38.15	39.48	39.48	39.48	39.48

Table 3.3 The nondimensional relative critical load P_{rc} for varying spring location, where Q_1:Q_2=0:1, k=100

a	Perfect column	ABAQUS for perfect column
0.1	11.63	11.64
0.2	15.58	15.58
0.3	20.45	20.46
0.4	25.78	25.79
0.5	29.29	29.30

4. DYNAMIC RESPONSE

4.1 Elastic analysis

4.1.1 Galerkin's method

If the brace is suddenly removed at t=0, and if the column is made with perfectly elastic material, the column moves away from its previous equilibrium state. The characteristic behavior of elasticity makes the column vibrate, and this vibration will continue unless damping effects are taken into account. Viscous and viscoelastic damping effects are considered in the analysis. The quantities $\bar{\eta}$ and $\bar{\beta}$ represent the coefficients of viscous and viscoelastic damping, respectively. The column deflection at time $\bar{t}$ and position $\bar{x}$ is denoted $\bar{y}(\bar{x},\bar{t})$, and for simplicity, the section properties of the column throughout the length L are considered to be constant. At the instant of losing the brace, the load Q_1 is also removed from the column. Consequently, this load is not involved in the equation of motion, which is given by:

$$EI\frac{\partial^4(\bar{y}-\bar{w}_0)}{\partial\bar{x}^4}+\bar{\eta}EI\frac{\partial^5\bar{y}}{\partial^4\bar{x}\partial\bar{t}}+\bar{\beta}\frac{\partial\bar{y}}{\partial\bar{t}}+Q_2\frac{\partial^2\bar{y}}{\partial\bar{x}^2}+\bar{\mu}\frac{\partial^2\bar{y}}{\partial\bar{t}^2}=0 \qquad (4.1)$$

where $\bar{\mu}$ is the mass per unit length.

Additional nondimensional quantities are defined as

$$y = \frac{\bar{y}}{L},\ t = \bar{t}\alpha,\ \eta = \frac{\bar{\eta}}{\alpha},\ \beta = \frac{\bar{\beta}L^4}{\alpha EI}$$

$$\text{where } \alpha = \sqrt{\frac{\bar{\mu}L^4}{EI}}. \tag{4.2}$$

Equation (4.1) now has the form

$$\frac{\partial^2 y}{\partial t^2} + \frac{\partial^4 y}{\partial x^4} - \frac{\partial^4 w_0}{\partial x^4} + \eta\frac{\partial^5 y}{\partial x^4 \partial t} + \beta\frac{\partial y}{\partial t} + \gamma_2^2\frac{\partial^2 y}{\partial x^2} = 0. \tag{4.3}$$

Let the deflection be approximated by

$$y(x,t) = \sum_{k=1}^{n} a_k(t)\theta_k(x) = \sum_{k=1}^{n} a_k(t)\sin(k\pi x) \tag{4.4}$$

and define the initial deflection as equation (3.6). By substituting these two functions into equation (4.3) and applying the method of Galerkin, equation (4.3) is rearranged as follows, where primes and dots denote differentiation with respect to x and t, respectively:

$$\begin{aligned}&\sum_{k=1}^{n}\int_0^1 \theta_j(\ddot{a}_k\theta_k + a_k\theta_k'''' + \eta\dot{a}_k\theta_k'''' + \beta\dot{a}_k\theta_k + \gamma_2^2 a_k\theta_k'')dx \\ &= \sum_{m=1}^{M}\int_0^1 \theta_j R_m(m\pi)^4\sin(m\pi x)dx\end{aligned} \tag{4.5}$$

where θ_j is the set of orthogonal eigenfunctions defined in equation (4.4) and j=1,2,...,n.

Introducing the following quantitative notations for convenience,

$$d_{jk} = \int_0^1 \theta_j\theta_k dx$$

$$f_{jk} = \int_0^1 (\eta\theta_j\theta_k'''' + \beta\theta_j\theta_k)dx \qquad (4.6)$$

$$g_{jk} = \int_0^1 (\theta_j\theta_k'''' + \gamma_2^2\theta_j\theta_k'')dx$$

$$h_{jm} = R_m(m\pi)^4 \int_0^1 \theta_j \sin(m\pi x)dx$$

one can obtain the simplified form:

$$\sum_{k=1}^{n}[d_{jk}\ddot{a}_k(t) + f_{jk}\dot{a}_k(t) + g_{jk}a_k(t)] = \sum_{m=1}^{M} h_{jm} \,. \qquad (4.7)$$

With the eigenfunction taken as $\theta_j = \sin(j\pi x)$, one can make use of orthogonality as follows:

$$\int_0^1 \sin(j\pi x)\sin(k\pi x)dx = 0 \qquad \text{if } j \neq k \text{ or}$$

$$= 1/2 \qquad \text{if } j = k. \qquad (4.8)$$

By utilizing orthogonality, equation (4.5) forms the following diagonal matrix equation:

$$\begin{bmatrix} d_{11} & 0 & 0 & 0 \\ 0 & \bullet & 0 & 0 \\ 0 & 0 & \bullet & 0 \\ 0 & 0 & 0 & d_{nn} \end{bmatrix} \begin{Bmatrix} \ddot{a}_1 \\ \bullet \\ \bullet \\ \ddot{a}_n \end{Bmatrix} + \begin{bmatrix} f_{11} & 0 & 0 & 0 \\ 0 & \bullet & 0 & 0 \\ 0 & 0 & \bullet & 0 \\ 0 & 0 & 0 & f_{nn} \end{bmatrix} \begin{Bmatrix} \dot{a}_1 \\ \bullet \\ \bullet \\ \dot{a}_n \end{Bmatrix} + \begin{bmatrix} g_{11} & 0 & 0 & 0 \\ 0 & \bullet & 0 & 0 \\ 0 & 0 & \bullet & 0 \\ 0 & 0 & 0 & g_{nn} \end{bmatrix} \begin{Bmatrix} a_1 \\ \bullet \\ \bullet \\ a_n \end{Bmatrix} = \sum_{m=1}^{M} \begin{Bmatrix} h_{1m} \\ \bullet \\ \bullet \\ h_{nm} \end{Bmatrix}$$

(4.9)

Equation (4.9) can be integrated exactly for given initial conditions. At t=0, they are $y(x,0) = w(x)$ and $\dot{a}_k(0) = 0$, and one can obtain the approximate motion in terms of the sine series. During motion, the deflection changes of the column at $x = 0.6$ are shown in Fig. 4.1 for one, two, three and four terms in the approximate motion, where $P_2 = 6.8836$, k=100, and the spring location is $a = 0.4$. In Table 4.1, values are listed. For $n \geq 3$, the change is negligible. As seen in Table 4.1 and Fig. 4.1, the first mode dominates the column deflection. Results shows that three or four terms in the sine series of the deflection are enough to closely approximate the solution. In this study, the motion is approximated by the first three terms in equation (4.4).

4.1.2 Results for damped column

As described in section 4.1.1, the initial deflection y(x,0) must be equal to the deflection w(x) under static loading. If the damping effects are considered in the equation of motion, the final deflection of the column, when time goes to infinity, is identical to the deflection $w_s(x)$ of the static case with an axial end loading only (Appendix). One percent of critical damping for the first mode is taken as the damping magnitude. If the viscous and the viscoelastic dampings are assumed to have equal contributions to the total damping for the first mode, the values of $\eta = 0.001$ and $\beta = 0.0987$ provide one percent of the critical damping. Specific explanations are given in section 4.1.3.

To test the formulation, the final deflection of the dynamic case for large values of t (in the analysis, t=100) is compared to that of the static case. This is shown in Fig. 4.2. For applied loads $\frac{Q_1 L^2}{EI}$=16 and $\frac{Q_2 L^2}{EI}$=8, the spring location a=0.7 and the spring stiffness k=500, the time-dependent motion is depicted. Since viscous and viscoelastic damping are included, the motion y(x,t) decays and finally approaches the static equilibrium state. The final state y(x,100) coincides with $w_s(x)$.

Figures 4.3 to 4.12 show the maximum deflection y(x,t) during the motion for different bracing locations and stiffnesses, where 1 % of the critical damping is applied. The maximum deflections are calculated and the effects of bracing stiffness are investigated for the following loading cases.

case 1. load ratio $Q_1:Q_2 = P_1:P_2 = 0:1$

$P_1 = 0,\ P_2 = 3$ Figs. 4.3 and 4.4.

$P_1 = 0,\ P_2 = 9$ Figs. 4.5 and 4.6

case 2. load ratio $Q_1:Q_2 = P_1:P_2 = 0.5:1$

$P_1 = 2,\ P_2 = 4$ Figs. 4.7 and 4.8

case 3. load ratio $Q_1:Q_2 = P_1:P_2 = 1:1$

$P_1 = 4,\ P_2 = 4$ Figs 4.9 and 4.10

case 4. load ratio $Q_1:Q_2 = P_1:P_2 = 2:1$

$P_1 = 4,\ P_2 = 2$ Figs. 4.11 and 4.12

a. Case 1.

If the internal load is not included. the maximum deflections are consistent with the higher spring stiffness (Figs. 4.3 to 4.6). Since the column is prevented from bending by the spring, as spring stiffness grows, the strain energy stored in the column becomes larger. When the column loses its bracing abruptly, the larger strain energy release results in a larger deflection during motion. Therefore, as k grows, the maximum deflections are also increased. Unlike the lower loading case (Fig. 4.3), when the spring is attached near the supports and higher load is applied, the maximum deflection can be greatly decreased by a lower spring stiffness.

b. Case 2

By adding the internal load in the static state, the maximum deflections at a=0.9 for k=100 are unexpectedly high compared with those in case 1 (Fig. 4.7). At this state, the maximum deflection occurs not in the dynamic state, but in the static state. Interestingly, in those cases, higher k's do not necessarily provide lower maximum deflections. The spring stiffness k=300 produces the lowest maximum deflection at a=0.9 in Figs. 4.7 and 4.8. Results show that, for some cases, the maximum deflection in the static state is much higher than subsequent local maximum values during the dynamic response (for example, at k=100 and 200 if a=0.9).

c. Case 3

Similar to case 2, the maximum deflection does not always occur for the higher spring stiffness. As seen in Fig. 4.9, at a=0.9 the highest spring stiffness, k=500, produces

the lowest maximum deflection, which occurs in the static state. The lowest among the maximum deflections is estimated at a=0.1 and k=100 (Fig. 4.10). Figure 4.10 shows that, at a=0.9 maximum deflections decrease as k increases. At a=0.85, maximum deflections decrease as k increases up to 300, and increase as k increases above 300. At the spring location a=0.9, the maximum deflection is governed by the static loading. At a=0.85, up to k=200 the maximum deflection occurs in the static state. However, if k is higher than 300, the maximum deflection occurs during the dynamic response.

d. Case 4

Inconsistency of relations between spring stiffnesses and spring locations is found when a is between 0.8 and 0.9 (Fig. 4.11). For cases a=0.8, a=0.85, and a=0.9, the maximum deflection decreases as k increases. For cases a=0.3, a=0.5, and a=0.7, the maximum deflection increases as k increases (Fig. 4.12). The deflection curve for a=0.1 fluctuates as k increases. These features depend on the loading states and loading ratio.

To find the maximum deflection of the column during motion, the length of the column is divided into 100 sections, and the deflections are checked at every section point after every time step $\bar{t}$ =0.01. The maximum deflection, if it occurs during motion, always occurs at the center of the column in the cases studied here.

Table 4.1 The deflection changes during motion for n=1,2,3,4 (unit= in $\times 10^{-2}$), Q_1=0, Q_2= 170 kips (P_2=6.8836), k=100, a=0.4, for W8 $\times$ 40 Column with L=240 in.

t (sec)	n=1	n=2	n=3	n=4
0	30.65	31.05	30.98	31.03
0.008	32.63	32.48	32.48	32.45
0.016	38.38	38.11	38.18	38.16
0.024	47.40	47.77	47.76	47.81
0.032	58.90	58.89	58.82	58.77
0.040	71.85	71.49	71.50	71.50
0.048	85.12	85.41	85.47	85.52
0.056	97.53	97.67	97.66	97.60
0.064	108.00	107.61	107.54	107.56
0.072	115.59	115.77	115.78	115.82
0.080	119.65	119.90	119.97	119.92
0.088	119.80	119.43	119.41	119.44
0.096	116.04	116.07	116.00	116.02
0.104	108.69	109.04	109.06	109.01
0.112	98.41	98.11	98.18	98.22
0.120	86.11	86.00	85.97	85.97
0.128	72.87	73.26	73.19	73.15
0.136	59.85	59.66	59.69	59.74
0.144	48.20	47.96	48.02	48.01
0.152	38.96	39.34	39.31	39.27
0.160	32.94	32.89	32.83	32.89
0.168	30.67	30.33	30.37	30.33
0.176	32.34	32.65	32.71	32.69
0.184	37.82	37.91	37.87	37.93
0.192	46.62	46.23	46.17	46.13
0.200	57.95	58.16	58.20	58.20

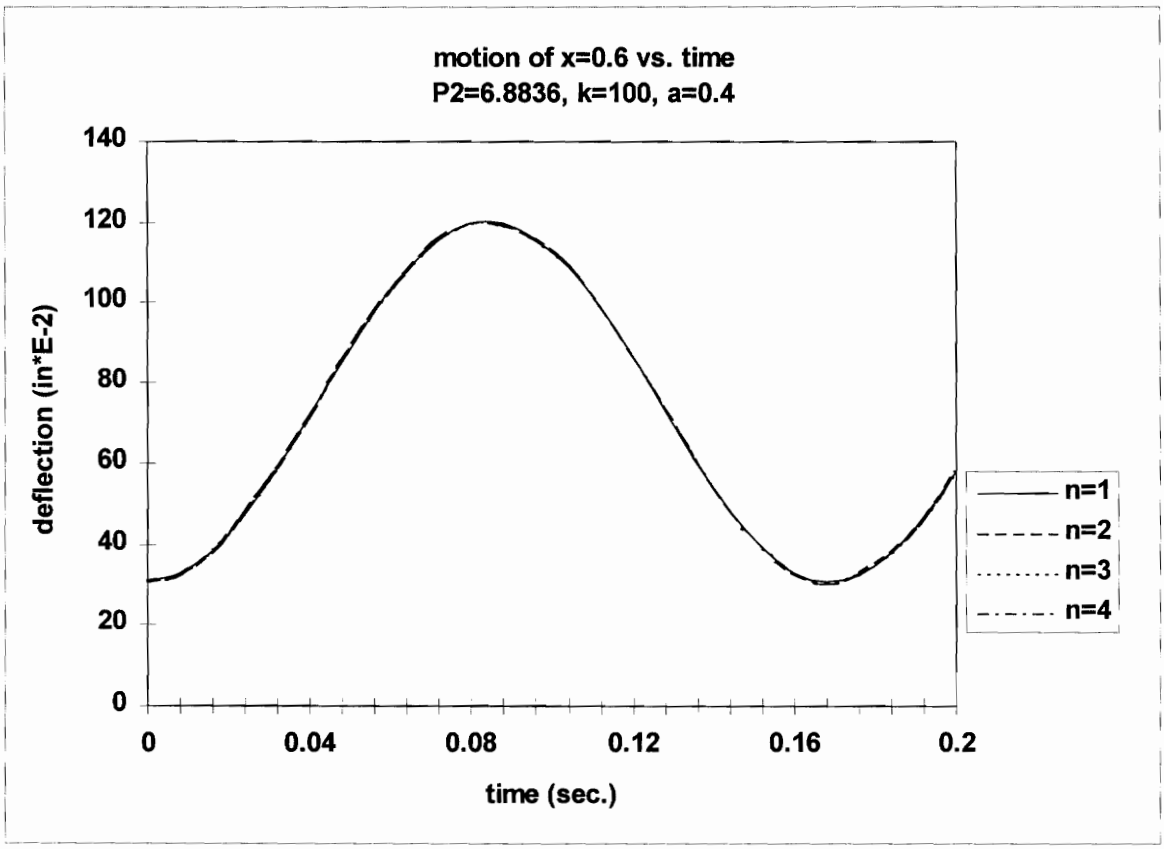

Fig. 4.1 The deflection changes during motion for n=1,2,3,4 (unit= in $\times 10^{-2}$)
Q_1=0, Q_2= 170 kips (P_2=6.8836), k=100, a=0.4, for W8 $\times$ 40 Column with L=240 in.

x	y(x,0)	y(x,0.02)	y(x,0.05)	y(x,0.1)	y(x,0.5)	y(x,100)	ws(x)
0.00	0.000	0.000	0.000	0.000	0.000	0.000	0.000
0.05	0.655	0.604	0.375	0.220	1.091	0.826	0.826
0.10	1.276	1.179	0.742	0.450	2.152	1.631	1.631
0.15	1.832	1.697	1.096	0.699	3.152	2.397	2.397
0.20	2.297	2.134	1.429	0.972	4.064	3.103	3.103
0.25	2.651	2.474	1.735	1.271	4.864	3.733	3.733
0.30	2.880	2.705	2.007	1.591	5.531	4.271	4.271
0.35	2.981	2.825	2.239	1.922	6.050	4.704	4.704
0.40	2.957	2.837	2.423	2.249	6.410	5.021	5.021
0.45	2.822	2.751	2.555	2.552	6.604	5.214	5.214
0.50	2.595	2.583	2.628	2.811	6.632	5.279	5.279
0.55	2.300	2.352	2.639	3.002	6.497	5.214	5.214
0.60	1.964	2.078	2.582	3.104	6.205	5.021	5.021
0.65	1.614	1.781	2.457	3.099	5.769	4.704	4.704
0.70	1.274	1.478	2.264	2.975	5.200	4.271	4.271
0.75	0.962	1.183	2.005	2.726	4.516	3.733	3.733
0.80	0.691	0.907	1.686	2.356	3.733	3.103	3.103
0.85	0.466	0.653	1.315	1.876	2.871	2.397	2.397
0.90	0.283	0.420	0.901	1.305	1.948	1.631	1.631
0.95	0.133	0.206	0.458	0.669	0.984	0.826	0.826
1.00	0.000	0.000	0.000	0.000	0.000	0.000	0.000

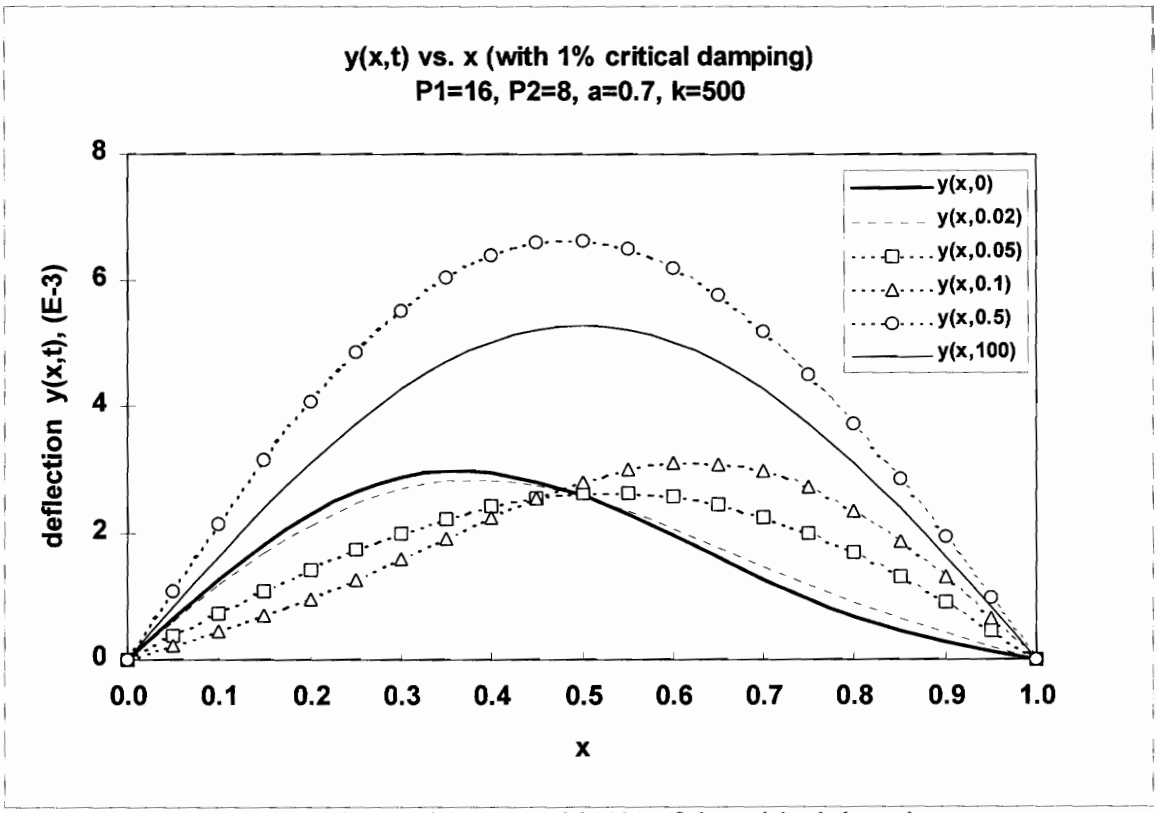

Fig. 4.2 The mode y(x,t) with 1% of the critical damping,
$P_1 = 16$, $P_2 = 8$, a=0.7, k=500

a	k=100	k=200	k=300	k=400	k=500
0.1	1.52	1.57	1.61	1.63	1.65
0.2	1.63	1.69	1.72	1.74	1.75
0.3	1.70	1.75	1.78	1.79	1.80
0.4	1.74	1.78	1.80	1.81	1.82
0.5	1.75	1.79	1.81	1.82	1.83
0.6	1.74	1.78	1.80	1.81	1.82
0.7	1.70	1.75	1.78	1.79	1.80
0.8	1.63	1.69	1.72	1.74	1.75
0.9	1.52	1.57	1.61	1.63	1.65

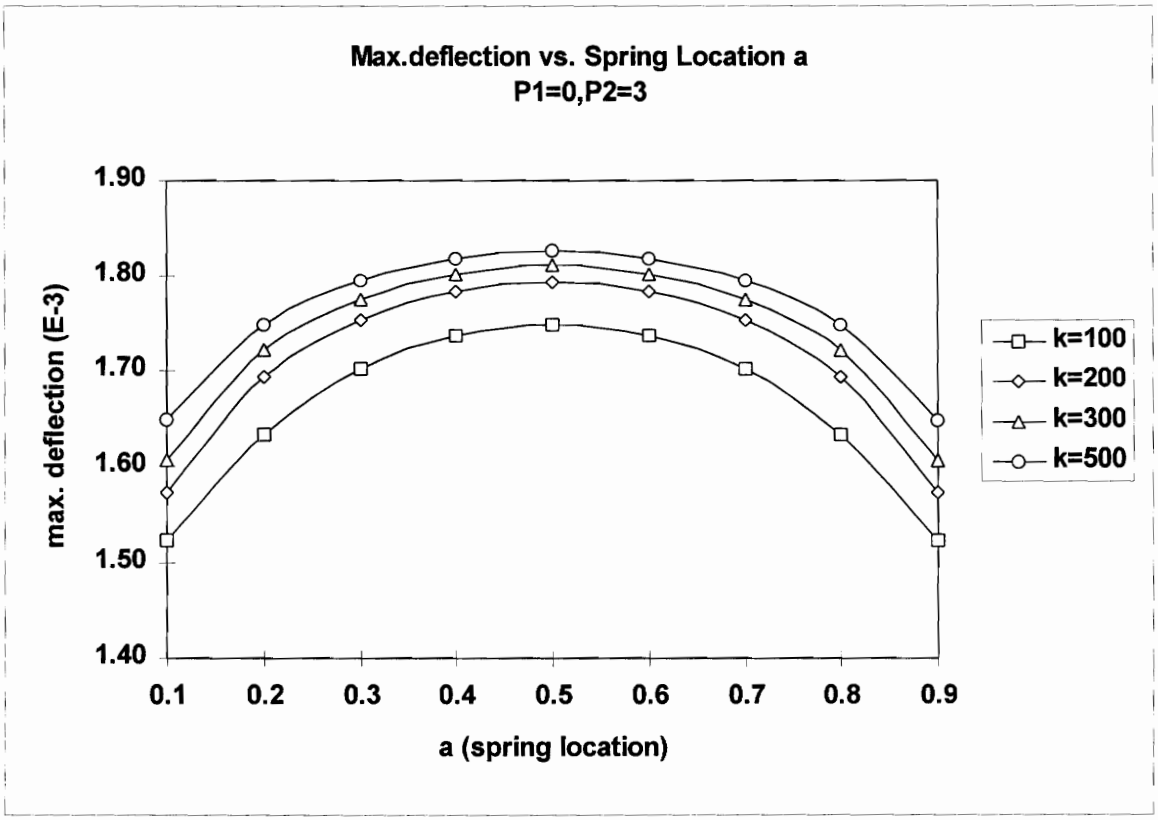

Fig. 4.3 Maximum deflection vs. spring location a
$P_1 = 0,\ P_2 = 3$

a	k=100	k=200	k=300	k=400	k=500
0.1	1.52	1.57	1.61	1.63	1.65
0.15	1.58	1.64	1.68	1.70	1.71
0.2	1.63	1.69	1.72	1.74	1.75
0.3	1.70	1.75	1.78	1.79	1.80
0.4	1.74	1.78	1.80	1.81	1.82
0.5	1.75	1.79	1.81	1.82	1.83
0.6	1.74	1.78	1.80	1.81	1.82
0.7	1.70	1.75	1.78	1.79	1.80
0.8	1.63	1.69	1.72	1.74	1.75
0.85	1.58	1.64	1.68	1.70	1.71
0.9	1.52	1.57	1.61	1.63	1.65

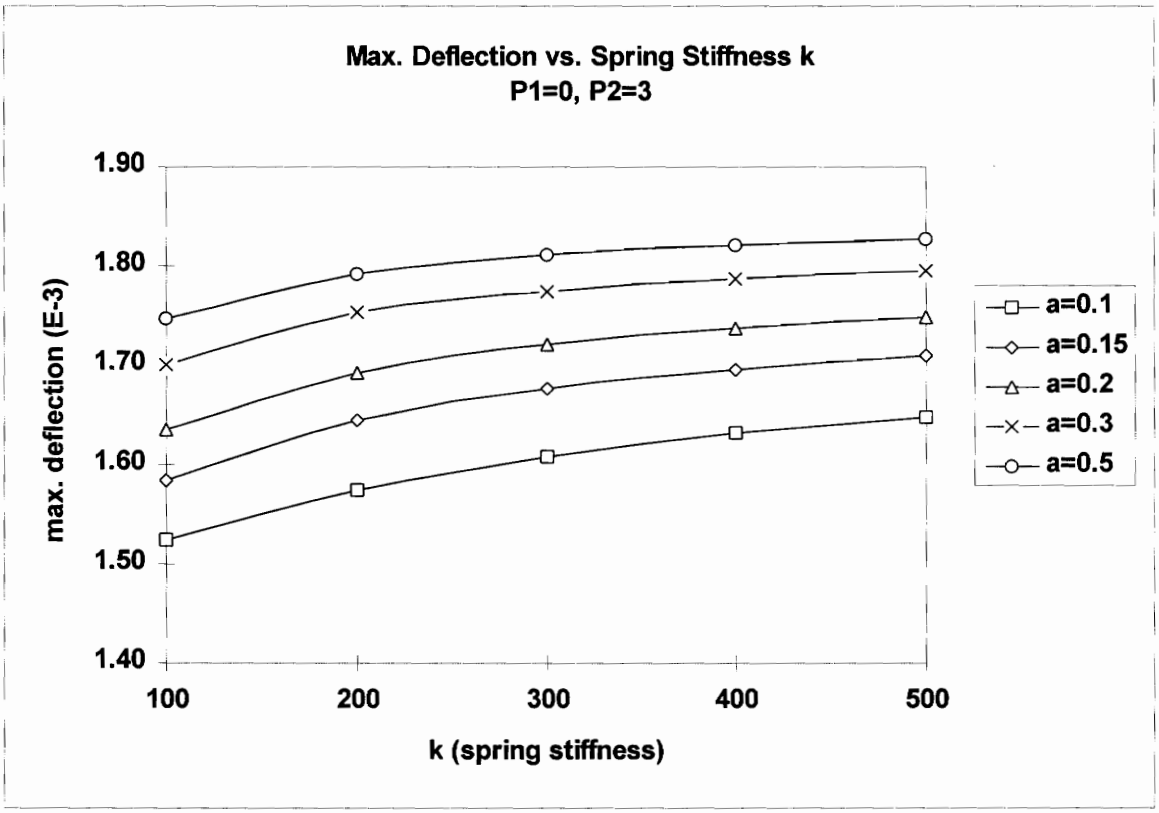

Fig. 4.4 Maximum deflection vs. spring stiffness k
$P_1 = 0,\ P_2 = 3$

a	k=100	k=200	k=300	k=400	k=500
0.1	1.76	1.87	1.92	1.94	1.96
0.2	1.95	1.99	2.01	2.02	2.02
0.3	2.00	2.03	2.04	2.04	2.04
0.4	2.02	2.04	2.05	2.05	2.05
0.5	2.03	2.05	2.05	2.06	2.06
0.6	2.02	2.04	2.05	2.05	2.05
0.7	2.00	2.03	2.04	2.04	2.04
0.8	1.95	1.99	2.01	2.02	2.02
0.9	1.76	1.87	1.92	1.94	1.96

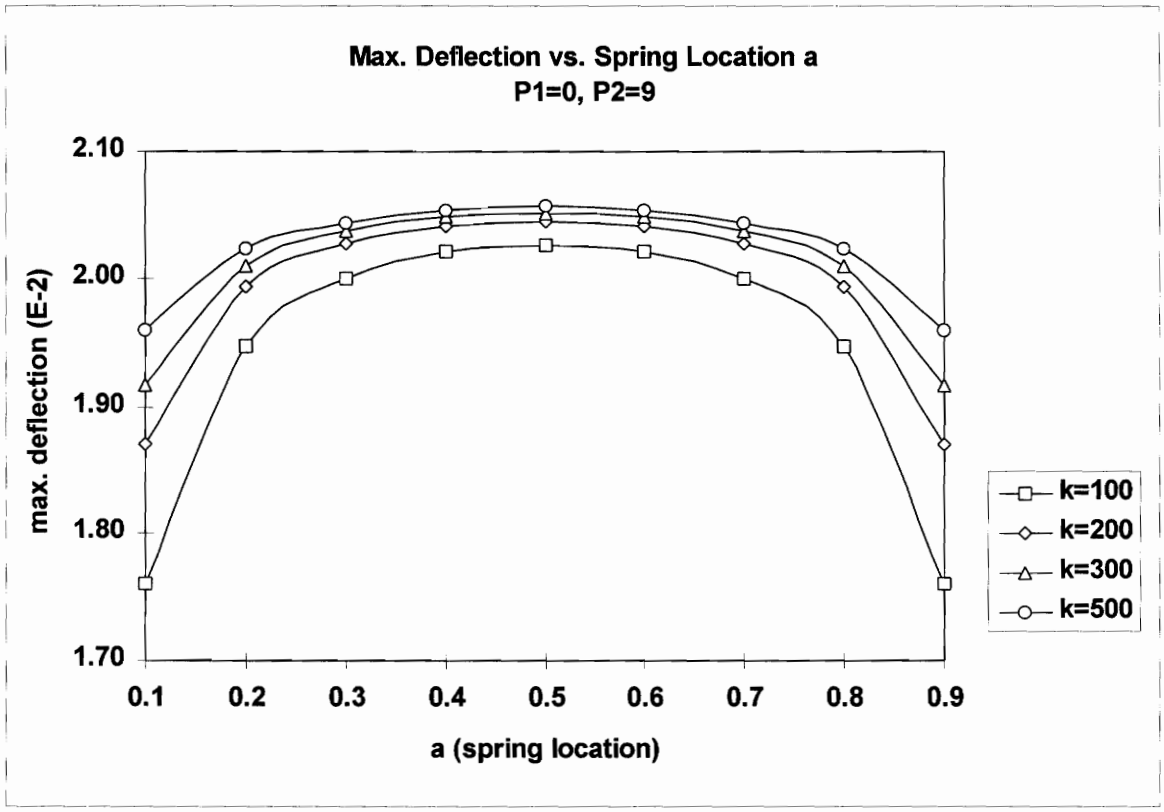

Fig. 4.5 Maximum deflection vs. spring location a
$P_1 = 0,\ P_2 = 9$

a	K=100	K=200	K=300	K=400	K=500
0.1	1.76	1.87	1.92	1.94	1.96
0.15	1.89	1.96	1.98	2.00	2.00
0.2	1.95	1.99	2.01	2.02	2.02
0.3	2.00	2.03	2.04	2.04	2.04
0.4	2.02	2.04	2.05	2.05	2.05
0.5	2.03	2.05	2.05	2.06	2.06
0.6	2.02	2.04	2.05	2.05	2.05
0.7	2.00	2.03	2.04	2.04	2.04
0.8	1.95	1.93	2.01	2.02	2.02
0.85	1.89	1.96	1.98	2.00	2.00
0.9	1.76	1.87	1.92	1.94	1.96

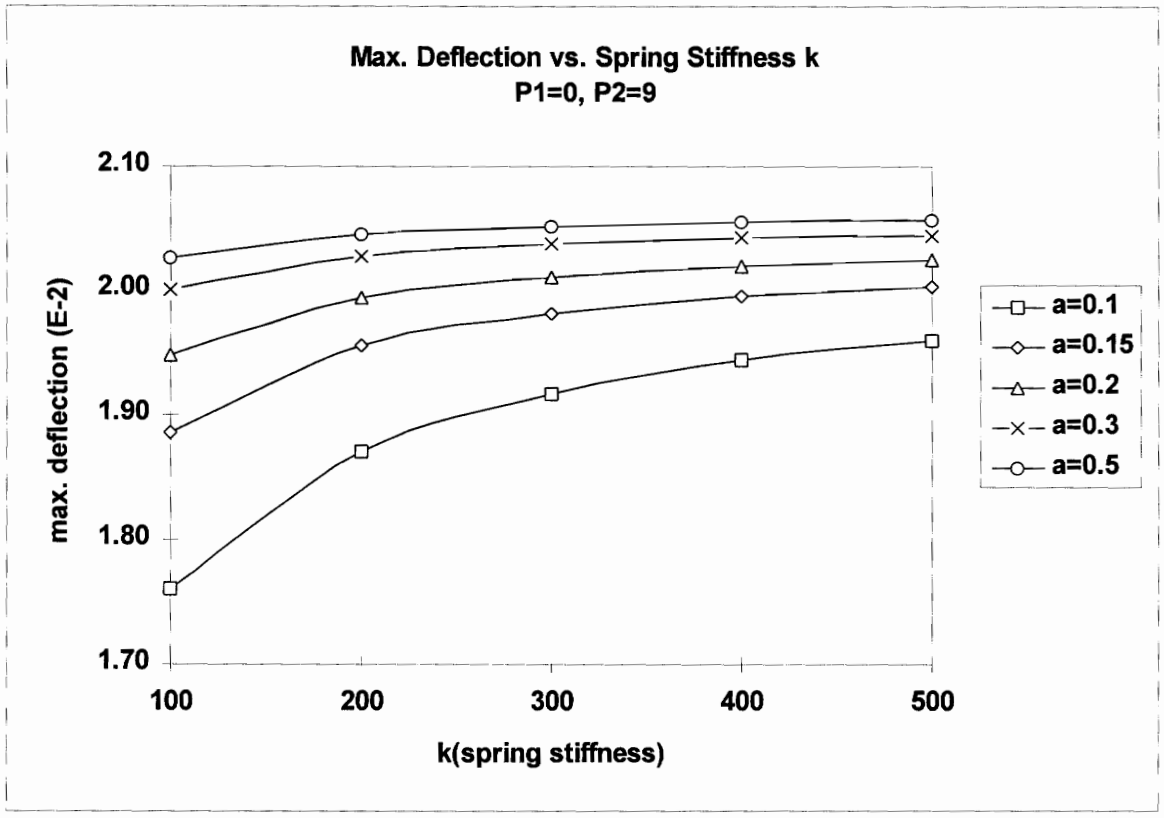

Fig. 4.6 Maximum deflection vs. spring stiffness k
$P_1 = 0,\ P_2 = 9$

a	k=100	k=200	k=300	k=400	k=500
0.1	1.76	1.87	1.93	1.98	2.01
0.2	1.95	2.07	2.12	2.15	2.17
0.3	2.06	2.16	2.20	2.23	2.24
0.4	2.12	2.21	2.25	2.26	2.28
0.5	2.14	2.22	2.26	2.27	2.28
0.6	2.11	2.20	2.24	2.25	2.27
0.7	2.02	2.13	2.17	2.20	2.21
0.8	1.84	1.98	2.05	2.08	2.10
0.9	1.95	1.77	1.71	1.78	1.83

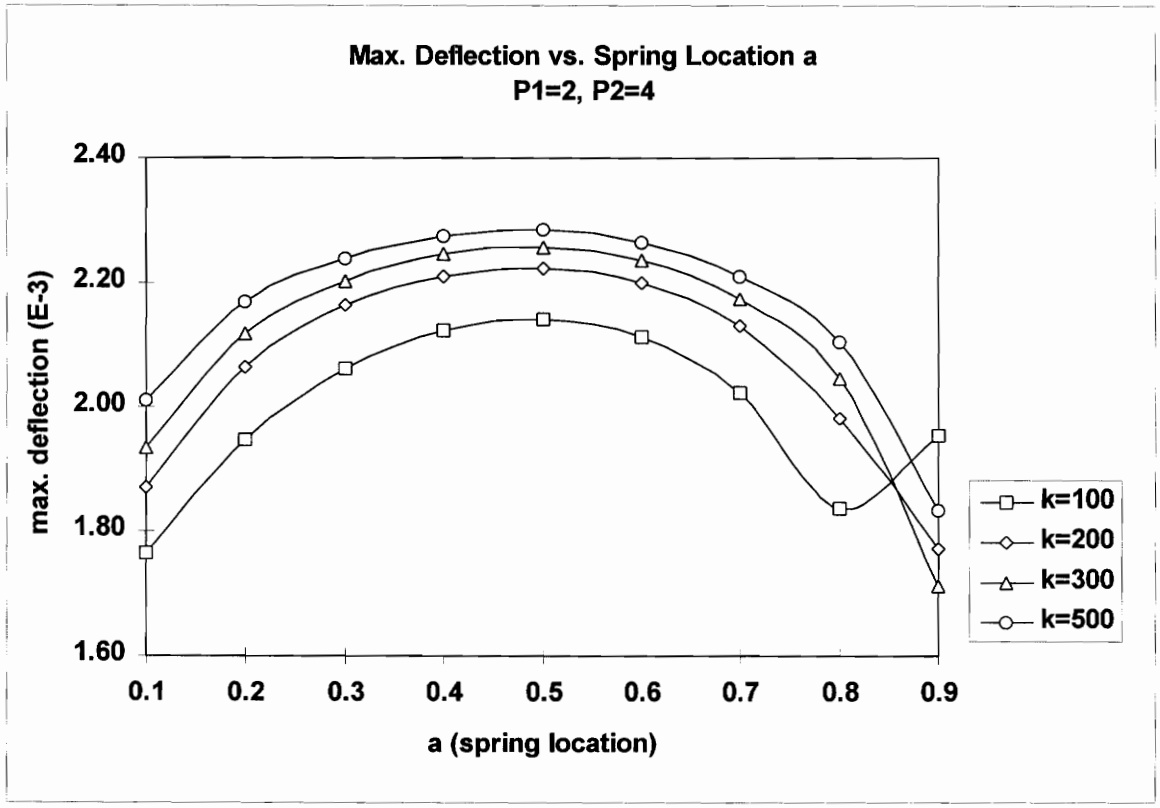

Fig. 4.7 Maximum deflection vs. spring location a
$P_1 = 2,\ P_2 = 4$

	k=100	k=200	k=300	k=400	k=500
a=0.1	1.76	1.87	1.93	1.98	2.01
a=0.15	1.86	1.98	2.05	2.08	2.11
a=0.2	1.95	2.07	2.12	2.15	2.17
a=0.3	2.06	2.16	2.20	2.23	2.24
a=0.4	2.12	2.21	2.25	2.26	2.28
a=0.5	2.14	2.22	2.26	2.27	2.28
a=0.6	2.11	2.20	2.24	2.25	2.27
a=0.7	2.02	2.13	2.17	2.20	2.21
a=0.8	1.84	1.98	2.05	2.08	2.10
a=0.85	1.70	1.84	1.93	1.98	2.01
a=0.9	1.95	1.77	1.71	1.78	1.83

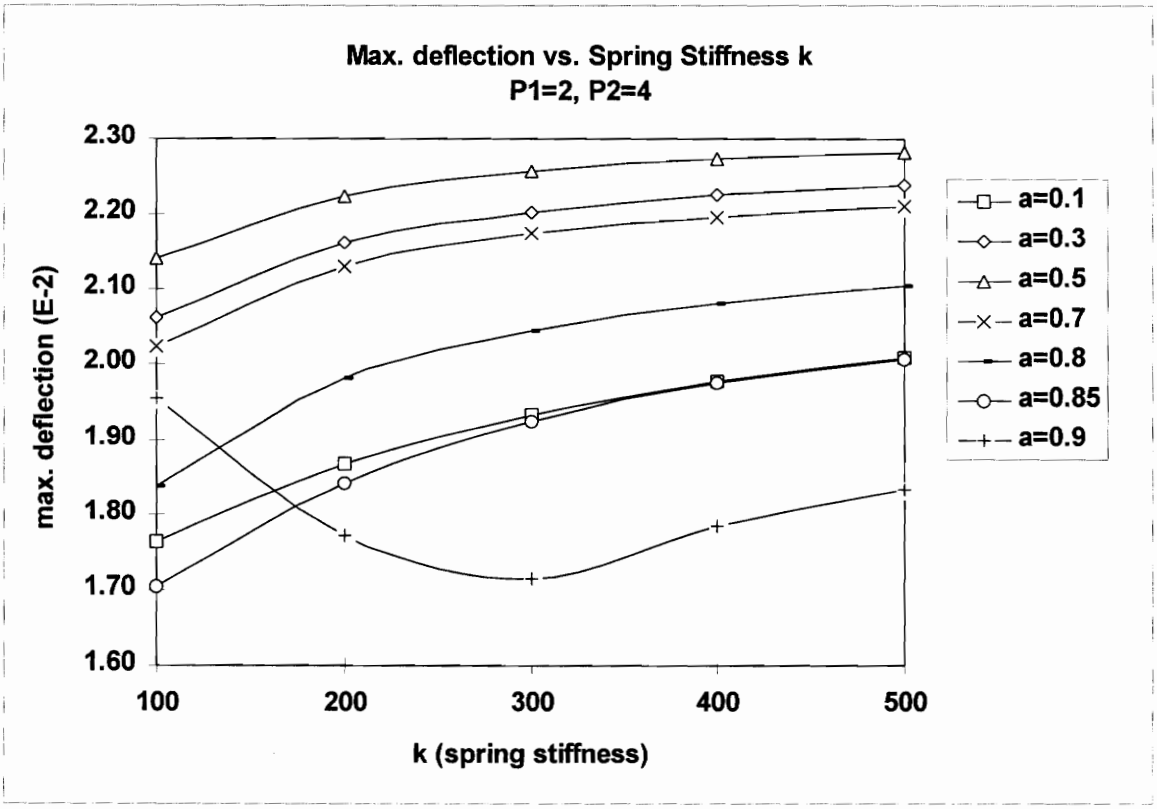

Fig. 4.8 Maximum deflection vs. spring stiffness k
$P_1 = 2,\ P_2 = 4$

a	k=100	k=200	k=300	k=400	k=500
0.1	1.68	1.81	1.89	1.94	1.98
0.2	1.87	2.02	2.09	2.13	2.15
0.3	2.00	2.13	2.18	2.21	2.23
0.4	2.07	2.19	2.23	2.25	2.27
0.5	2.09	2.20	2.24	2.26	2.27
0.6	2.05	2.16	2.21	2.23	2.24
0.7	1.91	2.06	2.12	2.15	2.17
0.8	1.80	1.82	1.92	1.97	2.01
0.9	2.73	2.32	2.10	1.96	1.87

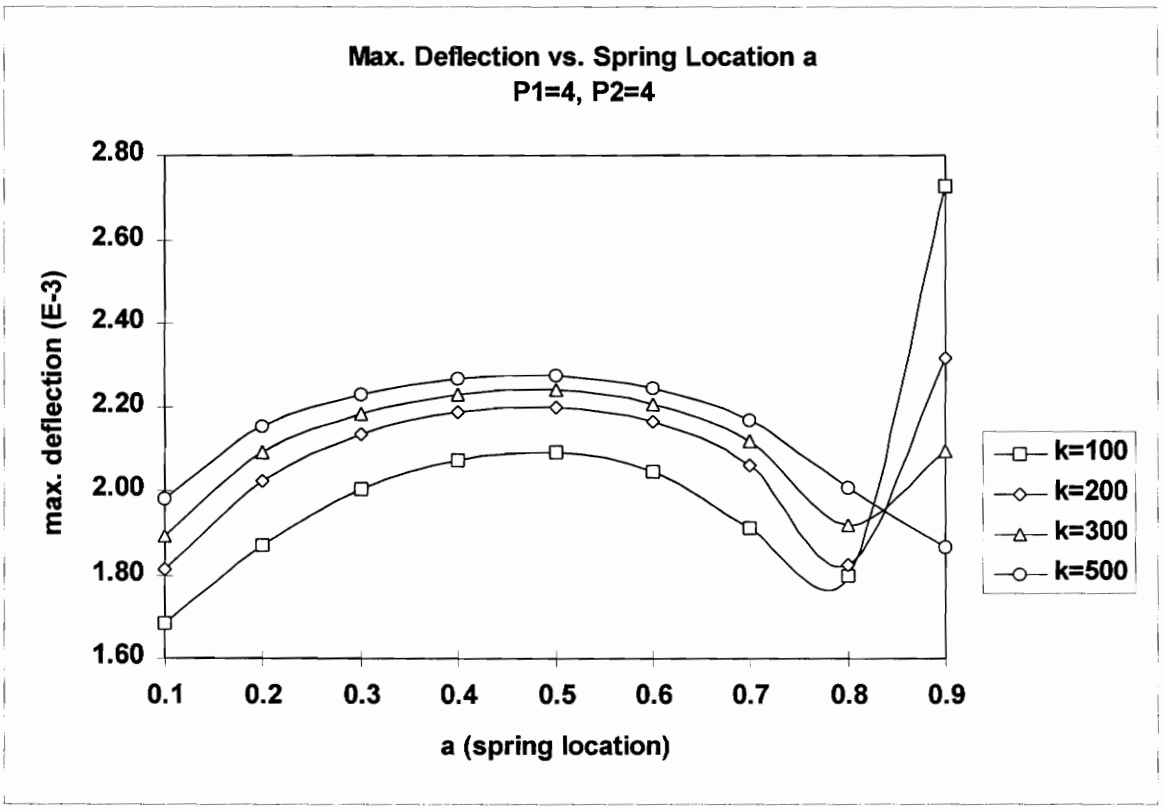

Fig. 4.9 Maximum deflection vs. spring location a
$P_1 = 4,\ P_2 = 4$

a	k=100	k=200	k=300	k=400	k=500
0.1	1.68	1.81	1.89	1.94	1.98
0.15	1.78	1.94	2.01	2.06	2.09
0.2	1.87	2.02	2.09	2.13	2.15
0.3	2.00	2.13	2.18	2.21	2.23
0.4	2.07	2.19	2.23	2.25	2.27
0.5	2.09	2.20	2.24	2.26	2.27
0.6	2.05	2.16	2.21	2.23	2.24
0.7	1.91	2.06	2.12	2.15	2.17
0.8	1.80	1.82	1.92	1.97	2.01
0.85	2.14	1.82	1.72	1.80	1.85
0.9	2.73	2.32	2.10	1.96	1.87

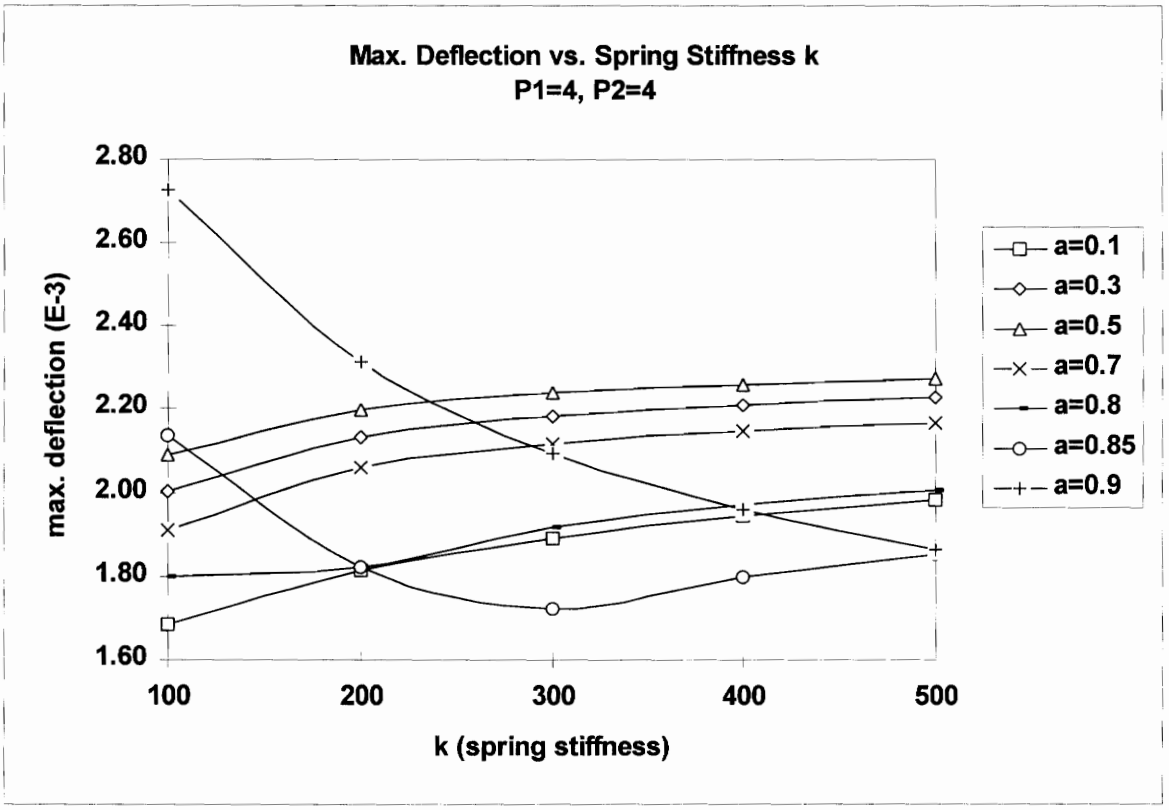

Fig. 4.10 Maximum deflection vs. spring stiffness k
$P_1 = 4,\ P_2 = 4$

a	k=100	k=200	k=300	k=400	k=500
0.1	1.31	1.26	1.29	1.31	1.33
0.2	1.26	1.33	1.37	1.39	1.40
0.3	1.31	1.38	1.41	1.43	1.44
0.4	1.34	1.41	1.43	1.45	1.46
0.5	1.35	1.41	1.44	1.45	1.46
0.6	1.32	1.39	1.41	1.43	1.44
0.7	1.27	1.32	1.36	1.38	1.39
0.8	1.46	1.34	1.29	1.27	1.29
0.9	1.85	1.71	1.62	1.56	1.51

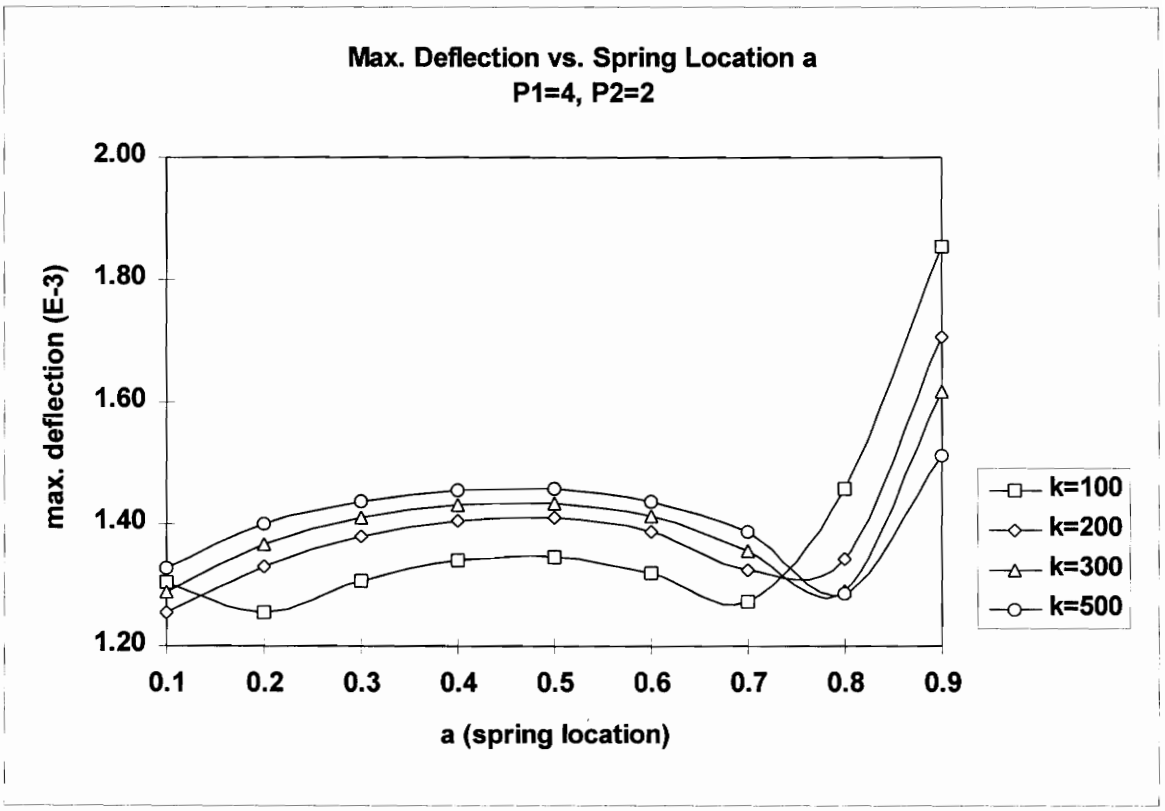

Fig. 4.11 Maximum deflection vs. spring location a
$P_1 = 4,\ P_2 = 2$

a	k=100	k=200	k=300	k=400	k=500
0.1	1.31	1.26	1.29	1.31	1.33
0.15	1.28	1.30	1.33	1.36	1.37
0.2	1.26	1.33	1.37	1.39	1.40
0.3	1.31	1.38	1.41	1.43	1.44
0.4	1.34	1.41	1.43	1.45	1.46
0.5	1.35	1.41	1.44	1.45	1.46
0.6	1.32	1.39	1.41	1.43	1.44
0.7	1.27	1.32	1.36	1.38	1.39
0.8	1.46	1.34	1.29	1.27	1.29
0.85	1.62	1.48	1.41	1.37	1.34
0.9	1.85	1.71	1.62	1.56	1.51

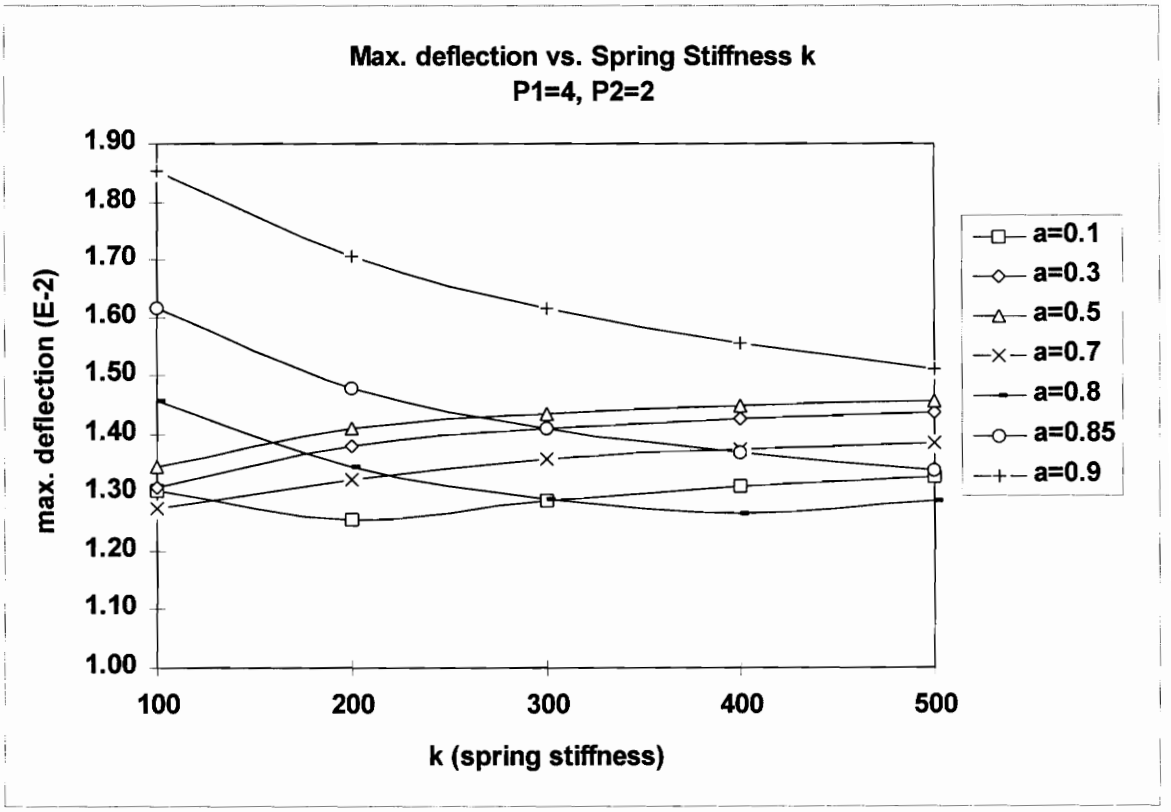

Fig. 4.12 Maximum deflection vs. spring stiffness k
$P_1 = 4,\ P_2 = 2$

4.1.3 Damping effects

The damping effect on the dynamic response of the column is investigated. A damping coefficient of 1% of the critical damping is applied in both Galerkin's method and ABAQUS, and their results are compared to each other.

a. Galerkin's method

The coefficients of viscous and viscoelastic damping are specified, and the decaying motions of the column are obtained with these coefficients. The responses of the column with damping are investigated as functions of time, and the results from Galerkin's method are compared to those from the finite element method using ABAQUS.

The damping ratio, ξ, is generally defined as the ratio of damping to critical damping, $\frac{c}{c_{cr}}$. Once the damping ratio is specified, the actual coefficient of damping can be calculated. The deflection variation is traced using the Galerkin method. As explained in section 4.1.2 (Table 4.1, and Fig. 4.1), the dynamic response of the column is dominated by the first mode. If the axial loads and the initial deflection of the column are neglected, and if only the first mode is considered, the equation of motion becomes

$$d_{11}\ddot{a}_1(t) + f_{11}\dot{a}_1(t) + g_{11}a(t) = 0 \qquad (4.10)$$

By applying the eigenfunction as $\sin(\pi x)$, we have

$d_{11} = 0.5$, $f_{11} = 0.5\pi^4\eta + 0.5\beta$, and $g_{11} = 0.5\pi^4$.

The critical damping for equation (4.10) is $c_{cr}=2\sqrt{d_{11}g_{11}}=(f_{11})_{cr}$. If a damping ratio of 1% is used in the analysis, we have the following relationship;

$$\pi^4\eta+\beta=0.02\pi^2 \tag{4.11}$$

b. ABAQUS

ABAQUS uses Rayleigh damping with the direct integration method [24]. For the single-degree-of-freedom equation of motion $m\ddot{u}+c\dot{u}+ku=0$, Rayleigh damping defines the damping as $c=\overline{A}m+\overline{B}k$, where $\overline{A}$ is the mass damping factor and $\overline{B}$ is the stiffness damping factor. The critical damping is expressed as $c_{cr}=2m\omega_n=2\sqrt{mk}$, where $\omega_n=\sqrt{k/m}$, the undamped natural frequency.

By combining these equations, we can get the damping ratio, ξ :

$$\xi=\frac{c}{c_{cr}}=\frac{\overline{A}}{2\omega_n}+\frac{\overline{B}\omega_n}{2}. \tag{4.12}$$

With this relationship, $\overline{A}$ and $\overline{B}$ are to be selected.

c. Calibration of damping coefficients

For the system in Fig. 4.13, if the external load is not considered, the equation of motion becomes

$$EI\overline{w}''''+\mu A\ddot{\overline{w}}=0 \tag{4.13}$$

where μ = the mass per unit volume and A= area of the column section.

The natural frequencies for the simply supported column are

$$\omega_n = \left(\frac{n\pi}{L}\right)^2 \sqrt{\frac{EI}{\mu A}}, \; n = 1,2,3,\ldots \tag{4.14}$$

If the first natural frequency is considered as the major factor, we can assume

$$\omega_n = \omega_1 = \left(\frac{\pi}{L}\right)^2 \sqrt{\frac{EI}{\mu A}}. \tag{4.15}$$

When material properties, geometry, and the loading are as follows,

$$E=29000 \text{ ksi}, \; I = 49.052 \text{in}^4,$$

$$L=240 \text{ in}, \; Q_2 = 170 \text{kips},$$

$$A = 11.61 \text{in}^2, \; \mu = 7.3 \times 10^{-7} \text{klbf} \cdot \text{s}^2 / \text{in}^4$$

we have $\omega_1 = 70.2129$ rad/sec.

By assigning 1% of the critical damping to the ABAQUS model and substituting the natural frequency into equation (4.12) , we have

$\overline{A} = 0.7725$ when $\overline{B} = 0.0$, and $\overline{B} = 2.848 \times 10^{-4}$ when $\overline{A} = 0.0$.

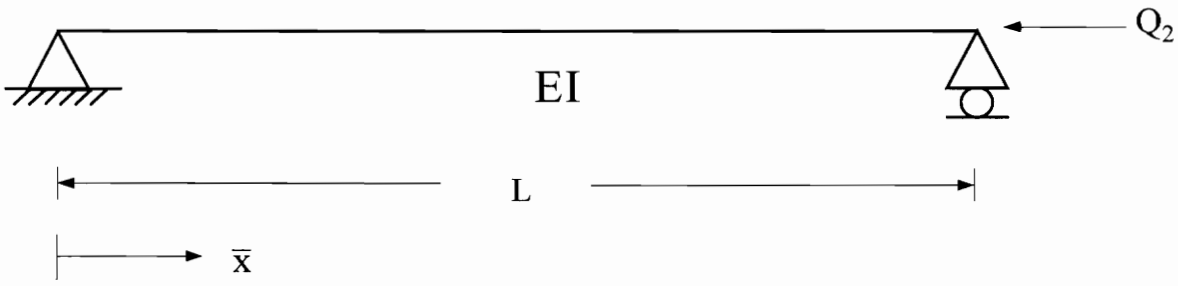

Fig. 4.13 Simply supported column

The following cases are tested and compared .

case 1:

Galerkin method : $\eta = 0$, $\beta = 0.1974$

ABAQUS : $\overline{A} = 0.7725$, $\overline{B} = 0.0$

case 2:

Galerkin method : $\eta = 0$, $\beta = 0.1974$

ABAQUS : $\overline{A} = 0.0$, $\overline{B} = 2.848 \times 10^{-4}$

Those damping parameters provide one percent of critical damping to both methods.

d. Comparison

The results from ABAQUS are tested for different numbers of elements and time steps, and compared to those of Galerkin's method. The motions from Galerkin's method are evaluated taking three terms in the deflection series.

In Fig. 4.14, the ABAQUS discretization is checked by investigating the motion of the midpoint of column. The ABAQUS dynamic analysis reduces to Newmark's method if the parameter α is chosen to be zero, as in this study. The parameters γ and β in Newmark's equations are taken as 1/2 and 1/4, respectively. These values provide constant average acceleration in every time increment [24-27]. When the system conditions are k=100, a=0.4, and $Q_2 = 170$ kips, and no damping is applied, no big

differences exist in the maximum deflection for 20 elements and for 40 elements. To save computational cost, 20 elements are selected in the analysis.

In the dynamic analysis, the magnitude of the time step is an important factor for numerical integration. The period of the motion is affected by the size of the time step, and by decreasing the time step, the period error can be reduced [28]. Figure 4.15 shows the motion of the column at x=0.5; the solid line represents Galerkin's method, and the dotted line and dashed line are for ABAQUS with time steps 0.01 and 0.02 seconds, respectively. As shown in Fig. 4.15, the time step of 0.01 second is small enough to provide a good approximation to the results from Galerkin's method. In this study, a time step of 0.002 seconds is used to provide more reliable results.

In Fig. 4.16, the damping effects in ABAQUS are investigated. The dashed line corresponds to case 1 where $\overline{A} = 1.4043$ and $\overline{B} = 0.0$, and the solid line represents case 2 where $\overline{A} = 0.0$, $\overline{B} = 2.848 \times 10^{-4}$. The results show that the two lines are identical during motion, so different combination of $\overline{A}$ and $\overline{B}$ can be used to provide one percent of critical damping to the system.

The results of Galerkin's method and ABAQUS are compared in Fig. 4.17. One percent of critical damping is given to both methods, and decaying motions are investigated. After a few cycles, compared to Galerkin's method, some delay in period is detected in ABAQUS. This is due to the size of the time step. If a smaller time step is

used and more terms in Galerkin's method are considered, the difference between the periods can be reduced.

For the axial loading case, the natural frequency is found as

$$\omega_n = \left(\frac{n\pi}{L}\right)^2 \sqrt{\frac{EI}{\mu A}} \sqrt{1 - \frac{P}{P_{cm}}} \tag{4.16}$$

where $P_{cm} = \dfrac{n^2\pi^2 EI}{L}$ = n-th buckling load [29].

According to equation (4.16), as the magnitude of the axial load P increases, the frequency squared, ω^2, is decreased linearly. The vibration frequencies for the axial load P are easily calculated by equation (4.15). With the properties in equation (4.14), we have $P_{cr1} = 243.74$ kips .

The first natural frequency (at P_1=0) is $\omega_1 = 38.626$ rad/sec. Finally, the natural period of this system is $T_1 = 2\pi / \omega_1 = 0.1627$ second. Figure 4.18 shows the periods for each method. After one cycle, time intervals are checked between lowest deflection points. The periods for Galerkin's method and ABAQUS are 0.166 and 0.164 second, respectively. They show a good approximation, as expected, with the exact analysis. Small differences may be caused by the initial deflection of the column and numerical error. It can be concluded that the ABAQUS model is reliable in the dynamic elastic analysis, and this model will be used in the dynamic plastic analysis.

When one percent of the critical damping is applied, the maximum deflection from the damped system is about 2% lower than the result from the undamped system (Fig. 4.19).

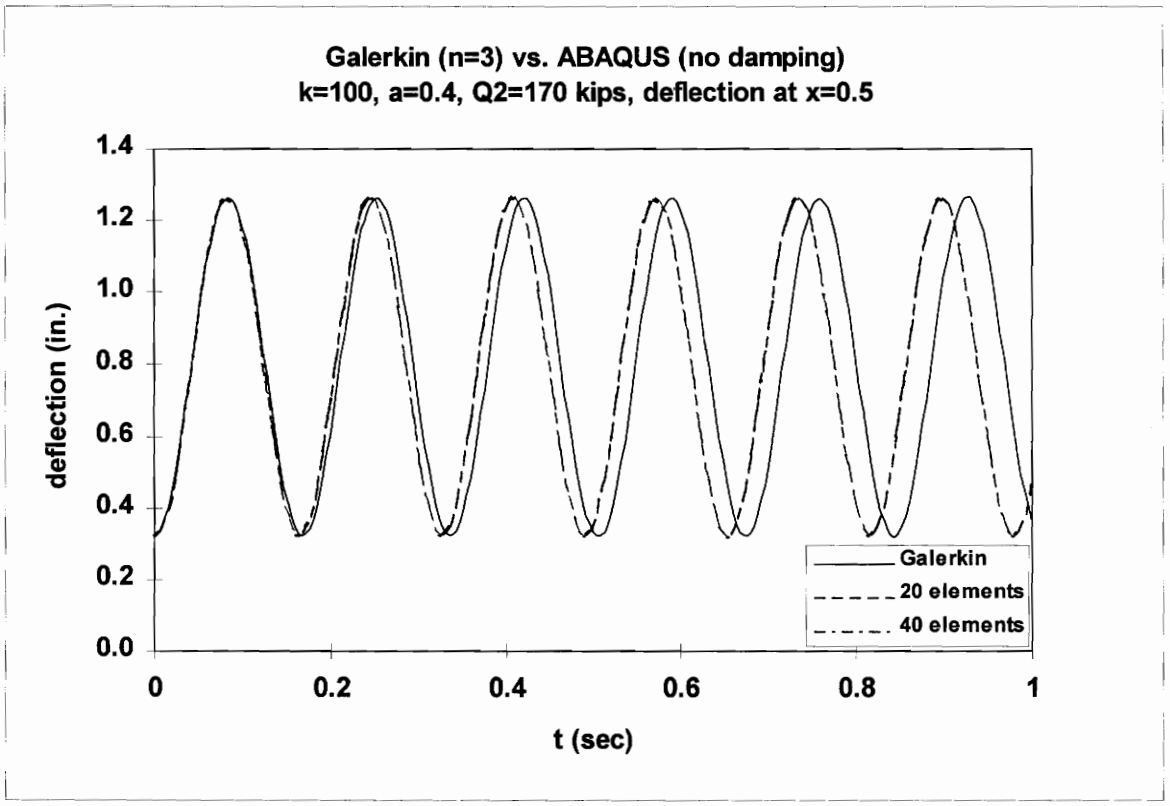

Fig. 4.14 The motions of the column at x=0.5 for Galerkin, ABAQUS 20-element model, and ABAQUS 40-element model.

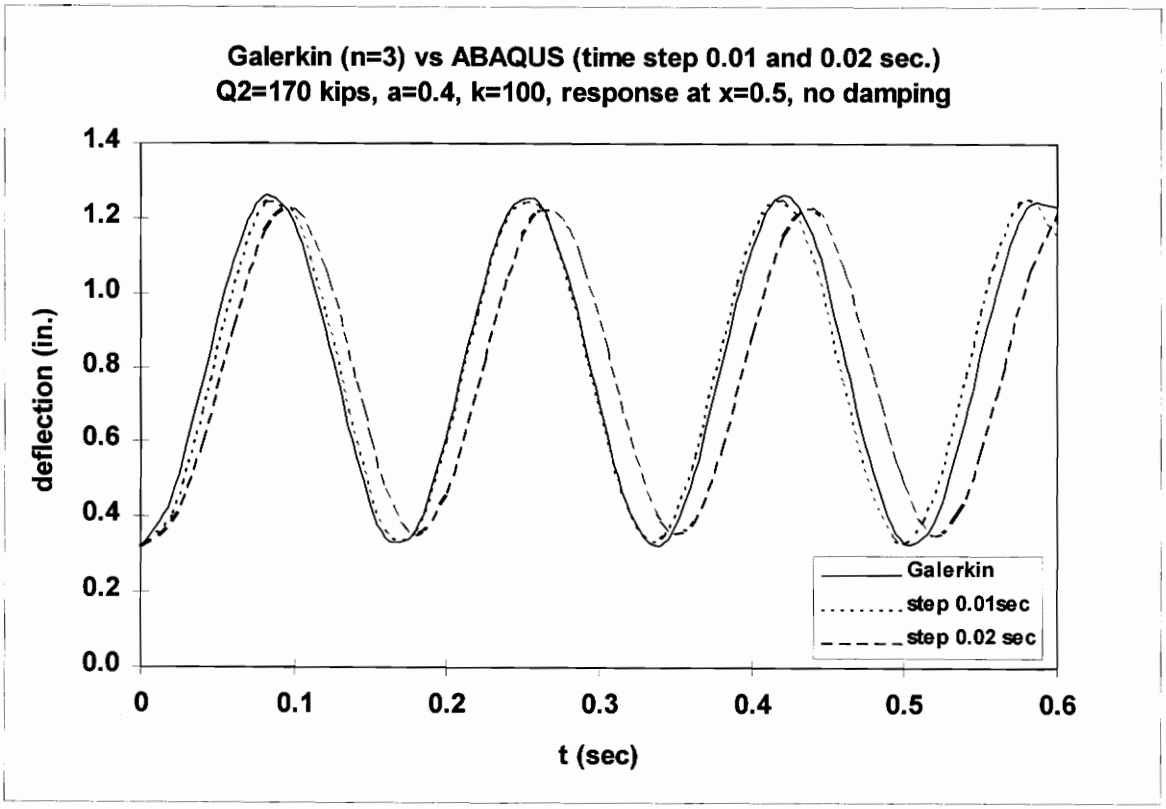

Fig. 4.15 Galerkin(n=3) vs. ABAQUS (time step 0.01 and 0.02 second) response at x=0.5, Q_2 =170 kips, k=100, a=0.4, no damping

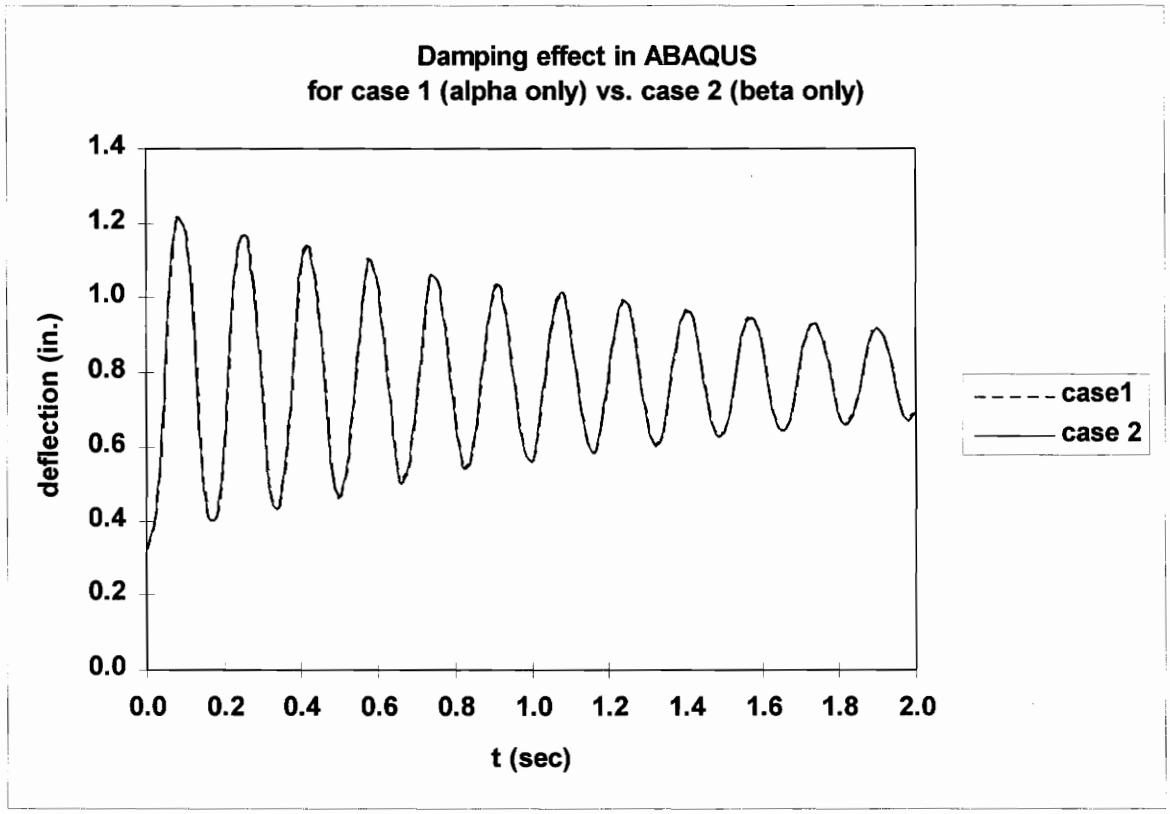

Fig. 4.16 The damping effects in ABAQUS

case 1 : $\overline{A}$ =1.4043, $\overline{B}$ =0

case 2 : $\overline{A}$ =0.0, $\overline{B} = 2.848 \times 10^{-4}$

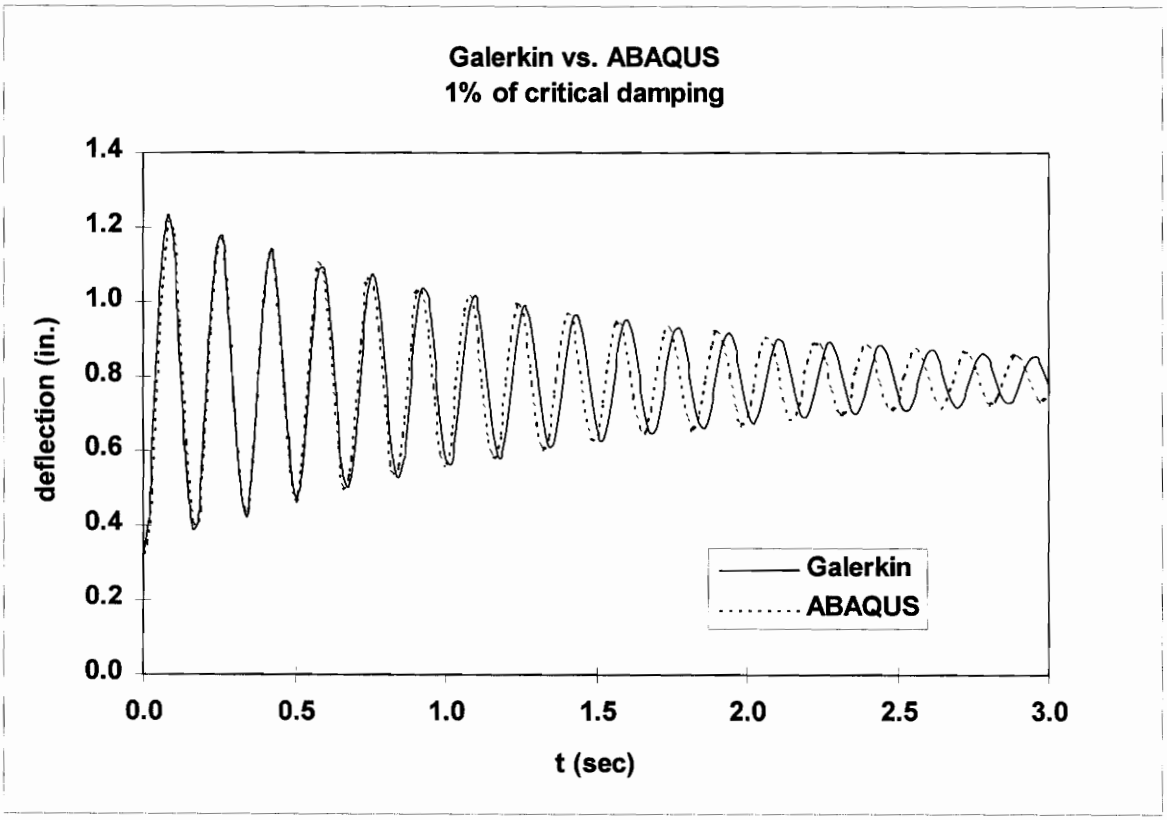

Fig. 4.17 Galerkin (n=3) vs. ABAQUS with 1% of critical damping;
response at x=0.5, Q_2=170 kips, a=0.4, k=100
($\overline{A}$: alpha, $\overline{B}$: beta in ABAQUS notation)

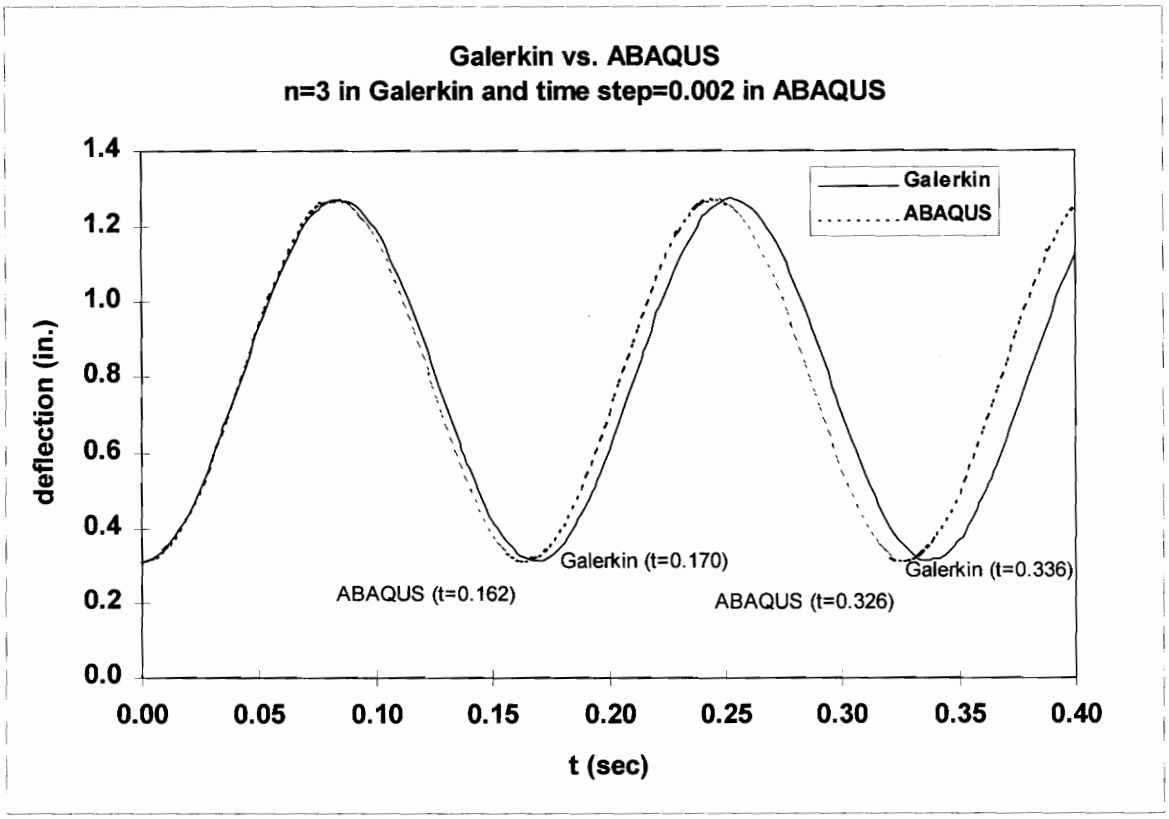

Fig. 4.18 Comparison for period,
response at x=0.5, Q_2=170 kips, a=0.4, k=100

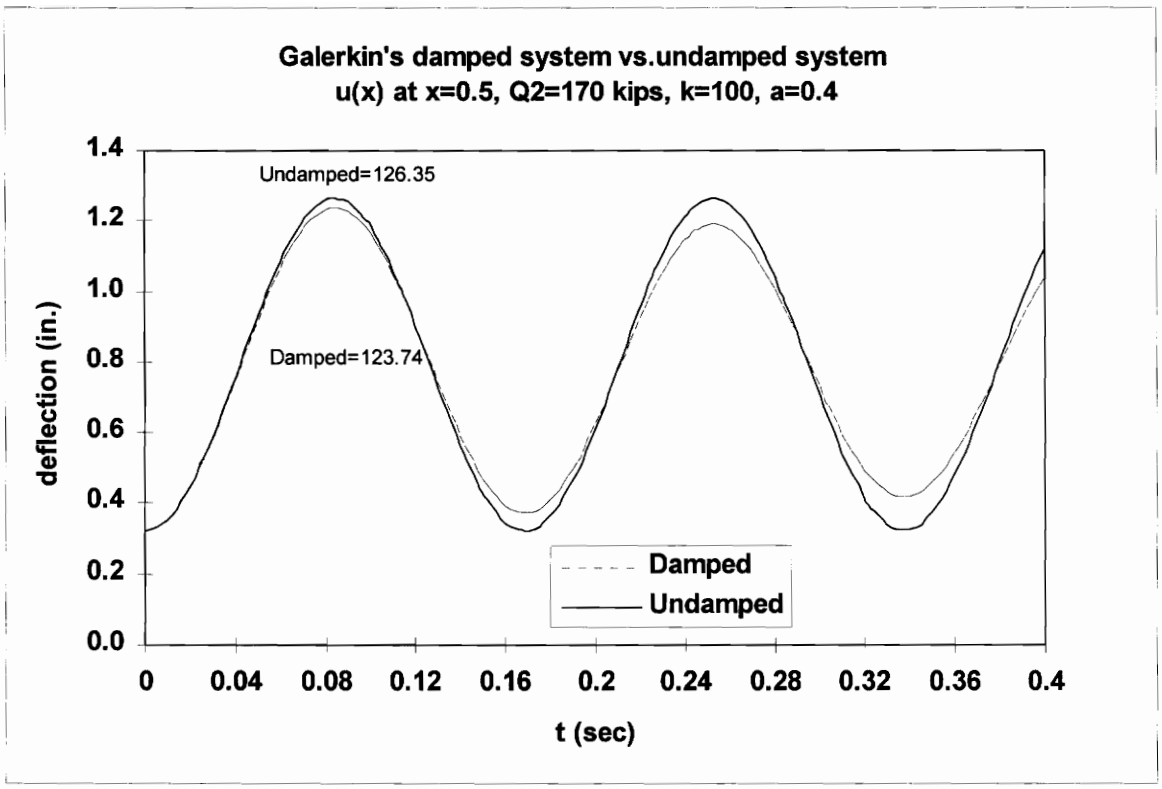

Fig. 4.19 The effect of damping on the deflection

4.2 Plastic analysis based on ABAQUS

Plastic zone analysis (or the distributed plasticity method) is the most comprehensive method to verify actual structural behavior [23]. In this analysis, the structure is discretized into multiple elements along the length and the stress-strain response can be monitored at a certain number of points throughout each elements. The spread of plasticity can be represented during both static and dynamic response of the structure.

To support plastic zone analysis, the program ABAQUS is used. This program has the ability to analyze three-dimensional models, and can display member performance. The actual residual stresses and the geometrical initial imperfections can be applied directly. According to Englekirk [30], a long column is dominated by the initial deformation and a short column will be affected most by the residual stresses.

Both initial deflection and residual stresses are included in the analysis, and the effect of damping on the column is also examined. A loading condition is selected to cause the plasticity in the column. To study the effects of the bracing location and the bracing stiffness on the column behavior, for cases with and without residual stresses, the maximum deflections during motion are sought and compared.

For some loading conditions, the effects of the spring location on the spread of the plasticity in the column are studied. Due to the size of the problem, using a workstation is not adequate. In this section, an IBM SP-2 computer is used.

4.2.1 Geometry and section profile in ABAQUS

The geometry, member and material properties, and loading are shown in Figs. 3.9 and 3.10. A 240 inch-long wide flange column ($W8 \times 40$) is selected and modeled with different values of a, k, and load. To provide residual stresses to the column section, eleven and three integration points are assigned to each flange and the web, respectively (Fig. 4.20).

The AISC specification defines the slenderness parameter , λ_c, as

$$\lambda_c = \frac{KL/r}{\pi}\sqrt{\frac{\sigma_y}{E}}$$

where K: the effective length factor

r: the least radius of gyration of the section

σ_y: the yield stress,

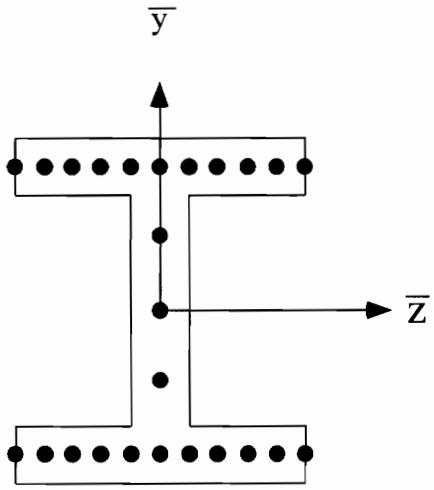

Fig. 4.20 The integration points in the column cross section

and defines the boundary between elastic and inelastic columns as λ_c=1.5.

If the column in Fig. 3.10 loses its bracing, by substituting the column properties, the slenderness parameter ,λ_c, is obtained as the value 1.32. This parameter is smaller than the boundary value, and this column exhibits inelastic behavior when it buckles. A 20-element model is selected with time step t=0.002 second for the ABAQUS dynamic analysis. Its accuracy was already verified in sections 3.4.3 and 4.1.3.

4.2.2 Residual stress distribution

As stated before, the strength of the column is affected by the residual stresses, as well as the initial imperfection of the column. Especially in the plastic analysis, the effects of residual stresses should be considered. Since at some position of the column the induced stresses due to the loads, along with residual stresses, may exceed the yield stress, an unexpected failure could occur. Residual stresses generally result from the uneven cooling or cold bending or welding, and their distribution depends largely on the type of cross section. The residual stresses in the I-section column are assumed to follow the distribution proposed by Galambos and Ketter [31] where the maximum compressive residual stress at the flange tips is $0.3\sigma_y$ (Fig. 4.21). The quantities σ_{rc} and σ_{rt} denote residual stresses in compression and tension, respectively.

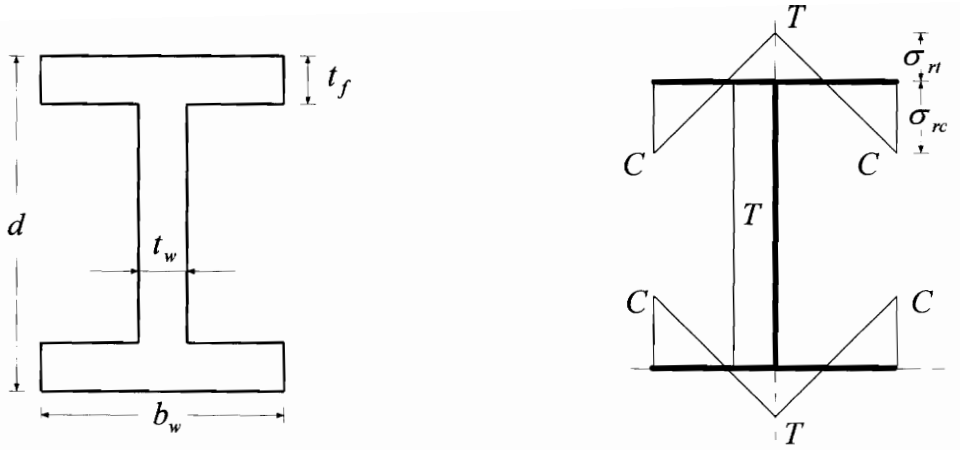

$$\sigma_{rc} = 0.3\sigma_y$$

$$\sigma_{rt} = \left[\frac{b_w t_f}{b_w t_f + t_w(d - 2t_f)}\right]\sigma_{rc}$$

Fig. 4.21 Residual stress distribution

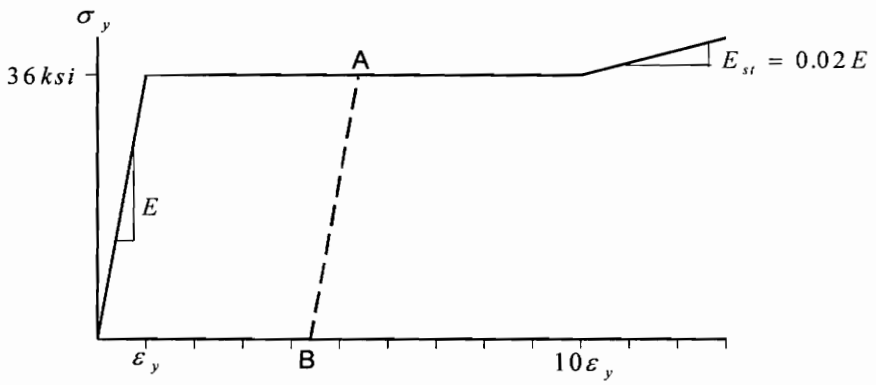

Fig. 4.22 Stress-strain relationship

In ABAQUS, residual stresses are stored in the integration points of the column section as the initial stress field. User subroutine SIGNI is used for this process with the option *INITIAL CONDITION, TYPE=STRESS, USER.

4.2.3 Material constitutive relationship

The amplitude of the strain in a compressed column depends on the magnitude of loading and supporting conditions. As the compressive load is increased, the strain in the column grows approximately linearly, and at a certain point, yielding is initiated. The stress-strain relationship in Fig. 4.22 is used in the plastic zone analysis. The modulus of elasticity is quantified for steel as 29000 $kips / in^2$, and the nominal strain at yield, ε_y, is F_y / E or 0.00124 for A36 steel. Strain hardening is assumed to occur if the strain is larger than $10\varepsilon_y$, and the strain-hardening modulus E_{st} is taken as 2% of E.

4.2.4 Plasticity and strain hardening

The model in Fig. 3.10 (a 20-element model) with k=100 and varying loads is tested to check if any strain hardening and plastic behavior occur after the sudden loss of bracing. Based on the LRFD manual [21], the design strength of an A36 $W8 \times 40$ column is 173 kips if no bracing between the column ends is considered. For a load slightly lower than the design strength, the strains at some part of the column may exceed the yield strain for a short period of time without the entire failure of the column. For a load above

the design strength, the column becomes unstable during motion, and plastic yielding and strain hardening can be expected. To investigate the response of the column, two loading conditions, 170 kips and 190 kips, are applied.

When the column loses its bracing, the maximum deflection occurs at x=0.5 if the spring location is a=0.5. During motion, the strains and stresses of the flange tip at the midpoint of the column, where their maximum values are expected, are checked with a time interval of t=0.002 second, and are plotted.

In Figs. 4.23 and 4.24, the results for the end load of 170 kips are presented, where the internal load is not included. The effects of the residual stress are considered and their results are shown in Figs. 4.25-4.27 for the load of 170 kips. In ABAQUS, residual stresses are given to each integration point of the column section, and the equilibrium state is checked. The distribution of residual stress in Fig. 4.21 provides the equilibrium of the column. From the numerical errors, small deflections due to applied residual stresses are detected, but the magnitude of deflection is so small that it can be neglected in the analysis. The motions of the center of the column are presented in Fig. 4.28 for the load of 170 kips with and without residual stresses. The results for the load of 190 kips are shown in Figs. 4.29 and 4.30.

With these figures, some explanations regarding the plastic behavior and strain hardening can be given as follows:

1. For $Q_2 = 170$ kips without residual stresses, Fig 4.23 shows the strain changes during motion. If the vibration is assumed to be a harmonic or decaying motion, the strain

at the first peak is the maximum value. The calculated strain value at that point is less than the yield strain, so the plasticity spread is not present. Since damping effects are not included, the column keeps vibrating with the harmonic motion.

2. For $Q_2 = 170$ kips with residual stresses, if the column contains residual stresses, the responses of the column show different features. Due to the additional compressive residual stress at the flange tip, the strain at the flange tip exceeds the yield strain (Fig. 4.25), and yielding occurs. Figure 4.26 shows the plasticity effect. When the strain exceeds the yield strain, the value of the stress remains constant (the yield stress). After the first maximum, the column unloads elastically and this stress becomes less than the yield stress again. However, during the second cycle, the stress does not reach the yield stress. The relation between the stress and the strain corresponding to this motion is shown in Fig. 4.27a and Fig. 4.27b. The first peak of the strain curve (point A in Fig. 4.27a) is 14.578×10^{-4}, at t=0.102 second. The strain at the second peak (point B in Fig. 4.27a) is 14.566×10^{-4}, at t=0.264 second. The maximum strain occurs at the first peak, and the response of the column becomes elastic after the first cycle. Its path in the stress and strain relationship then lies on the line AB in Fig. 4.22 or Fig. 4.27b.

In Fig. 4.27a, the strain reaches its yield value at t=0.068 second, but the yield stress is reached earlier (it occurs at t=0.040 second). At the point C in Fig. 4.27b where the stress reaches its yield value (36 ksi), the strain is 8.8×10^{-4} and is below the yield

strain (12.4×10^{-4}). This happens due to residual stresses which cause additional compressive stress at the flange tip.

3. For $Q_2 = 190$ kips without residual stresses, Fig. 4.29 shows that the strain keeps rising during motion. As a result, the column collapses after a short time. The stress change is shown in Fig. 4.30. Before the strain reaches $10\varepsilon_y$, stresses remain constant at the yield stress (36 ksi). After that, since stresses are governed by the strain hardening modulus, E_{st}, stresses become higher than σ_y. Finally, the column collapses.

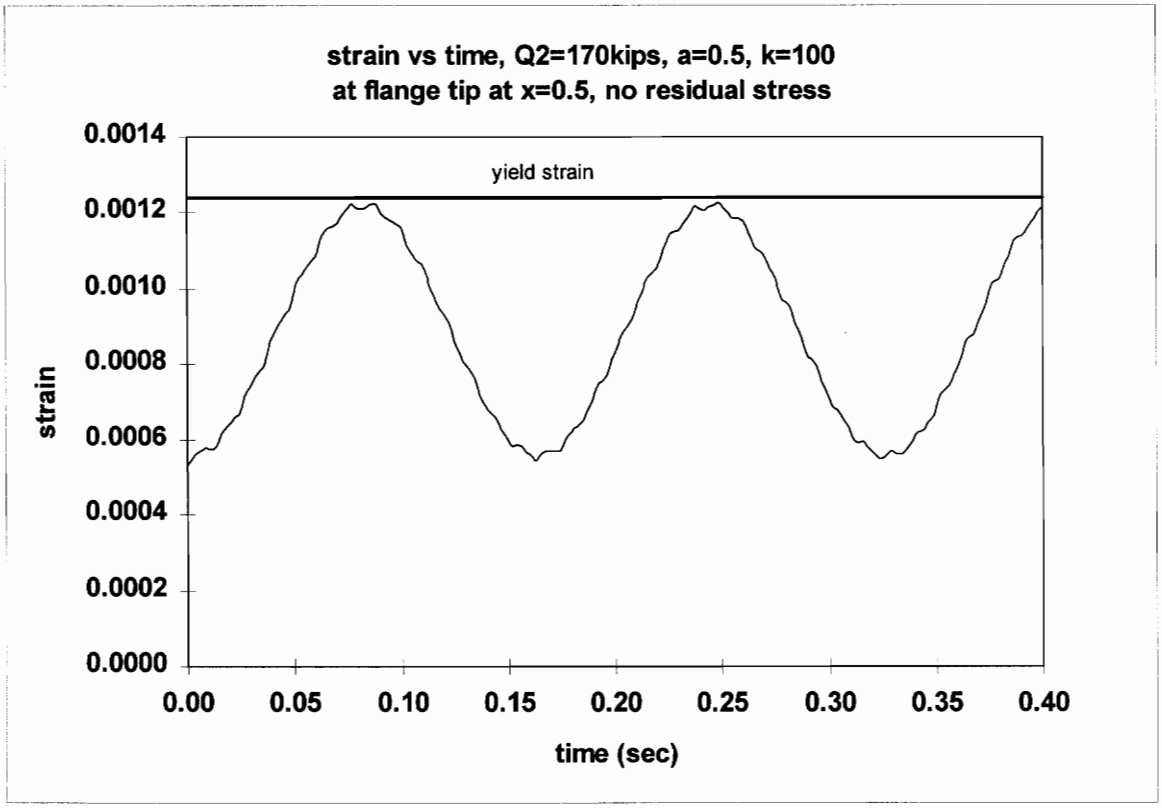

Fig. 4.23 Strain vs. time, Q_2=170 kips, a=0.5, k=100
at flange tip at x=0.5, no residual stress

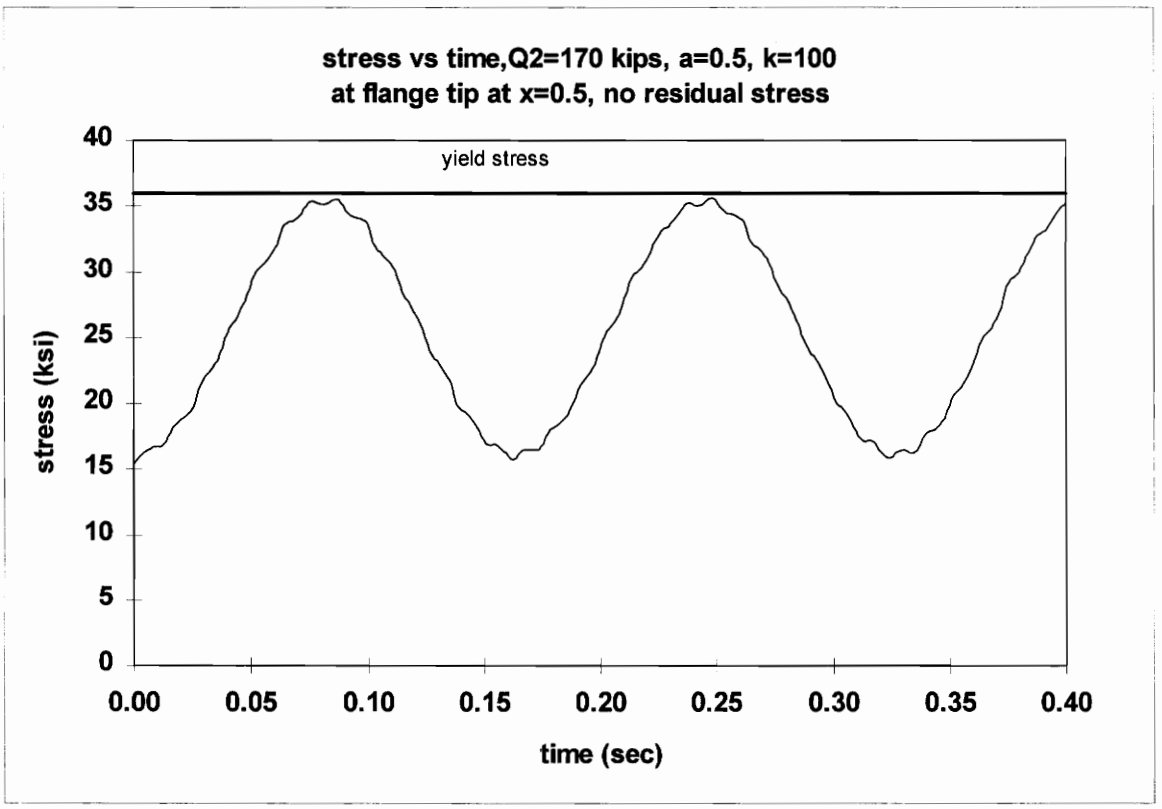

Fig. 4.24 Stress vs. time, Q_2=170 kips, a=0.5, k=100
at flange tip at x=0.5, no residual stress

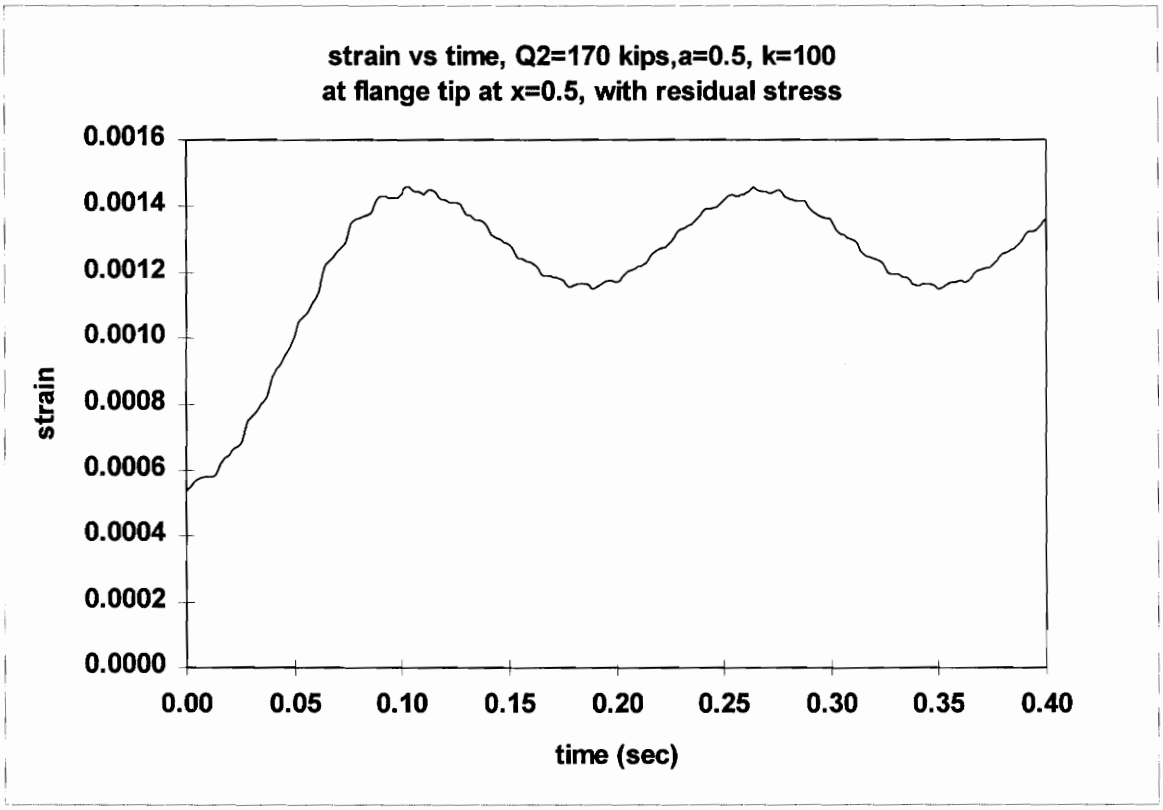

Fig. 4.25 Strain vs. time, Q_2=170 kips, a=0.5, k=100
at flange tip at x=0.5, with residual stress

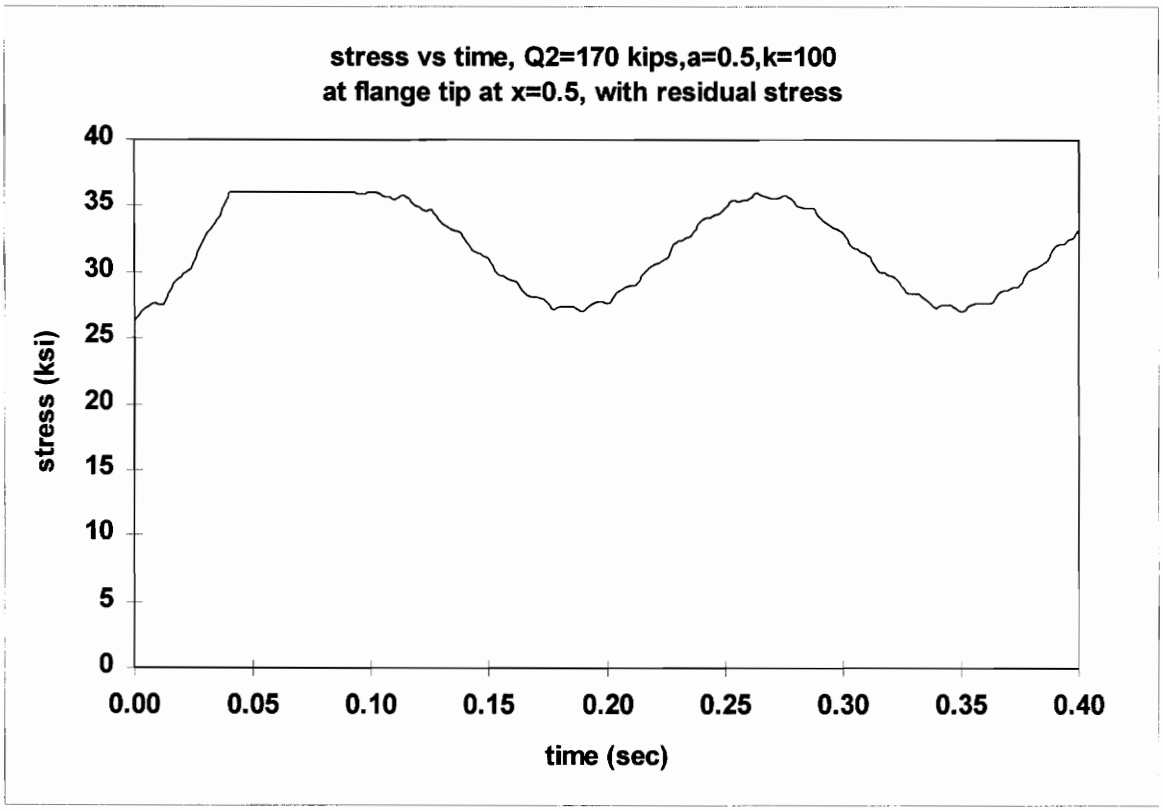

Fig. 4.26 Stress vs. time, Q_2=170 kips, a=0.5, k=100
at flange tip at x=0.5, with residual stress

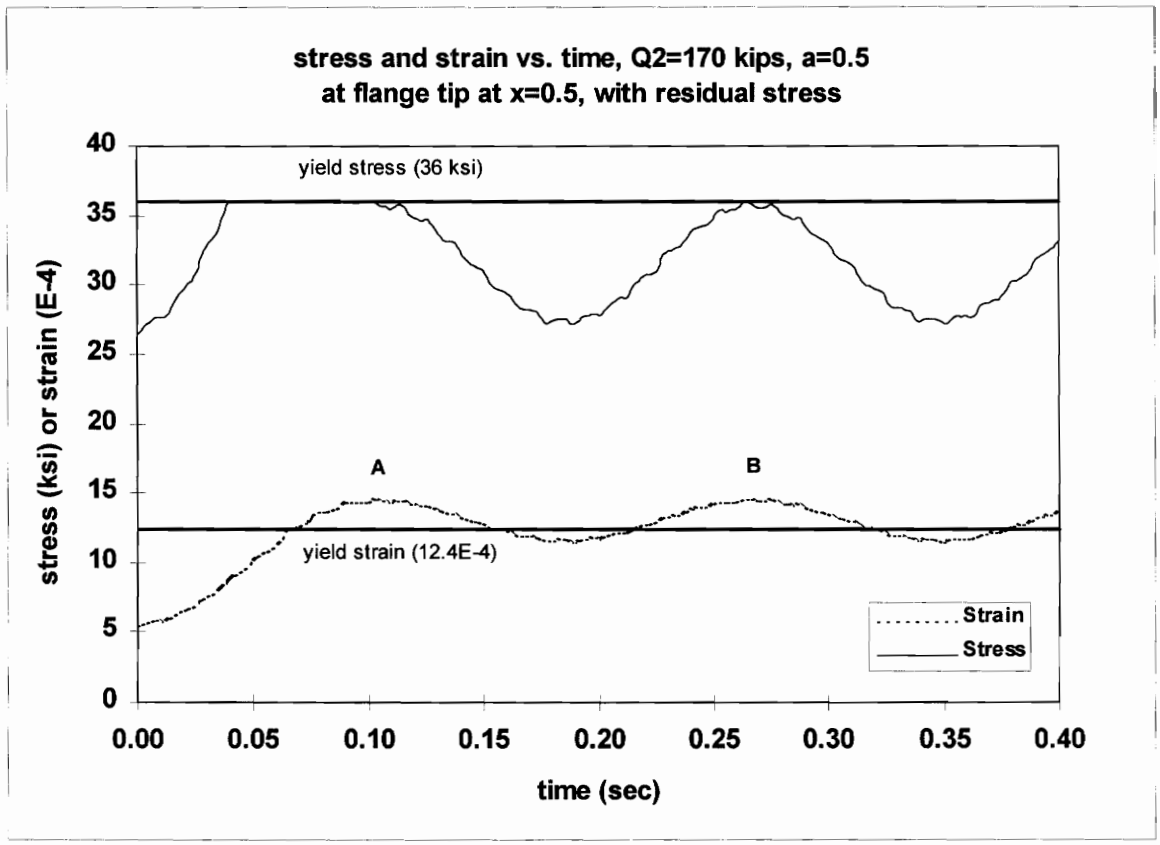

Fig. 4.27a Stress and strain vs. time, Q_2=170 kips, a=0.5, k=100
at flange tip at x=0.5, with residual stress

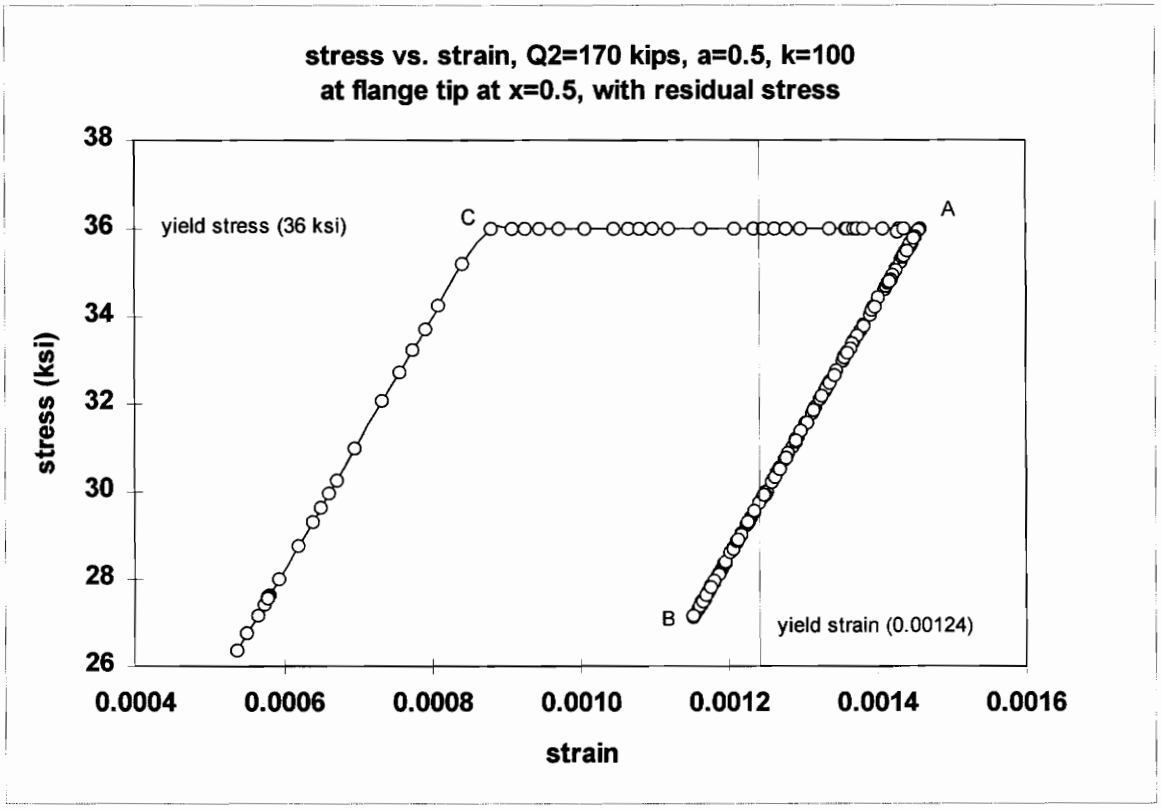

Fig. 4.27b Stress vs. strain, Q_2=170 kips, a=0.5, k=100 at flange tip at x=0.5, with residual stress

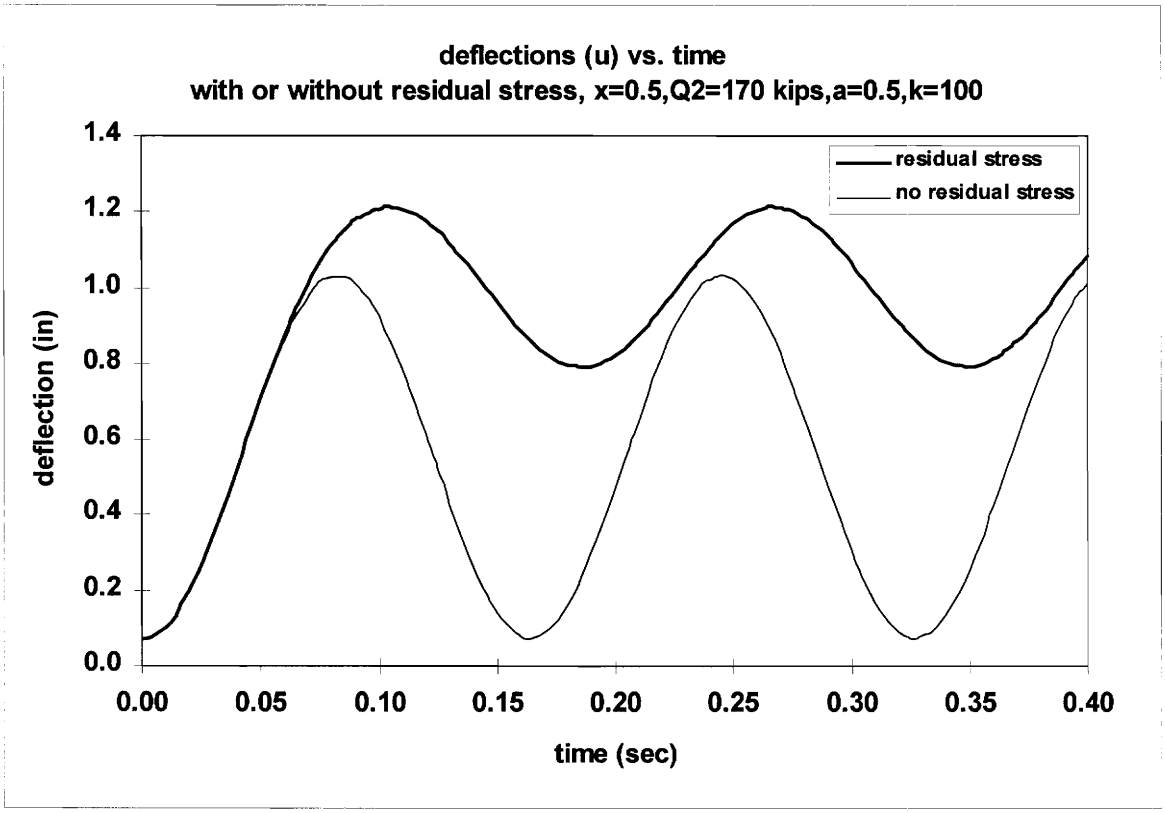

Fig. 4.28 Deflection u(x) vs. time
with or without residual stress, x=0.5, Q_2=170 kips, a=0.5, k=100

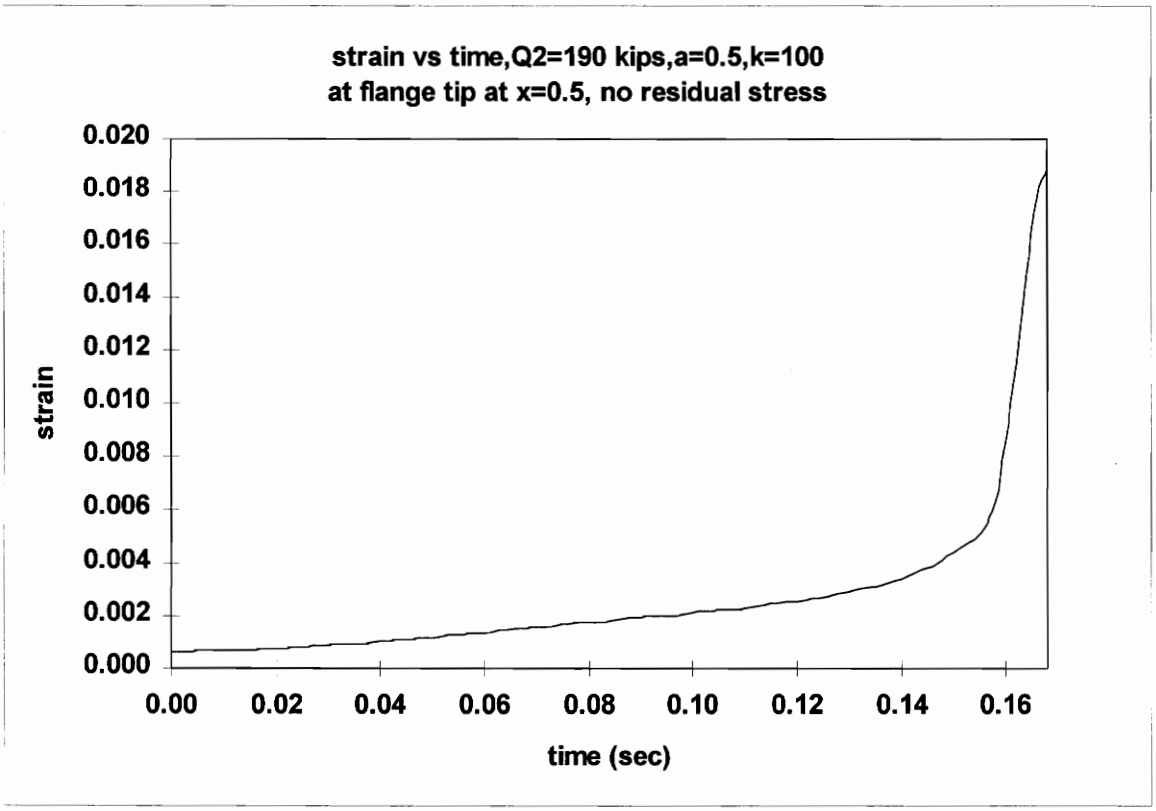

Fig. 4.29 Strain vs. time, Q_2 =190 kips, a=0.5, k=100
at flange tip at x=0.5, no residual stress

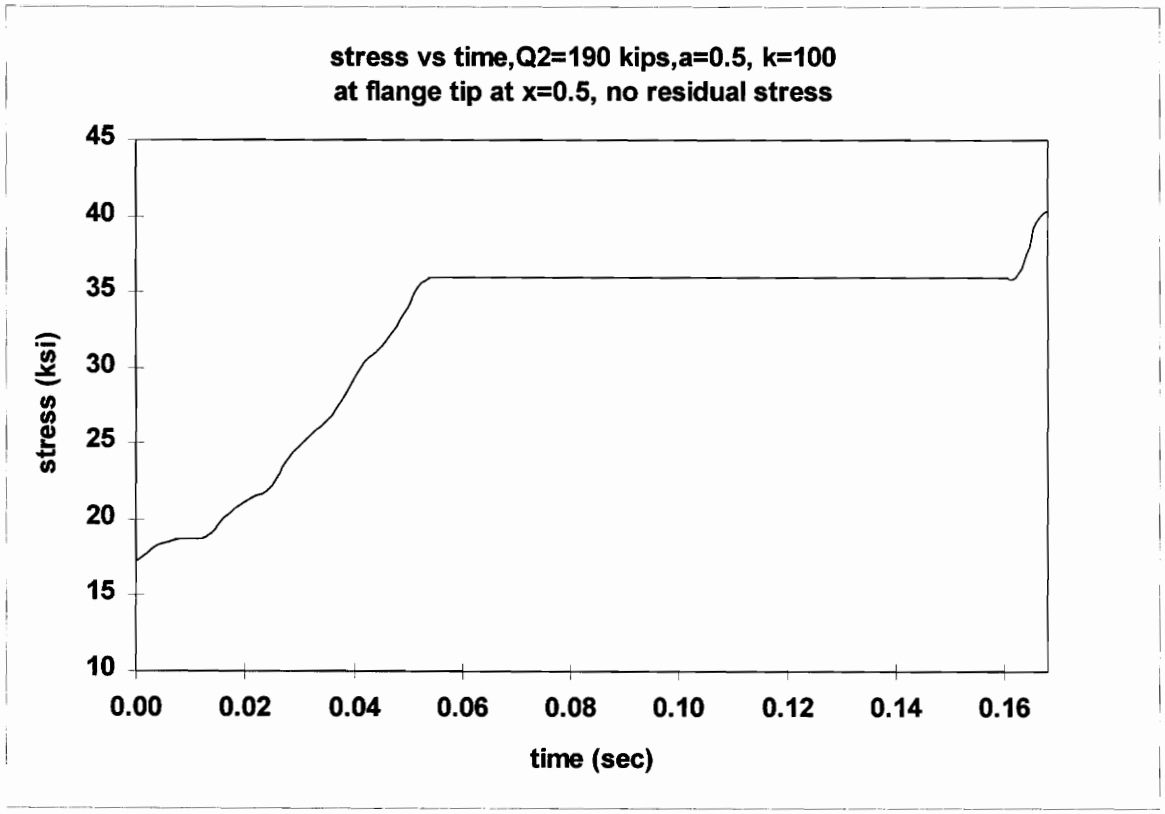

Fig. 4.30 Stress vs. time, Q_2=190 kips, a=0.5, k=100
at flange tip at x=0.5, no residual stress

4.2.5 The response of the column during motion

a. The maximum deflection during motion

The plastic response of the column is investigated using ABAQUS. The load of 170 kips which causes the spread of plasticity during motion is selected, and the maximum deflection corresponding to this load is calculated. The effects of the spring locations and spring stiffnesses are considered in the analysis.

Under this load, if residual stresses are not contained in the column section, stresses in the column are always below the yield stress. Therefore, the maximum deflections are the same as those in the elastic analysis. By including residual stresses, the column shows partial yielding along the column section, and this yielding causes a higher maximum deflection. Figures 4.31 to 4.34 show the shape of the column for different spring locations. The spring is at the center in Figs. 4.31 and 4.32 and at a=0.2 in Figs. 4.33 and 4.34. The initial deflection, deflected shape under the static loading, and the shapes at times when the first maximum and first local minimum deflection occur are depicted.

Figures 4.32 and 4.34 and Figs. 4.31 and 4.33 represent the cases with and without residual stresses, respectively. As stated in section 4.2.4, if plasticity occurs during the motion, it affects the amplitude and period of the motion and the magnitude of the maximum deflection. For the case with residual stresses, the spread of plasticity along the column length and cross section are explained in section 4.2.6.

The effects of spring location are shown in Fig. 4.35. Similar to the elastic case, the maximum deflection of the plastic state increases as the spring location approaches the center of the column. However, the incremental rate for the plastic state is higher than that for the elastic state. As in the elastic analysis, higher stiffness provides higher maximum deflection (Figs. 4.36 and 4.37).

b. Effects of residual stresses and damping

At the design strength of the column, with a load of 173 kips, an investigation is made into the effects of residual stresses and damping. When the spring location is a=0.5, and its stiffness is k=100, the deflection changes at the center of the column are shown in Fig. 4.38, where A, B, and C represent the following cases, respectively:

A: without residual stress and no damping

B: with residual stress and no damping

C: with residual stress and including damping

or without residual stress and including damping.

If residual stresses are not included in the analysis, stresses at all points of the column are below the yield stress (Fig. 4.39), so the response of the column is governed by the elastic analysis (line A in Fig. 4.38). On the other hand, if residual stresses are taken into account, the column collapses after a short time of period (line B in Fig. 4.38). As shown in Fig. 4.38, for a small time increment, the deflection increases sharply, and these increments are continuous with time. This state can be defined as failure. This

failure is caused by the excessive compressive stresses due to residual stresses. The change of stress corresponding to the failure is depicted in Fig. 4.40. The plasticity spreads during the motion, and finally the column collapses. However, by including damping effects (one percent of the critical damping, as stated in sections 4.1.2 and 4.1.3), the column become stable, even though residual stresses are included in the analysis (graph C in Fig. 4.38). Due to the damping, stresses do not reach the yield stress, and the motion decays slowly.

To show the effect of residual stresses without the failure of the column, the load of 170 kips, which is slightly lower than the design load, was applied. At this load, the changes of stresses and strains were shown in section 4.2.4. The influence of residual stresses on the response of the column was presented in Fig. 4.29. In addition to the results in Fig. 4.28, the damping term is included in Fig. 4.41. The deflections of the column at x=0.5 for the cases with and without residual stresses were monitored during the motion, where the deflections are measured from the static state. As seen in Fig. 4.28 and Fig. 4.41, due to the residual stresses, the maximum deflection is increased and the time at which the first peak is reached is delayed. However, the period of motion remains the same as in the non-residual stresses case (the elastic response). Since the plasticity spread occurs during the first cycle and it acts like a damping factor, the amplitude of motion becomes smaller. After the first cycle, no plasticity is detected, so the deflection exhibits harmonic motion with the decreased amplitude. As described in section 4.1.3, compared to the undamped system, the effects of 1% critical damping alone provided

about 2% difference in the maximum deflections. However, for the load of 170 kips and without damping, the difference between the cases with and without residual stresses is more than 15%.

x	w0(x,0)	w(x,0)	w(x,0.084)	w(x,0.164)
0	0.00	0.00	0.00	0.00
12	3.75	4.95	19.95	4.95
24	7.42	9.82	39.32	9.72
36	10.90	14.40	57.80	14.30
48	14.11	18.61	74.81	18.51
60	16.97	22.27	89.87	22.27
72	19.42	25.42	102.82	25.42
84	21.38	27.88	113.28	27.88
96	22.83	29.63	120.83	29.73
108	23.70	30.70	125.50	30.80
120	24.00	31.10	127.10	31.20
132	23.70	30.70	125.50	30.80
144	22.83	29.63	120.83	29.73
156	21.38	27.88	113.28	27.88
168	19.42	25.42	102.82	25.42
180	16.97	22.27	89.87	22.27
192	14.11	18.61	74.81	18.51
204	10.90	14.40	57.80	14.30
216	7.42	9.82	39.32	9.72
228	3.75	4.95	19.95	4.95
240	0.00	0.00	0.00	0.00

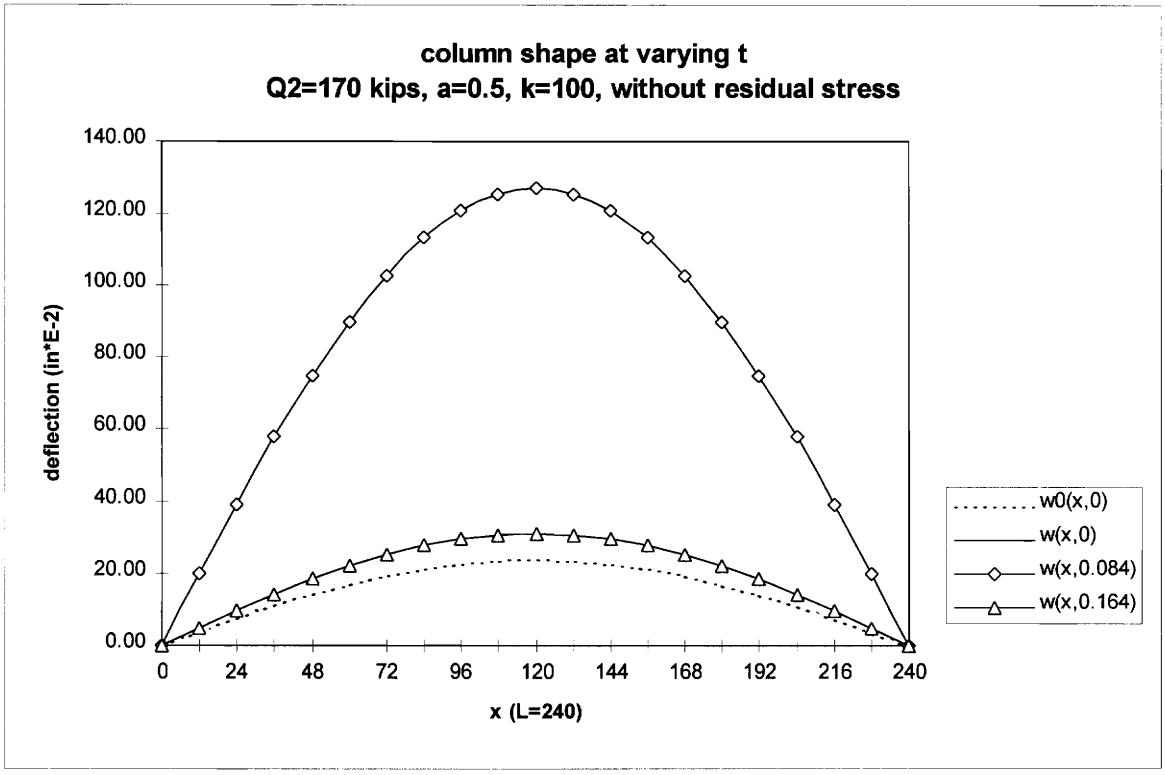

Fig. 4.31 Column shape at varying t
Q_2=170 kips, a=0.5, k=100, at flange tip at x=0.5, without residual stress

x	w0(x,0)	w(x,0)	w(x,0.104)	w(x,0.188)
0	0.00	0.00	0.00	0.00
12	3.75	4.95	22.15	15.65
24	7.42	9.82	43.82	31.02
36	10.90	14.40	64.60	45.70
48	14.11	18.61	83.91	59.41
60	16.97	22.27	101.27	71.77
72	19.42	25.42	116.32	82.42
84	21.38	27.88	128.68	91.28
96	22.83	29.63	137.83	97.83
108	23.70	30.70	143.40	101.80
120	24.00	31.10	145.30	103.20
132	23.70	30.70	143.40	101.80
144	22.83	29.63	137.83	97.83
156	21.38	27.88	128.68	91.28
168	19.42	25.42	116.32	82.42
180	16.97	22.27	101.27	71.77
192	14.11	18.61	83.91	59.41
204	10.90	14.40	64.60	45.70
216	7.42	9.82	43.82	31.02
228	3.75	4.95	22.15	15.65
240	0.00	0.00	0.00	0.00

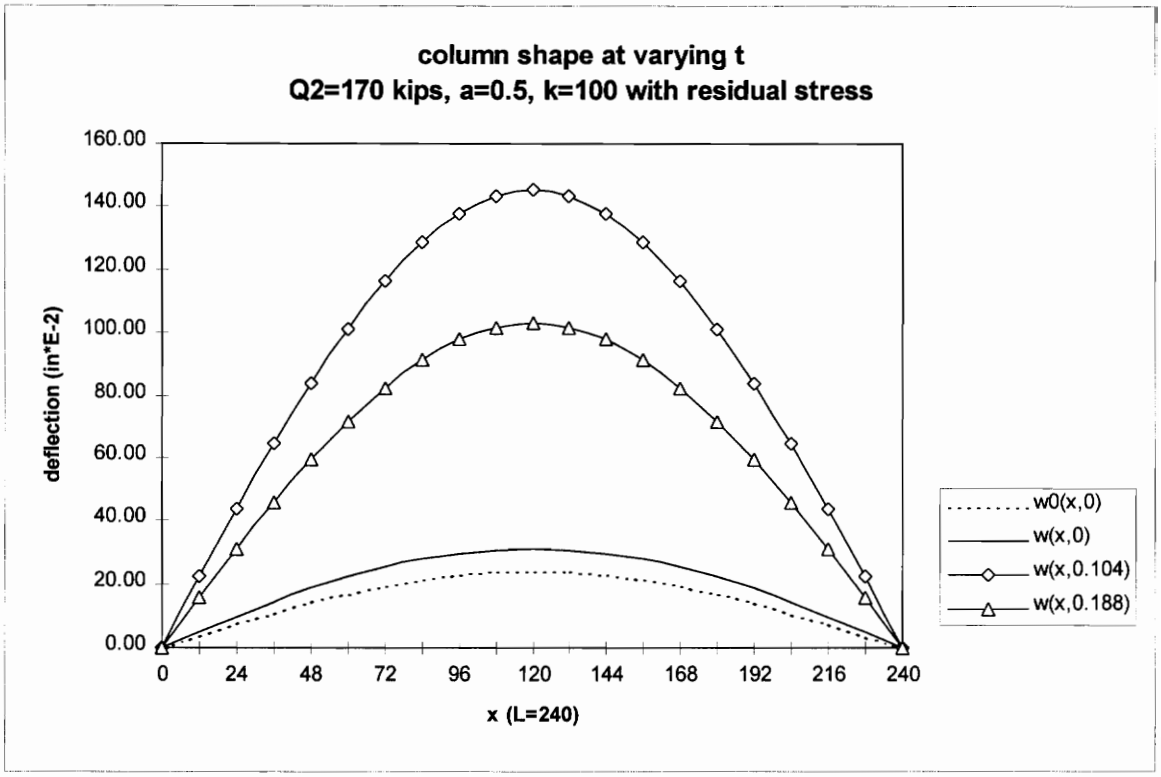

Fig. 4.32 Column shape at varying t
Q_2=170 kips, a=0.5, k=100, at flange tip at x=0.5, with residual stress

0.00	0.00	0.00	0.00
3.75	6.05	17.95	7.05
7.42	12.12	35.52	13.92
10.90	17.90	52.30	20.40
14.11	23.31	67.81	26.21
16.97	28.47	81.77	31.37
19.42	32.92	93.62	35.62
21.38	36.78	103.28	38.88
22.83	39.73	110.43	41.13
23.70	41.70	114.80	42.30
24.00	42.60	116.30	42.40
23.70	42.50	114.90	41.50
22.83	41.23	110.73	39.63
21.38	38.88	103.68	36.88
19.42	35.52	94.12	33.22
16.97	31.17	82.17	28.87
14.11	26.01	68.31	23.91
10.90	20.10	52.70	18.40
7.42	13.72	35.82	12.52
3.75	6.95	18.15	6.35
0.00	0.00	0.00	0.00

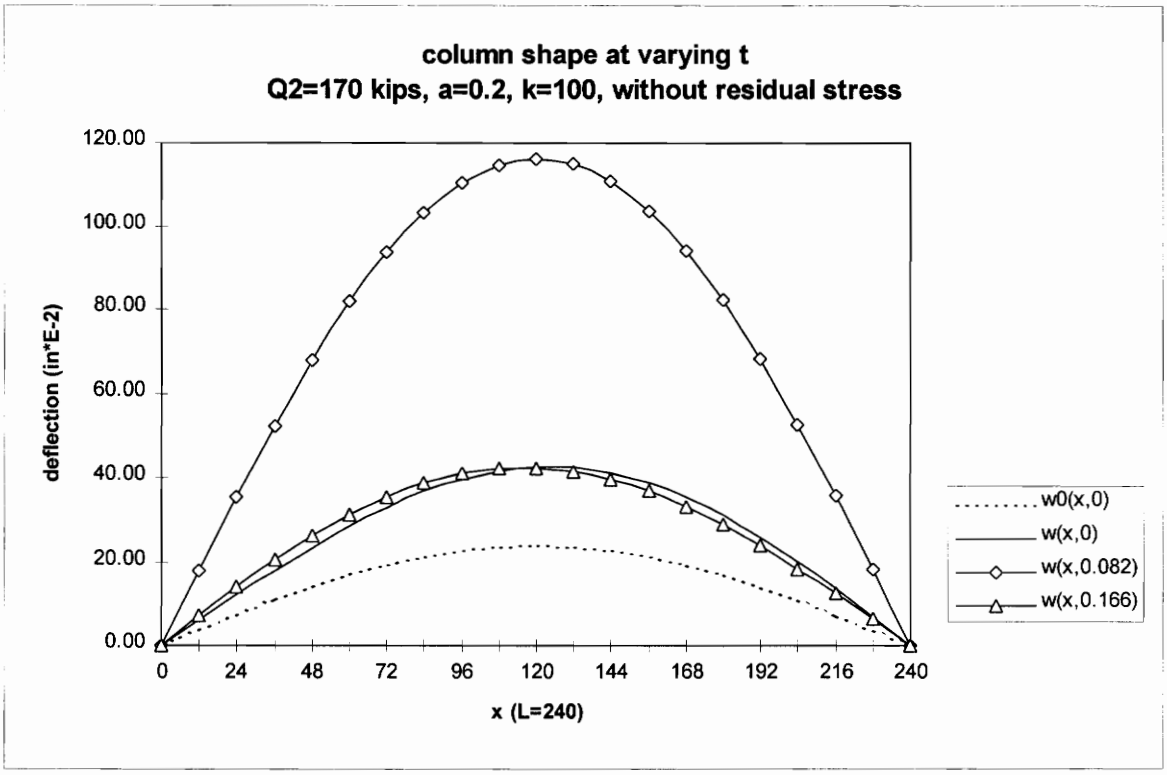

Fig. 4.33 Column shape at varying t
Q_2=170 kips, a=0.2, k=100, at flange tip at x=0.5, without residual stress

x	w0(x,0)	w(x,0)	w(x,0.094)	w(x,0.174)
0	0.00	0.00	0.00	0.00
12	3.75	6.05	19.45	12.55
24	7.42	12.12	38.42	24.72
36	10.90	17.90	56.60	36.40
48	14.11	23.31	73.31	47.31
60	16.97	28.47	88.37	57.17
72	19.42	32.92	101.22	65.72
84	21.38	36.78	111.68	72.78
96	22.83	39.73	119.23	78.03
108	23.70	41.70	123.70	81.30
120	24.00	42.60	125.10	82.50
132	23.70	42.50	123.20	81.50
144	22.83	41.23	118.13	78.43
156	21.38	38.88	110.28	73.28
168	19.42	35.52	99.72	66.32
180	16.97	31.17	86.77	57.87
192	14.11	26.01	71.91	47.91
204	10.90	20.10	55.40	36.90
216	7.42	13.72	37.62	25.12
228	3.75	6.95	19.05	12.65
240	0.00	0.00	0.00	0.00

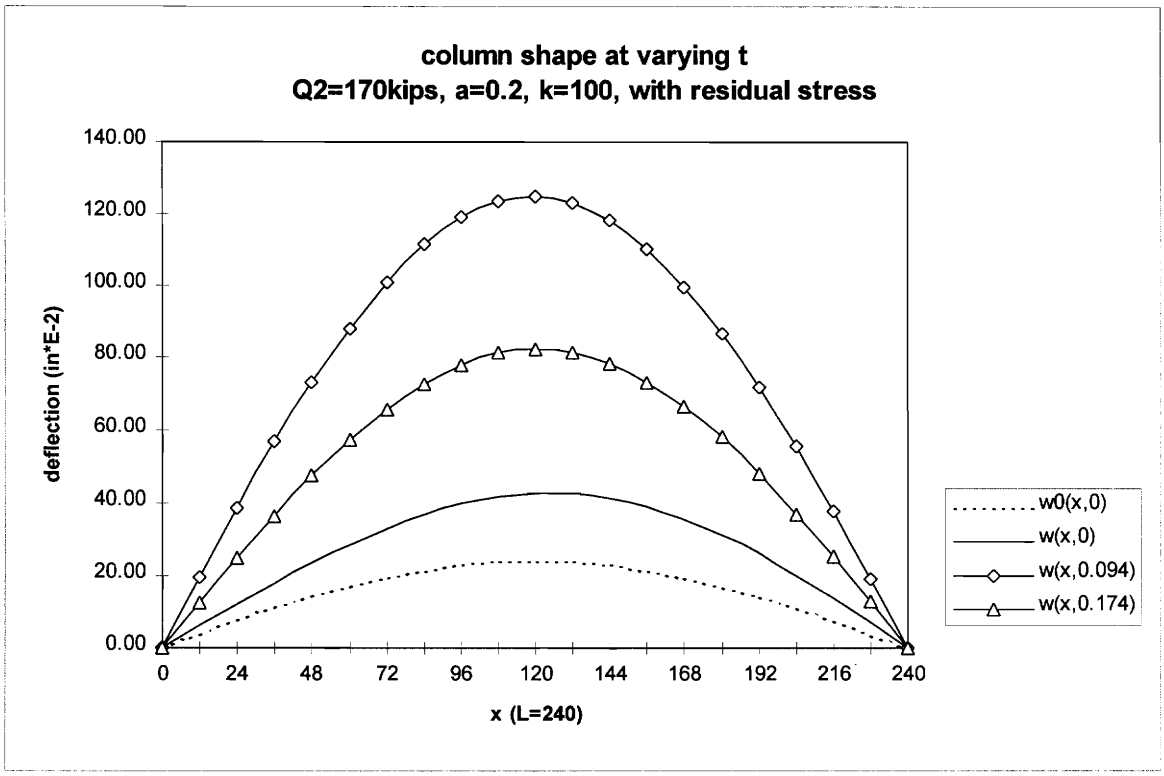

Fig. 4.34 Column shape at varying t
Q_2 =170 kips, a=0.2, k=100, at flange tip at x=0.5, with residual stress

a	with r.s.	without r.s.
0.1	103.4	100.1
0.2	125.1	116.3
0.3	137.0	123.2
0.4	143.3	126.2
0.5	145.3	127.1

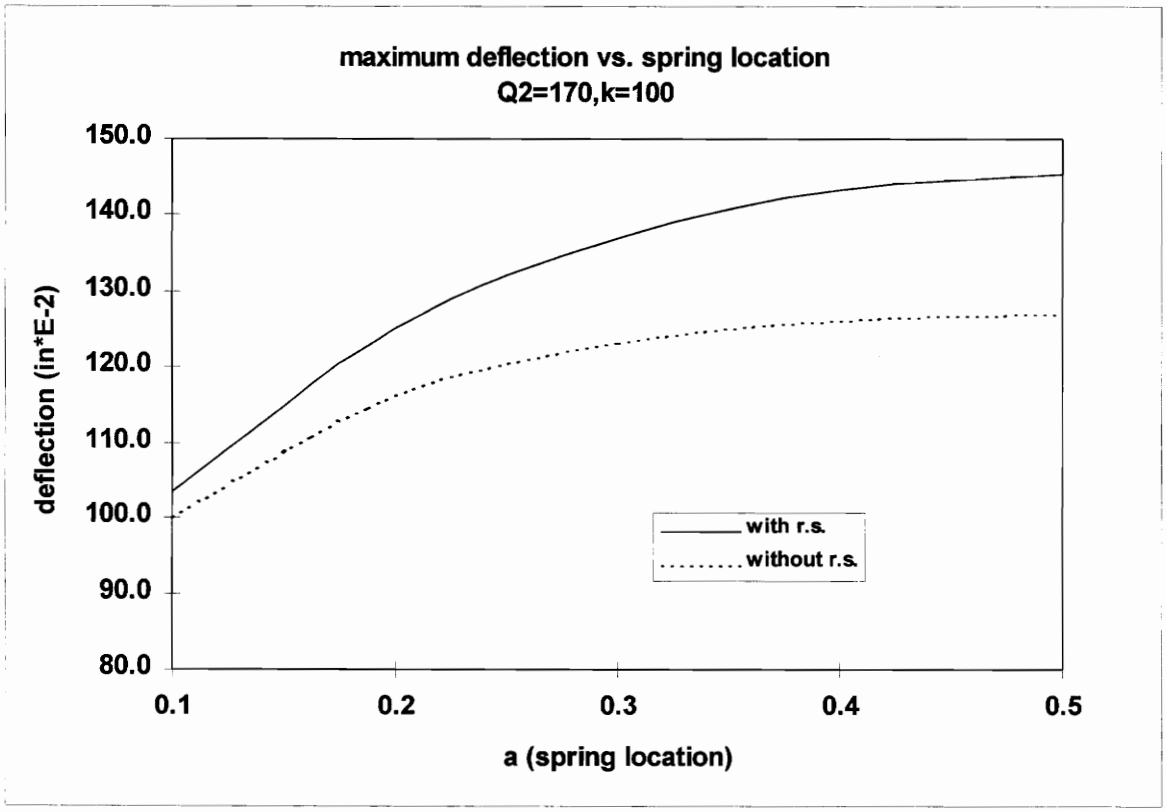

Fig. 4.35 Maximum deflection u(x) vs. spring location a
Q_2=170 kips, k=100

k	with r.s.	without r.s.
100	145.3	127.1
500	159.3	132.5
1000	161.8	133.3

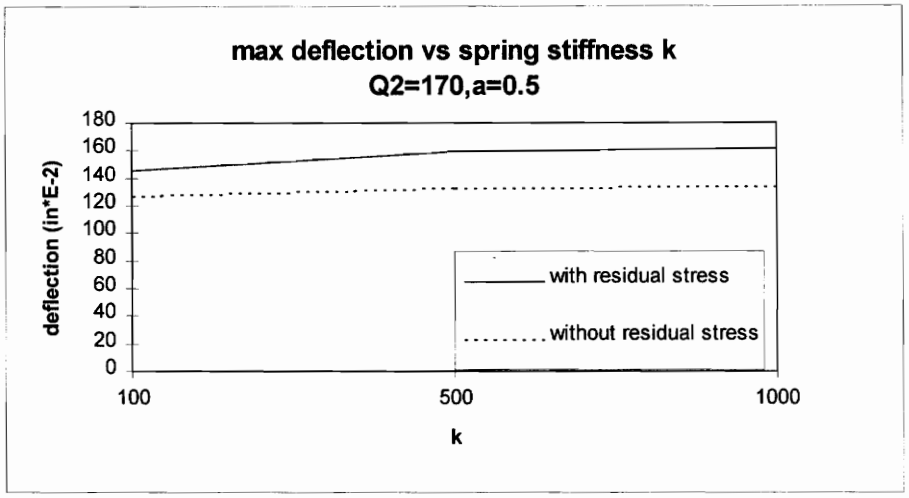

Fig. 4.36 Maximum deflection u(x) vs. spring stiffness k
Q_2=170 kips, a=0.5

k	with r.s.	without r.s.
100	125.1	116.3
500	146.5	127.2
1000	151.1	129

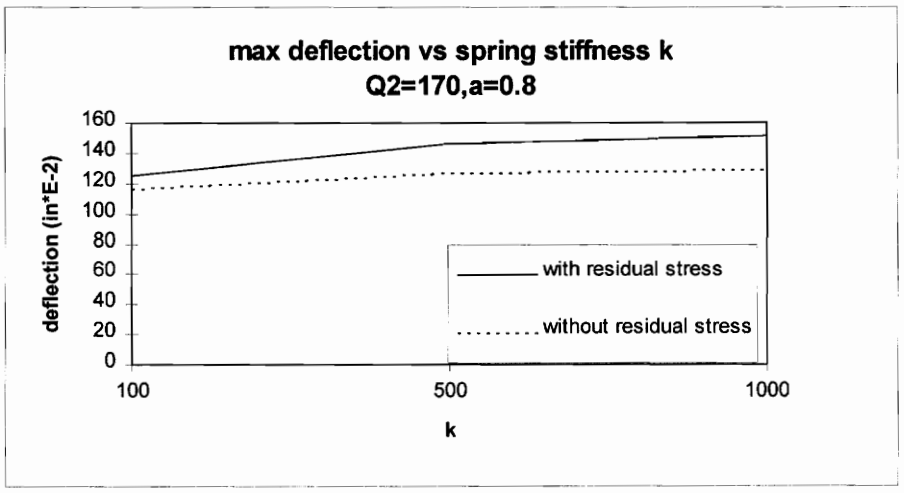

Fig. 4.37 Maximum deflection u(x) vs. spring stiffness k
Q_2=170 kips, a=0.8

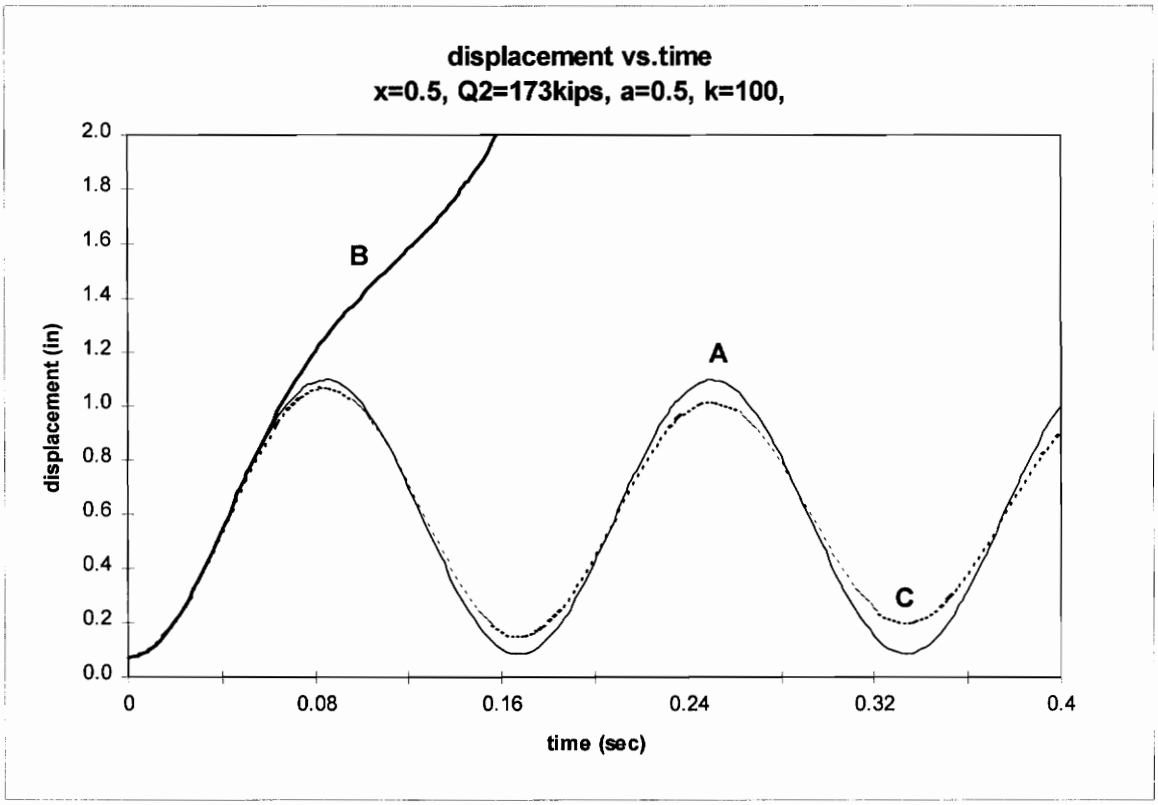

Fig. 4.38 Deflection u(x) vs. time
x=0.5, Q_2=173 kips, a=0.5, k=100

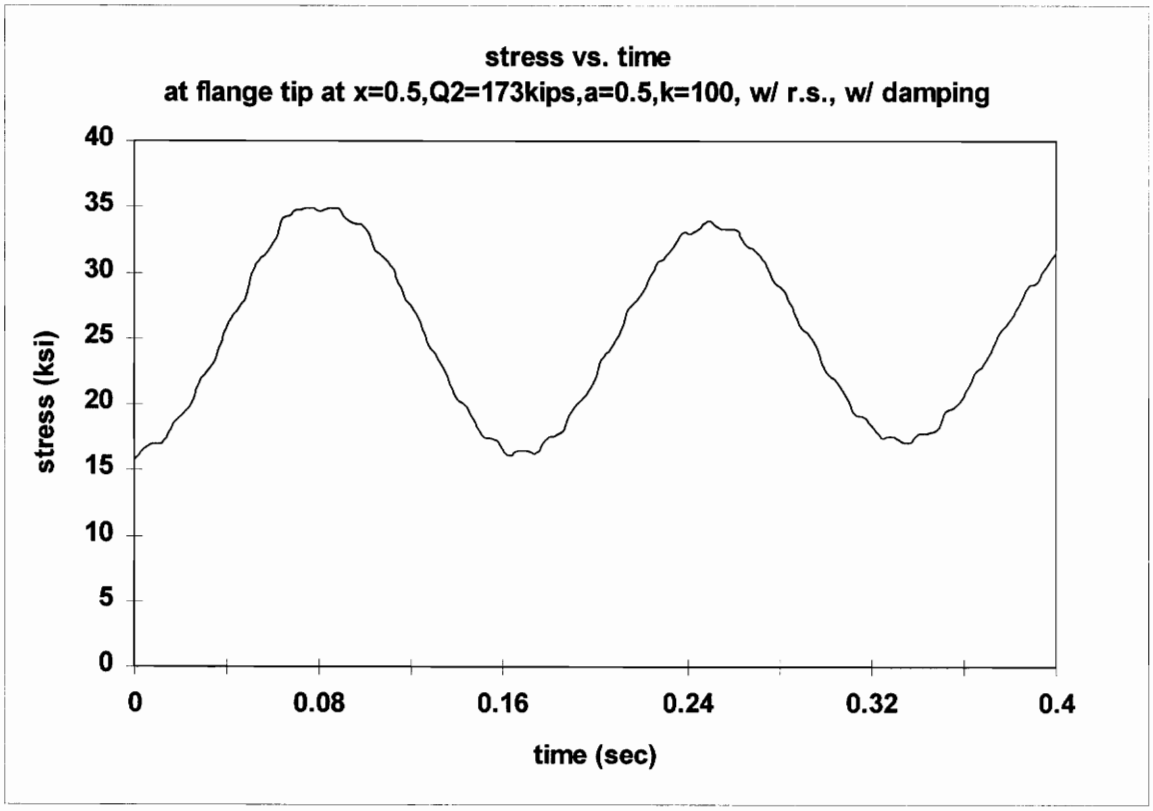

Fig. 4.39 Stress vs. time, Q_2=173 kips, a=0.5, k=100
at flange tip at x=0.5, with residual stress, with damping

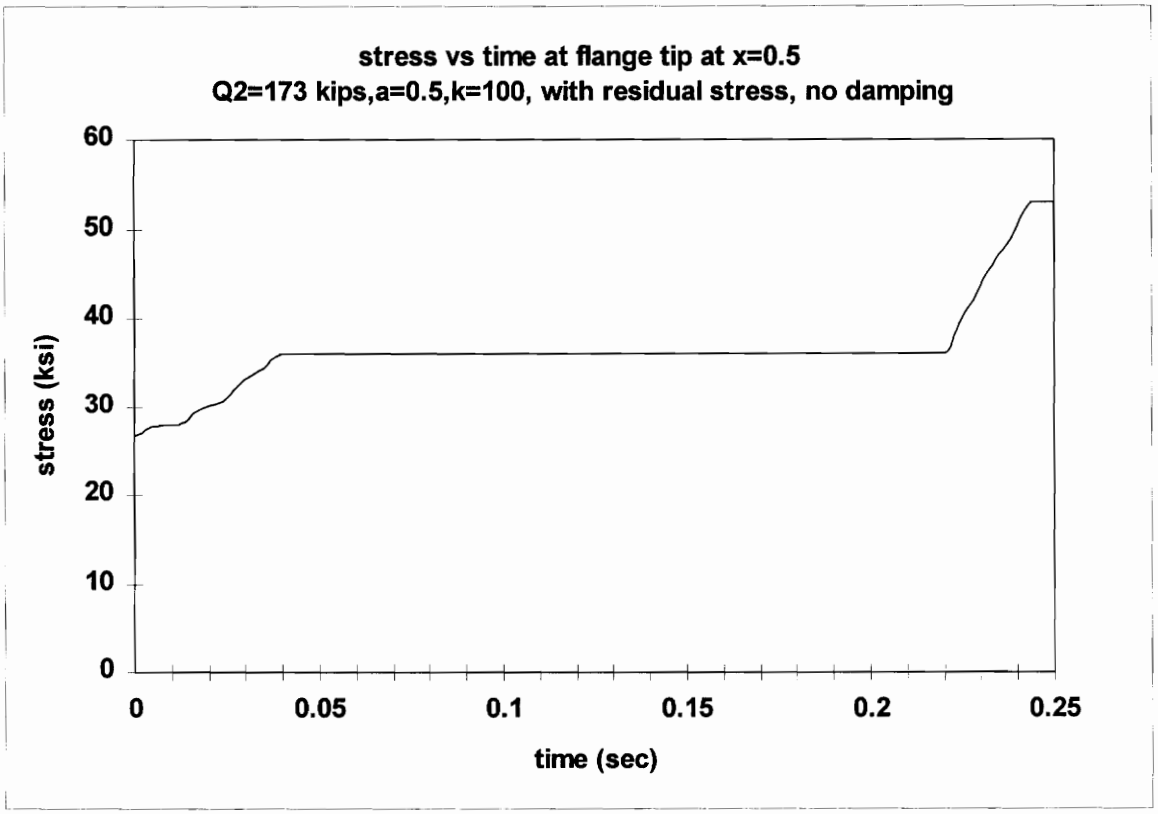

Fig. 4.40 Stress vs. time, Q_2=173 kips, a=0.5, k=100 at flange tip at x=0.5, with residual stress, no damping

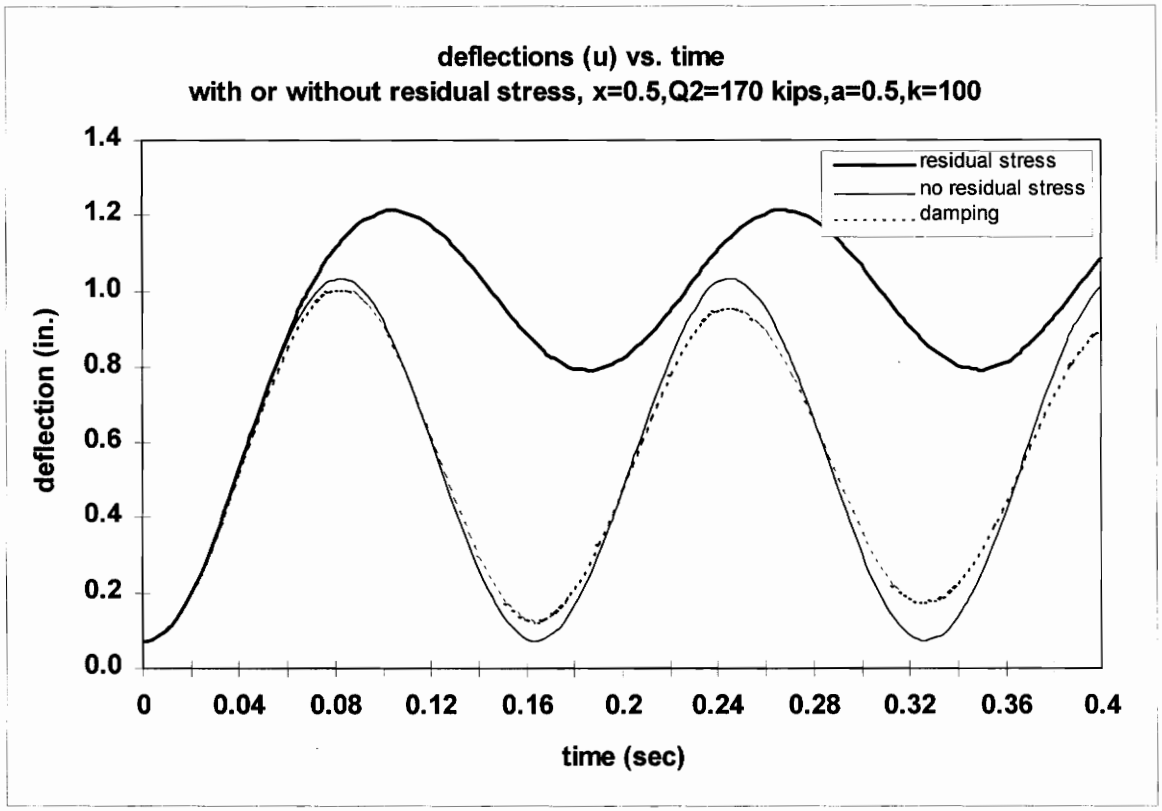

Fig. 4.41 Deflection u(x) vs. time
with or without residual stress, x=0.5, Q_2=170 kips, a=0.5, k=100

4.2.6 Plasticity spread

The advantage of the finite element method is that such factors as strain hardening, unloading, and residual stresses can be applied to the structural analysis. By subdividing the column into elements, the spread of yielding can be checked through the cross section and along the length of the column. In this study, to investigate the spread of yielding during the motion, the column in Fig. 3.10 is tested for different loadings and spring locations. The bending direction of the column is shown in Fig. 4.42, and the nondimensional spring stiffness is k=100. For the simply supported column, the design strength is 173 kips. To ensure yielding in the column, the loads Q_2=170 and 190 kips are examined. Stresses are checked at the eleven points of a column flange and 21 sections along the column length, and any point where the stress exceeds the yield stress is depicted as a dot in Figs. 4.43 to 4.46. Residual stresses are included, but the damping effects are not considered.

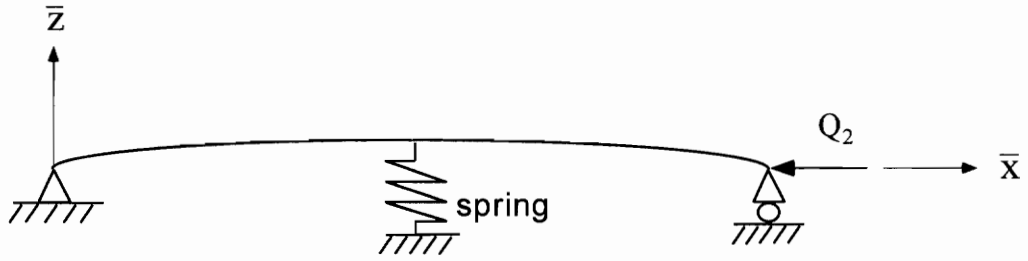

Fig. 4.42 The bending of the column

In the ABAQUS dynamic analysis, if the increment of strain is fifty times greater than that of the previous step, the calculation is stopped. This means that the small increment of load causes a large displacement. The collapse of the column is assumed to occur at this state.

Case 1. Q2=170 kips, a=0.5

Since the spring is located at the center of the column and the initial deflection is symmetric and Q_1=0, the motion of the column is perfectly symmetric after it loses its bracing. Using a time increment of 0.002 second, plasticity is first detected at t=0.040 second for this case. The maximum deflection of the column occurs at t=0.104 second; the shape of the column at that time was shown in Fig. 4.32. Figure 4.43 shows that the spread of plasticity is also symmetric about the center of the column. Yielding in compression initiates at the bottom edge of the column first, and spreads into the column cross section. At t=0.094 second, the column is not plastic at the center, due to elastic unloading. At t=0.100 second, yielding at the center of the column starts again, and finally after t=0.104 second, no plastic yielding occurs. Yielding in tension at the surface of the top edge of the column is not detected at this load. The column is only plastic during the first half-cycle of motion.

Case 2. Q2=170 kips, a=0.2

When the column is braced unsymmetrically, and released from the constraint, its response is far from symmetric. In Fig. 4.44, the spread of yielding fluctuates irregularly

as the column moves. It starts on the left side of the center, then moves to the right side, and so on. The maximum deflection of the column occurs at t=0.094 second, and the shape of the column at that time was shown in Fig. 4.34. Unlike case 1, the column also exhibits some yielding during the second cycle of motion (see last two drawings in Fig. 4.44).

Case 3. Q2=190 kips, a=0.5

Figure 4.45 shows the spread of yielding at a load higher than the design load. Like case 1, the spread is symmetric about the center of the column. Yielding in compression starts at the surface of the bottom edge of the column at t=0.032 second, and spreads along the length. Then it spreads into the cross section. Yielding in tension at the top edge of the flange is seen first at t=0.102 second and also spreads. After t=0.116 second, the column collapses.

Case 4. Q2=190 kips, a=0.2

This case is shown in Fig. 4.46. The first yielding starts a little bit earlier than in case 3. Like case 2, the spread of yielding is not symmetric. Yielding in compression starts at the surface of the bottom edge of the column at t=0.026 second, and spreads along the length. Yielding in tension at the top edge of the flange occurs first at t=0.104 second and also spreads. After t=0.118 second, the column collapses. When the column collapses, a wider spread of plasticity is observed than in case 3.

Comments on the plastic analysis

In the plastic analysis, a two-span 240-inch-long $W8 \times 40$ column (its slenderness parameter is 1.32) is investigated. This column exhibits inelastic behavior when it collapses. The load at the brace is not considered. As shown in section 4.2.5, for the case of the load ratio $Q_1:Q_2 = 0:1$, a=0.5, and k=100, the column subject to a compressive design load (173 kips) at its end is stable after sudden loss of bracing, if both residual stresses and damping effects are included in the analysis.

In this study, the initial deflection of the column is assumed as L/1000 rather than L/1500 specified in LRFD manual, so that results from the plastic analysis represent more conservative cases.

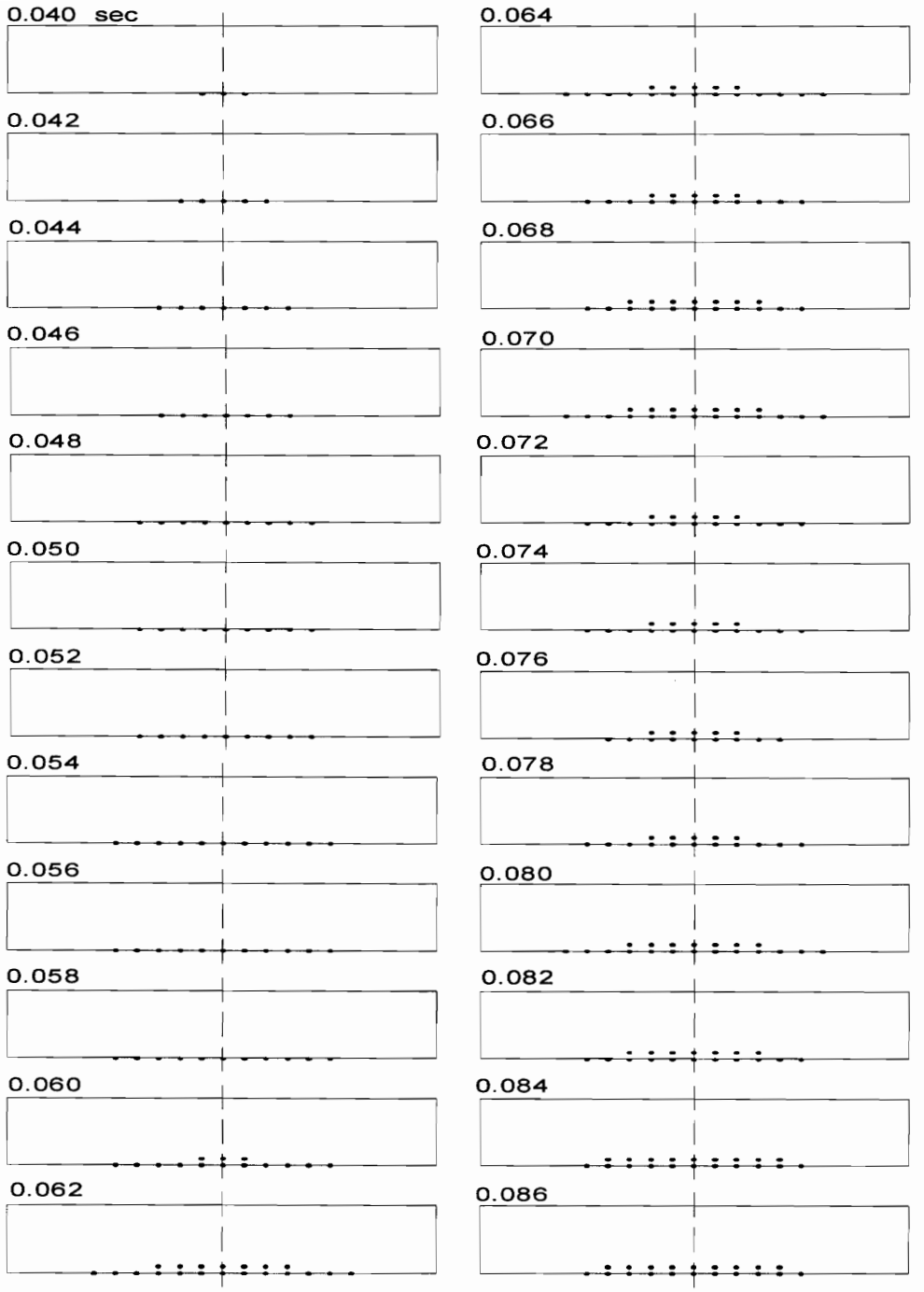

Fig. 4.43 Plasticity spread, Q_2=170 kips, a=0.5, k=100

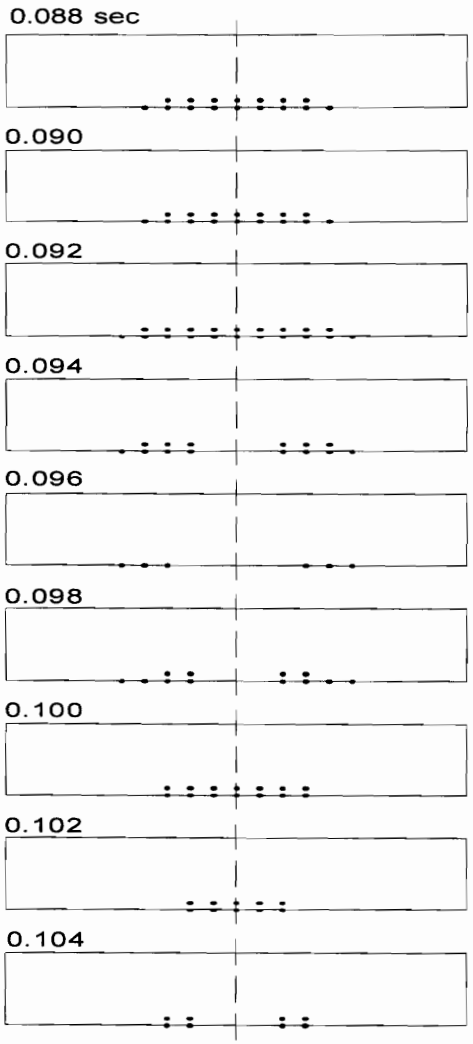

Fig. 4.43 (continued)

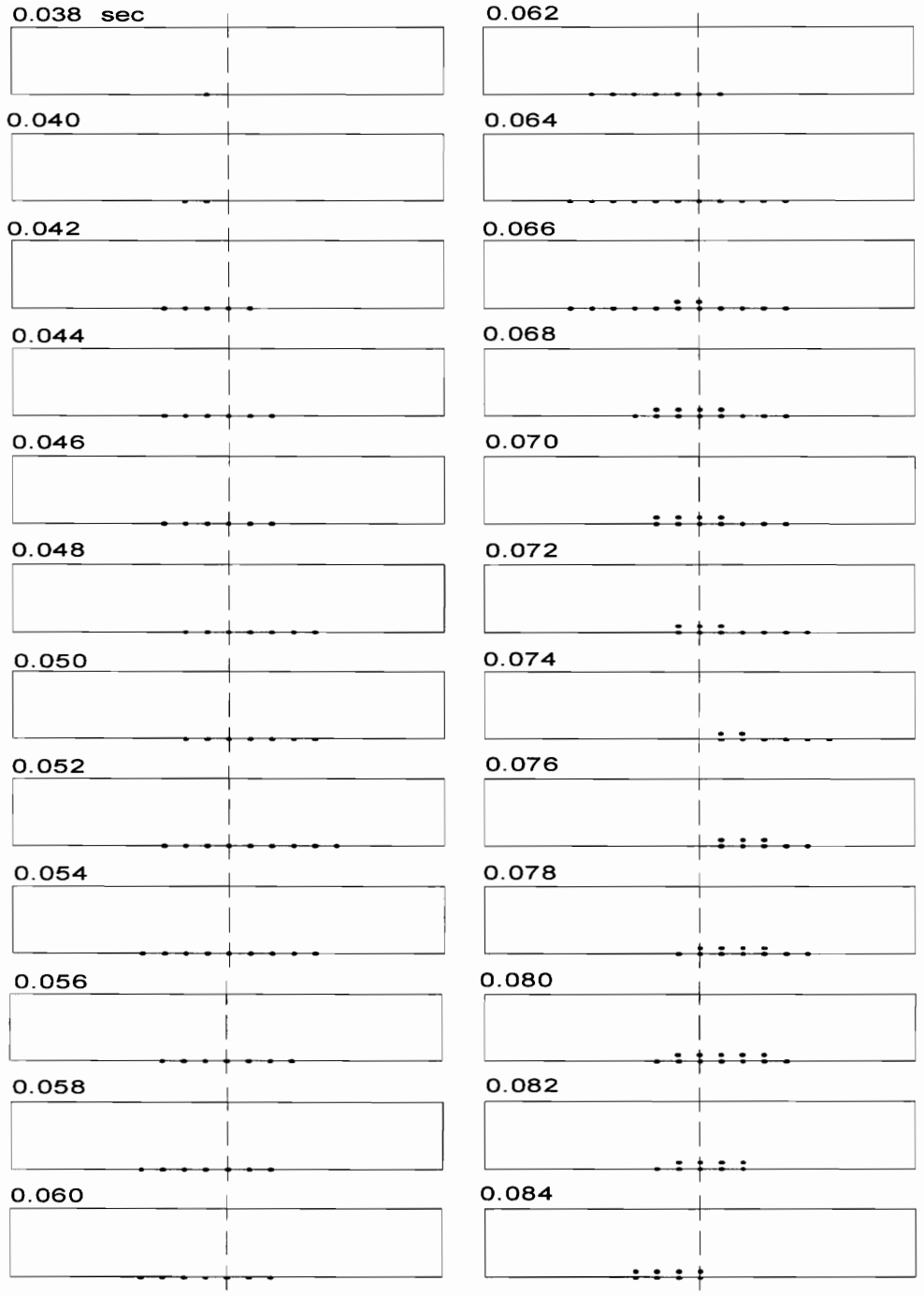

Fig. 4.44 Plasticity spread, Q_2=170 kips, a=0.2, k=100

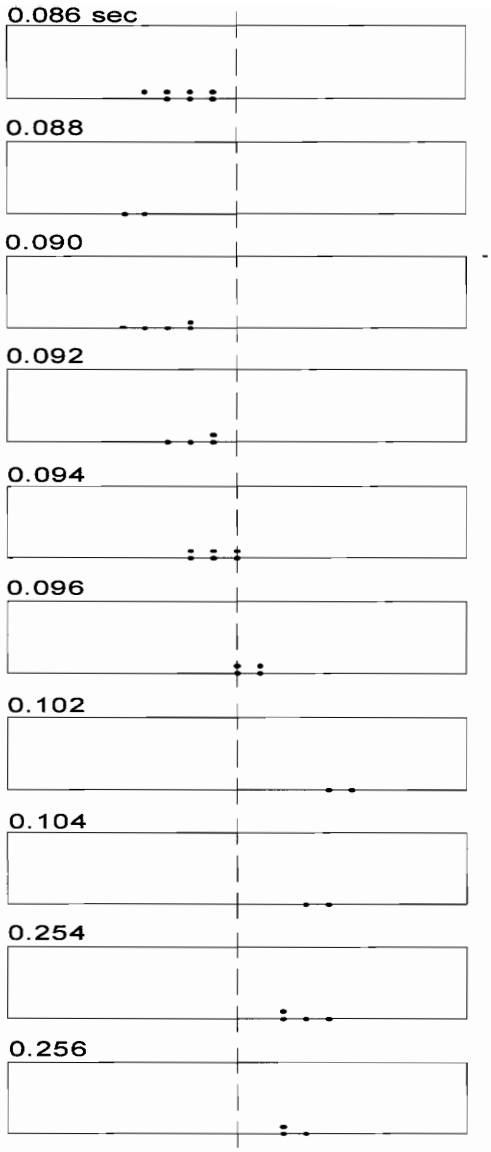

Fig. 4.44 (continued)

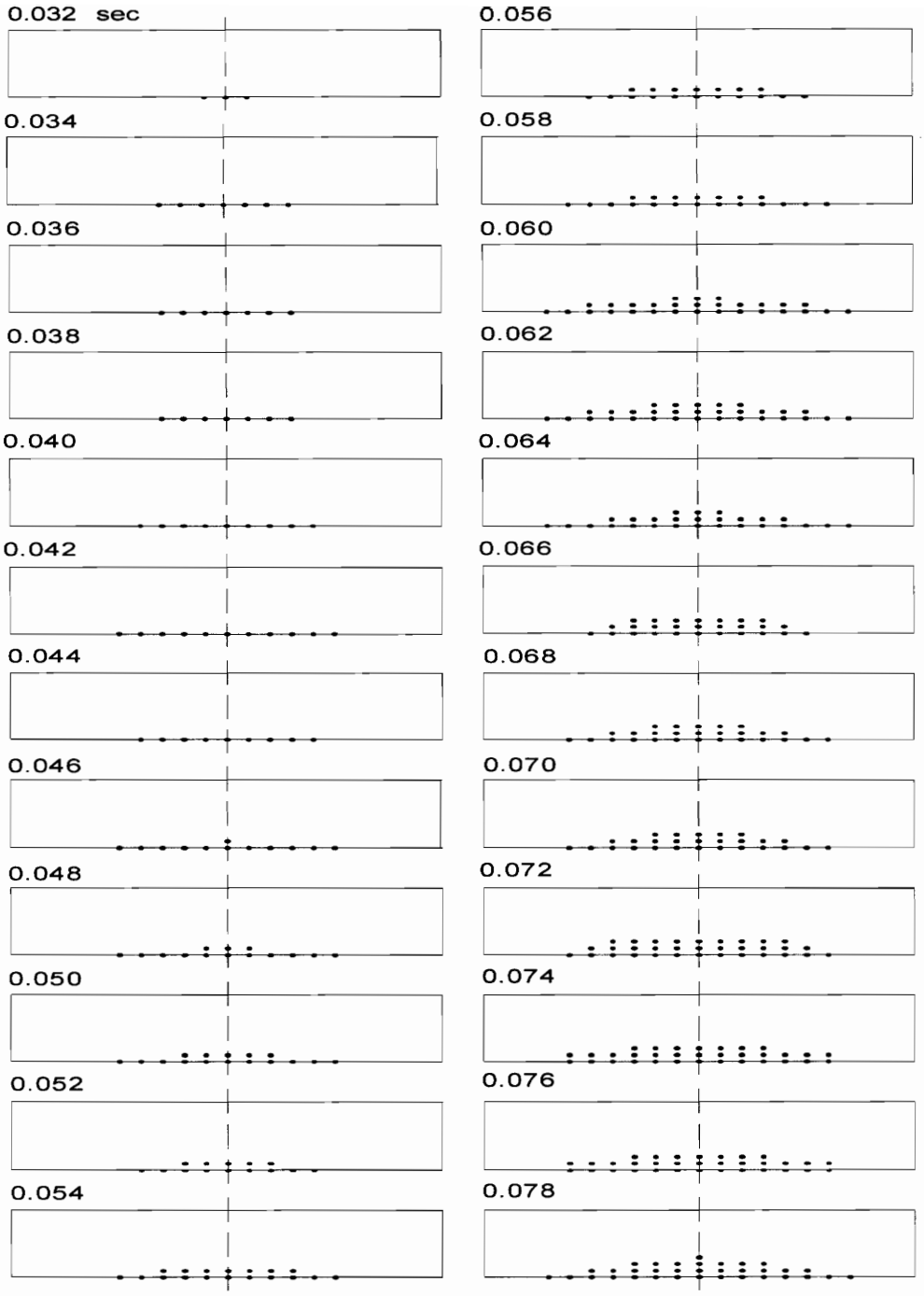

Fig. 4.45 Plasticity spread, Q_2=190 kips, a=0.5, k=100

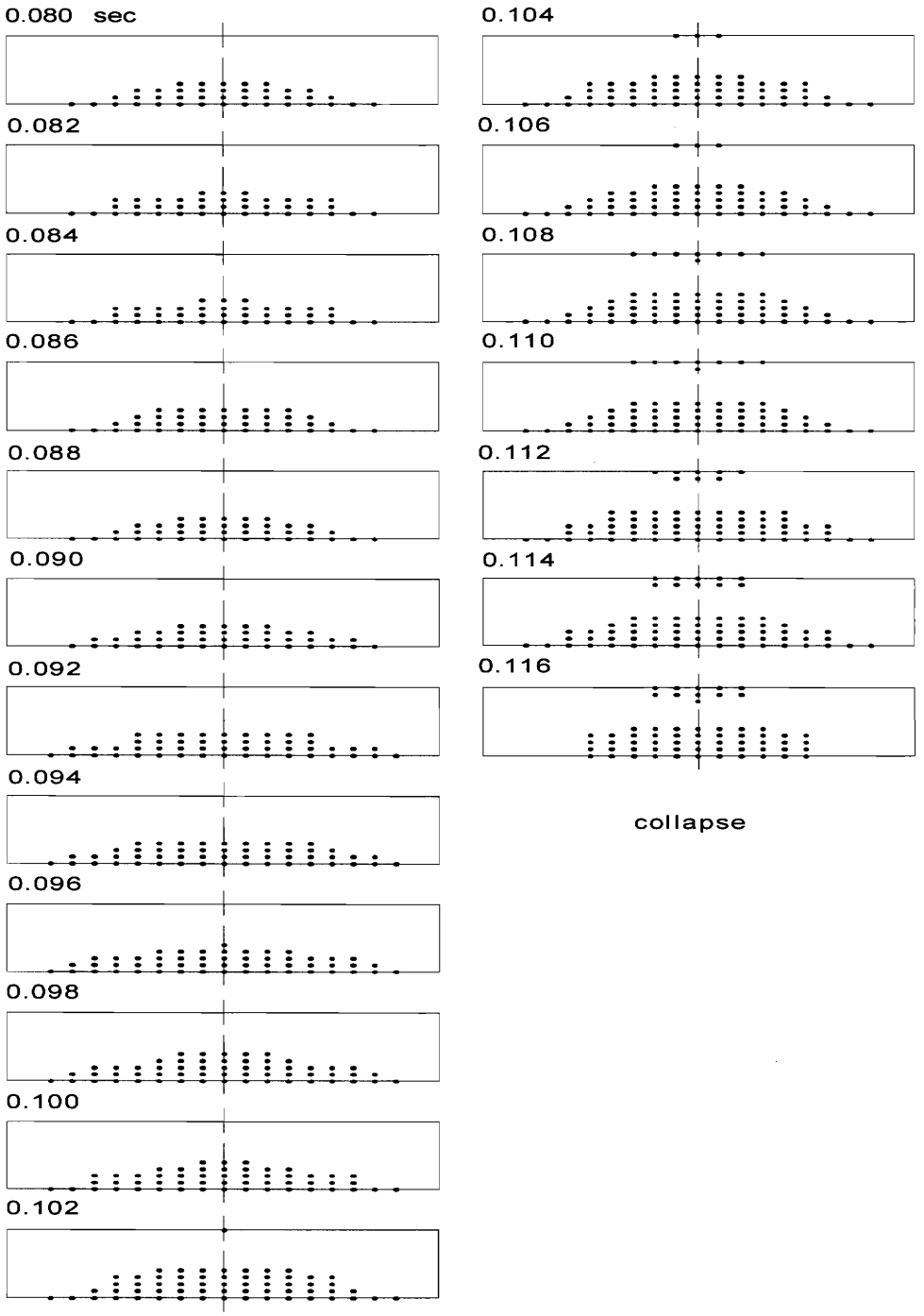

Fig. 4.45 (continued)

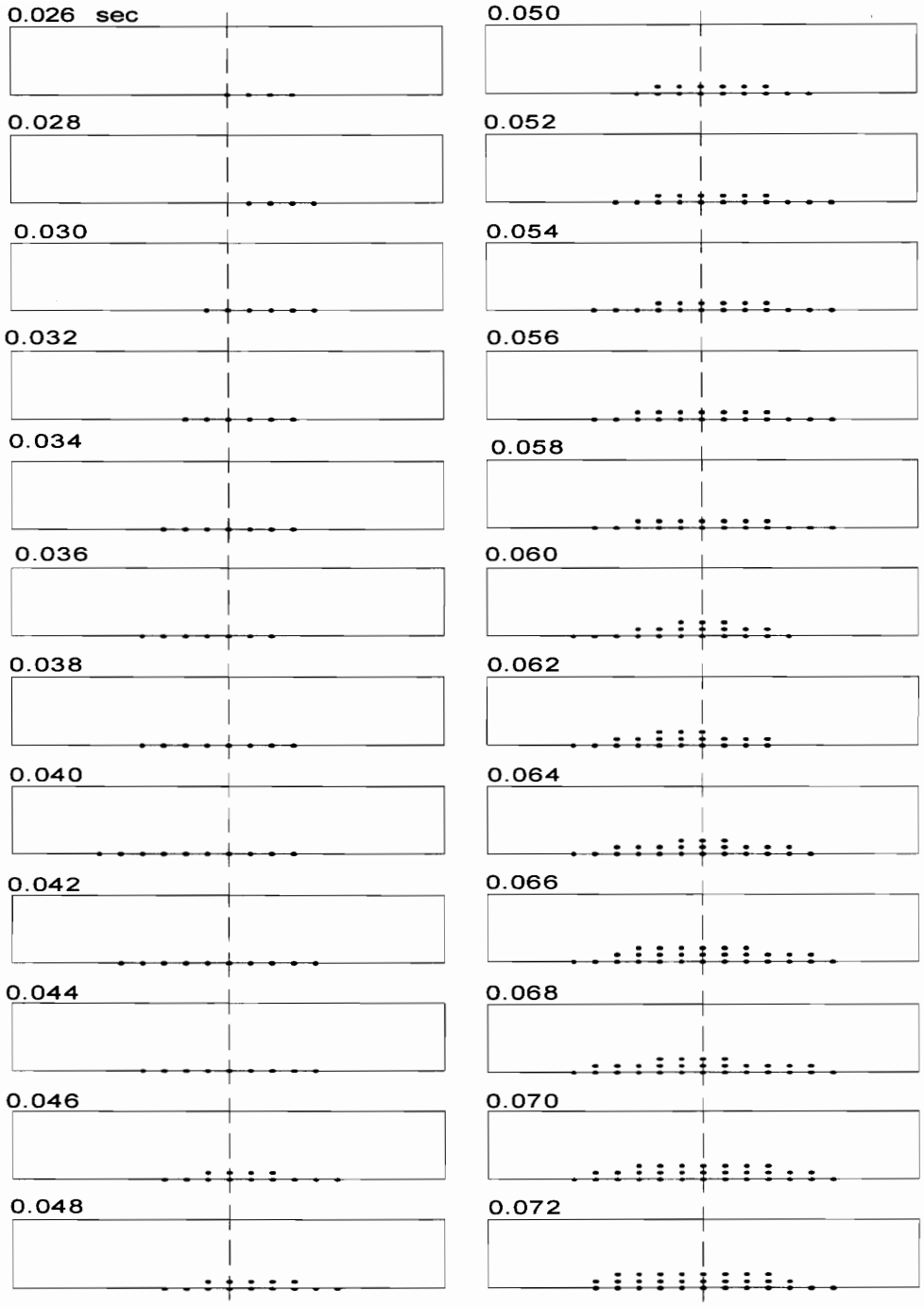

Fig. 4.46 Plasticity spread, Q_2=190 kips, a=0.2, k=100

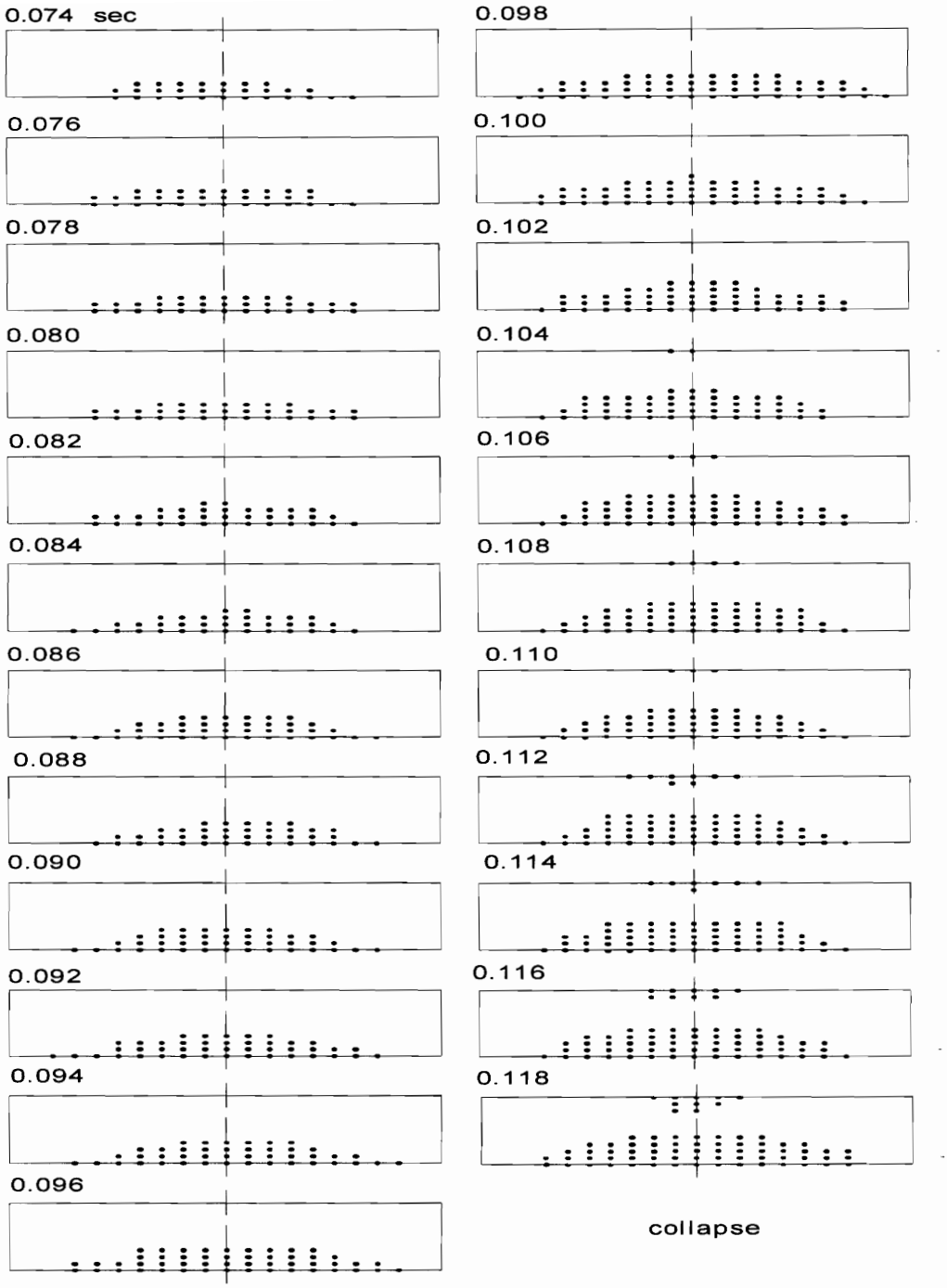

Fig. 4.46 (continued)

5. SUMMARY AND CONCLUSIONS

The static response of a pinned column with initial deflection and an internal brace is investigated first. The brace is modeled as a translational spring. Axial compressive loads are applied at the brace and the top of the column, and the equilibrium shape of the column is determined. The critical loads for the perfect column are computed analytically for the several loading conditions.

The dynamic response of the column after sudden loss of bracing is analyzed using Galerkin's method. With the consideration of the effects of the bracing location and the bracing stiffness, the maximum deflection of the column during motion is determined. The contribution of damping effects to the maximum deflection of the column is examined. Damping effects in the Galerkin method are compared to the results from the finite element method (based on ABAQUS).

The plastic dynamic analysis is carried out using ABAQUS. A 240-inch-long $W8 \times 40$ column (its slenderness parameter is less than 1.5) is used. Both residual stresses and damping effects are considered, and the spread of plasticity during the motion is investigated.

The following observations and conclusions are drawn from the study.

1. If the column spans are unequal and an axial compressive load is applied at the brace, as well as the top, an ideal spring stiffness does not exist. For the imperfect column, the maximum deflection grows after loss of bracing as the spring stiffness increases. The

maximum load capacity of the column is provided by the spring located at some position other than the center of the column.

2. In the elastic dynamic analysis, one percent of the critical damping of the first mode in Galerkin's method provides approximately a two percent decrease of the maximum deflection.

3. For some cases (e.g., $P_1 = 4$, $P_2 = 4$, and spring location a=0.9), the maximum deflection occurs at the static state. Generally, the maximum deflection is detected during the motion, and its point in the column is always the center of the column if $0.2 \leq a \leq 0.7$.

4. Without the internal load at the brace, the column subject to the compressive design load at its end is stable after sudden loss of bracing. With the design load alone at the end of the column, no plasticity in the column appears during motion. However, the dynamic response of the column is affected largely by residual stresses. Additional stresses due to residual stresses cause the plasticity spread in the column and result in the collapse of the column after loss of bracing. However, failure of the column can be prevented if damping effects are included.

5. When the column becomes plastic without failure, the maximum deflection is increased, and the time at which the first peak is reached is delayed. The period of motion remains the same as in the elastic response. Like the damping effects, plasticity reduces the amplitude of the vibration of the column.

Recommendations for future work

The following categories can be added to the future work:

1. Analysis of a column which has more than two spans;
2. In addition to the translational spring, the effect of a rotational spring at the braces;
3. Changing boundary conditions of the column;
4. The effect of the slenderness ratio on the results;
5. The effect of eccentric loads;
6. The shape of the column other than an I-section column;
7. In plastic dynamic analysis, finding the maximum load capacity of the column for different loading combinations;
8. The effect of the initial deflection shape of the column;
9. The effects of lateral load such as a blast load.

6. REFERENCES

[1] Winter, G. (1960). "Lateral bracing of columns and beams." *Trans. ASCE*, 125, Pt. I, 807-845.

[2] Galambos, T. V., ed. (1988). *Guide to Stability Design Criteria for Metal Structures*. 4th ed., Wiley, New York, N. Y.

[3] Plaut, R. H., and Yang, J. (1993). "Lateral bracing forces in columns with two unequal spans." *J. Struc. Engrg.*, 119, 2896-2912.

[4] Plaut, R. H., and Yang, Y. (1995). "Behavior of three-span braced columns with equal or unequal spans." *J. Struc. Engrg.*, 121, 986-994.

[5] Plaut, R. H. (1993). "Requirements for lateral bracing of columns with two spans." *J. Struc. Engrg.*, 119, 2913-2931.

[6] Yura, J. (1994). "Winter's bracing approach revisited." *Proc., Annual Technical Session of the Structural Stability Research Council*, 375-382.

[7] Olhoff, N., and Akesson B. (1991). "Minimum stiffness of optimally located supports for maximum value of column buckling loads." *Struct. Optimization*, 163-175.

[8] Stanway, G. D., Chapman, J. C., and Dowling, P. J. (1992). "A simply supported imperfect column with a transverse elastic restraint at any position. Part 2: Design models." *Proc., Institution of Civil Engineers, Structures and Buildings*, 94, 217-228.

[9] Stronge, W. J., and Yu, T. X. (1993). *Dynamic Models for Structural Plasticity*, Springer-Verlag, New York, N. Y.

[10] Yu, T. X., and Johnson, W. (1982). "Influence of axial force on the elastic-plastic bending and springback of a beam." *J. Mech. Working Tech.*, 6, 5-21.

[11] Ammann, W. (1984). "Applicability of dynamic plasticity theorems to impulsively loaded reinforced concrete structures." *Structural Impact and Crashworthiness*, Vol. 2, J. Morton, ed., Elsevier, London, 605-616.

[12] Sevin, E. (1960). "On the elastic bending of columns due to dynamic axial forces including effects of axial inertia." *J. Appl. Mech.* 27, 125-131.

[13] Elishakoff, I. (1978). "Axial impact buckling of a column with random imperfections." *J. Appl. Mech.*, 45, 361-365.

[14] Jones, N. (1989). *Structural Impact*, Cambridge University Press, Cambridge, England.

[15] Jones, N. (1971). "A theoretical study of the dynamic plastic behavior of beams and plates with finite deflections." *Int. J. Solids Structs.*, 7, 1007-1029.

[16] Lindberg, H. E., and Floence, A. L. (1987). *Dynamic Pulse Buckling*, Martinus Nijhoff Publishers, Boston.

[17] Lee, L. H. N. (1981). "Dynamic buckling of an inelastic column." *Int. J. Solids Structs.*, 17, 271-279.

[18] Cowper, G. R., and Symonds, P. S. (1957). "Strain-hardening and strain-rate effects in the impact loading of cantilever beams." Division of Applied Mathematics, Brown University, TR28.

[19] Hall, R. G., Al-Hassani, S. T. S., and Johnson, W. (1971). "The impulsive loading of cantilevers." *Int. J. Mech. Sci.* 13, 481-488.

[20] Martin, J. B., and Symonds, P. S. (1966). "Mode approximation for impulsively-loaded rigid-plastic structures." *J. Engrg. Mech. Div., ASCE*, 92, 43-66.

[21] AISC, (1994). *Manual of Steel Construction, Load & Resistance Factor Design* Vol. 1, 2nd ed., American Institute of Steel Construction, Chicago, IL.

[22] ASTM, (1995). *Annual Book of ASTM Standards*, Vol. 01.04, A6, American Society of Testing and Materials, Philadephia, PA.

[23] White, D. W., and Chen, W. F. eds. (1993). *Plastic Hinge Methods for Advanced Analysis and Design of Steel Structures*, Structural Stability Research Council, Bethlehem, PA.

[24] ABAQUS, (1994). *User's Manual* (version 5.4), Hibbitt, Karlsson & Sorensen, Pawtucket, RI.

[25] Chopra, A. K. (1995). *Dynamics of structures: Theory and Applications to Earthquake Engineering*, Prentice Hall, Englewood Cliffs, NJ.

[26] Cook, R. D. (1981). *Concepts and Applications of Finite Element Analysis*, John Wiley & Sons, New York, NY.

[27] Bathe, K. J. (1982). *Finite Element Procedures in Engineering Analysis*, Prentice Hall, Englewood Cliffs, NJ.

[28] Craig, Jr., R.R. (1981). *Structural Dynamics*, John Wiley & Sons, New York, NY.

[29] Bažant, Z. P., and Cedolin, L. (1991). *Stability of Structures: Elastic, Inelastic, Fracture, and Damage Theories*, John Wiley & Sons, New York, NY.

[30] Englekirk, R. (1994). *Steel Structures, Controlling Behavior Through Design.* John Wiley & Sons, New York, N. Y.

[31] Galambos, T. V., and Ketter, R. L. (1959). "Column under combined bending and thrust." *J. Eng. Mech. Div., ASCE*, 85, 1-30.

APPENDIX

1. Equilibrium shape of the column with brace

If the initial deflection of the column is $w_0 = \sum_{m=1}^{M} R_m \cdot \sin(m\pi x)$, by utilizing nondimensional quantities, the equilibrium equations of the system in Fig. 2.1 become:

$$w_1''''(x) - w_0''''(x) + \gamma_1^2 w_1''(x) = 0, \quad \text{for } 0 \le x \le a$$

$$w_2''''(x) - w_0''''(x) + \gamma_2^2 w_2''(x) = 0, \quad \text{for } a \le x \le 1 \qquad \text{(A1)}$$

where $\gamma_1^{\,2} = \dfrac{(Q_1 + Q_2)L^2}{EI_1}$, $\gamma_2^{\,2} = \dfrac{Q_2 L^2}{EI_2}$.

The solutions of Equation (A1) are

$$w_1(x) = A_1 \sin\gamma_1 x + A_2 \cos\gamma_1 x + A_3 x + A_4 + W_{P1}(x), \ (0 \le x \le a)$$

$$w_2(x) = B_1 \sin\gamma_2 x + B_2 \cos\gamma_2 x + B_3 x + B_4 + W_{P2}(x), \ (a \le x \le 1)$$

where $W_{P1}(x) = \sum_{m=1}^{M} \dfrac{R_m (m\pi)^2}{(m\pi)^2 - \gamma_1^{\,2}} \cdot \sin(m\pi x)$

and $W_{P2}(x) = \sum_{m=1}^{M} \dfrac{R_m (m\pi)^2}{(m\pi)^2 - \gamma_2^{\,2}} \cdot \sin(m\pi x)$.

The boundary and transition conditions are:

at x=0 : $w_1 = 0$

$$w_1'' - w_0'' = 0$$

at x=a : $w_1 = w_2$

$$w_1' = w_2'$$

$$w_1'' - w_0'' = \varepsilon(w_2'' - w_0'')$$

$$w_1''' - w_0''' + qw_1' = \varepsilon(w_2''' - w_0''') + k(w_1 - w_0)$$

at x=1 : $w_2 = 0$

$$w_2'' - w_0'' = 0 \qquad \text{(A2)}$$

where $\varepsilon = \dfrac{EI_2}{EI_1}$ and $q = \gamma_1^2 - \varepsilon\gamma_2^2$.

Using Equations (A2), we have

$A_1 = \delta_4 \cdot \delta_{15} + \delta_5$

$A_2 = 0$

$A_3 = \delta_9 \cdot \delta_{15} + \delta_{10}$

$A_4 = 0$

$B_1 = \delta_{15}$

$B_2 = \delta_1 \cdot \delta_{15}$

$B_3 = \delta_{11} \cdot \delta_{15} + \delta_{12}$

$$B_4 = -\delta_{11} \cdot \delta_{15} - \delta_{12}$$

where

$$\sigma_1 = \gamma_1 \cdot a$$

$$\sigma_2 = \gamma_2 \cdot a$$

$$\delta_1 = -\tan \gamma_2$$

$$\delta_2 = -\frac{\varepsilon}{{\gamma_1}^2 \cdot \sin \sigma_1}$$

$$\delta_3 = \frac{\left[W_{P1}''(a) - w_0''(a)\right]}{{\gamma_1}^2 \cdot \sin \sigma_1}$$

$$\delta_4 = -\delta_2({\gamma_2}^2 \cdot \sin \sigma_2 + \delta_1 \cdot {\gamma_2}^2 \cdot \cos \sigma_2)$$

$$\delta_5 = \delta_2\left[W_{P2}''(a) - w_0''(a)\right] + \delta_3$$

$$\delta_6 = q - ka$$

$$\delta_7 = \delta_4 \cdot {\gamma_1}^3 \cdot \cos \sigma_1 - q \cdot \delta_4 \cdot \gamma_1 \cdot \cos \sigma_1 - \varepsilon \cdot {\gamma_2}^3 \cdot \cos \sigma_2 + \varepsilon \cdot \delta_1 \cdot {\gamma_2}^3 \cdot \sin \sigma_2 + k \cdot \delta_4 \cdot \sin \sigma_1$$

$$\delta_8 = \delta_5 \cdot {\gamma_1}^3 \cdot \cos \sigma_1 - W_{P1}'''(a) + w_0'''(a) - q\left[\delta_5 \cdot \gamma_1 \cdot \cos \sigma_1 + W_{P1}'(a)\right]$$

$$+\varepsilon\left[W_{P2}'''(a) - w_0'''(a)\right] + k\left[\delta_5 \cdot \sin \sigma_1 + W_{P1}(a) - w_0(a)\right]$$

$$\delta_9 = \frac{\delta_7}{\delta_6}$$

$$\delta_{10} = \frac{\delta_8}{\delta_6}$$

$$\delta_{11} = \delta_4 \cdot \gamma_1 \cdot \cos \sigma_1 + \delta_9 - \gamma_2 \cdot \cos \sigma_2 + \delta_1 \cdot \gamma_2 \cdot \sin \sigma_2$$

$$\delta_{12} = \delta_5 \cdot \gamma_1 \cdot \cos\sigma_1 + \delta_{10} + W_{P1}'(a) - W_{P2}'(a)$$

$$\delta_{13} = \delta_4 \cdot \sin\sigma_1 + \delta_9 \cdot a - \sin\sigma_2 - \delta_1 \cdot \cos\sigma_2 + \delta_{11}(1-a)$$

$$\delta_{14} = \delta_{12} \cdot a - \delta_{12} + W_{P2}(a) - \delta_5 \cdot \sin\sigma_1 - \delta_{10} \cdot a - W_{P1}(a)$$

$$\delta_{15} = \frac{\delta_{14}}{\delta_{13}}.$$

2. Equilibrium shape of the column without brace and internal load

The equilibrium equation is

$$w_s''''(x) - w_0''''(x) + \gamma_2^2 w_s''(x) = 0, \quad \text{for } 0 \le x \le 1. \tag{A3}$$

The solution of equation (A3) becomes

$$w_s(x) = C_1 \sin\gamma_2 x + C_2 \cos\gamma_2 x + C_3 x + C_4 + W_{P0}(x)$$

where $W_{P0}(x) = \sum_{m=1}^{M} \frac{R_m (m\pi)^2}{(m\pi)^2 - \gamma_2^2} \cdot \sin(m\pi x)$.

The boundary conditions are:

at x=0 : $w_s = 0$

$$w_s'' - w_0'' = 0$$

at x=1 : $w_s = 0$

$$w_s'' - w_0'' = 0 .$$

All $C_i = 0$ from boundary conditions. Therefore

$$w_s(x) = \sum_{m=1}^{M} \frac{R_m (m\pi)^2}{(m\pi)^2 - \gamma_2^{\,2}} \cdot \sin(m\pi x) \ .$$

VITA

Rae Hak Yoo was born on June 15, 1961, in Seoul, Korea. In 1980, he matriculated at Kookmin University in Seoul, Korea, and subsequently received his Bachelor of Engineering (1984) and an M.S. (1986) in Civil Engineering. After finishing the military service as a second lieutenant in the Korean Army (1987), he worked for Ssangyong Construction Co. as a field engineer in Seoul, Korea. He entered the graduate school at Virginia Polytechnic Institute in 1992, and completed requirements for the Ph.D. in the Department of Civil Engineering (Structure) in December of 1995.